博士論文

# Cosmological evolution of pseudo-moduli and its impact on the gravitino relic abundance

（擬モジュライの宇宙論的進化と
グラヴィティーノ暗黒物質）

福島　　啓

平成２５年

Ph.D thesis

# Cosmological evolution of pseudo-moduli and its impact on the gravitino relic abundance

Hiraku Fukushima

*Department of Physics, Tohoku University, Sendai, Japan*

# Contents

# 1 Introduction

## 1.1 Overview

The existence of dark matter (DM) is fairly confirmed by various observations, and about twenty percent of the total energy density of the Universe is occupied by the unknown particle; the candidate of DM is absent in the Standard Model (SM). Among various candidates, the hypothesis of gravitino dark matter is very attractive as gravitino always exists in supersymmetric (SUSY) theories and is often the lightest superparticle (LSP) since its mass is suppressed by the Planck scale. The gauge mediated SUSY breaking (GMSB) scenario [1, 2] is an explicit realization of the gravitino LSP. The superpartners of the SM particles are fed masses through the SM gauge interactions which can be mach heavier than gravitino.

Gravitinos are produced in the early Universe from the thermal bath of the particles in the minimal supersymmetric standard model (MSSM). The production rate has been calculated in the literature [5, 6, 7, 8, 9, 10, 11, 12, 13, 14], by using the supergravity Lagrangian. According to the studies, the production process is more effective at high temperatures, and thus the relic abundance is proportional to the reheating temperature after inflation, $\Omega_{\rm DM} \propto T_R$. This gives an upper bound on $T_R$ so as not for the gravitino abundance to exceed the observed DM abundance, $\Omega_{\rm DM}h^2 \simeq 0.1$. The upper bound is $T_R \lesssim 10^6$GeV for $m_{3/2} \sim 1$ GeV and it becomes more severe for a lighter gravitino. It is, therefore, difficult to realize the gravitino DM compatible with the thermal leptogenesis [16], where the maximal baryon asymmetry is also proportional to $T_R$. In order to explain the baron asymmetry of the Universe, we need $T_R \gtrsim 10^9$ GeV [17, 18, 19, 20]. The ratio $\Omega_{\rm DM}/\Omega_B$ is predicted to be too large compared to the observed one, i.e., $\Omega_{\rm DM}/\Omega_B \gg 5$. The situation does not change even if there is an entropy injection at late-time since both the baryon and DM are diluted while fixing the ratio, $\Omega_{\rm DM}/\Omega_B$.

In the GMSB models, however, the above estimates should be modified if the reheating temperature of the Universe is extremely high, i.e., higher than the messenger scale $M_{\rm mess}$. It has been argued in Ref. [22], and recently confirmed in Ref. , that for temperature $T \gg M_{\rm mess}$, the production rate of gravitino is suppressed by $\sim M_{\rm mess}^2/T^2$ compared to the one for $T \ll M_{\rm mess}$. This indicates that the relic abundance of the gravitino is proportional to the messenger scale, $\Omega_{\rm DM} \propto M_{\rm mess}$ rather than $T_R$ for $T_R \gg M_{\rm mess}$. Therefore, in this occasion, there is no reason to abandon thermal leptogenesis. Given that the gravitino abundance does not depend on $T_R$, the ratio $\Omega_{\rm DM}/\Omega_B$ can be fixed to the observed value, $\sim 5$, with a suitable $T_R$. We study this possibility in this thesis.

Although the observed DM-baryon ratio can be explained by the thermal leptogenesis, the scenario requires a late-time entropy production by some mechanism, because the produced amount of gravitino is still larger than the observation, $\Omega_{\rm DM}h^2 \gg 0.1$, in order to explain the $\Omega_{\rm DM}/\Omega_B$ ratio. Interestingly, we already have a source of the entropy production in GMSB models; there is a pseudo-moduli field in generic low-energy SUSY breaking models, which can supply a large amount of entropy by its decay.

It has been recently found in Ref. [33] that a wide class of dynamical SUSY breaking (DSB) models reduces to a weakly-coupled description at low-energy, which always has a pseudo-moduli field. Therefore, the cosmological scenario is well motivated also from the viewpoint of model buildings. We study the general features of the pseudo-moduli in low-energy SUSY breaking models together with a few examples.

One general symptom of realistic SUSY breaking models is the meta-stability; in many models of SUSY breaking including the one in Ref. [33], there is a SUSY preserving true vacuum other than the SUSY breaking one. In such a model, the existence of a SUSY breaking local minimum is not a sufficient condition to be adopted as a mechanism of SUSY breaking. One should check that the SUSY breaking state is actually selected along the thermal history of the Universe, not falling into SUSY preserving true vacuum. Together with other cosmological constraints, we summarize the requirements that should be equipped with in a realistic SUSY breaking model.

As seen from above, in order for the gravitino DM scenario to be realized, the SUSY breaking sector should pass through a distinctive thermal history. We demonstrate the scenario in a simple model of gauge mediation and confirm that the scenario indeed works as the mechanism to produce the right amount of the gravitino DM.

The sketch of the scenario is as follows; the reheating of the Universe occurs at a high $T_R$ so that the gravitino abundance is independent of $T_R$. With an appropriate reheating temperature, the ratio of energy densities $\Omega_{\rm DM}/\Omega_B$ can be fixed at the observed value, $\Omega_{\rm DM}/\Omega_B \sim 5$. Then, during the radiation dominated era, the SUSY breaking pseudo-moduli starts coherent oscillation about the minimum of the potential, and the oscillation energy eventually dominates the Universe. A sizable amount of entropy is released by the subsequent decay, and the pre-existing gravitinos and baryons are diluted by a same amount to realize the observed values. While the model exhibits meta-stable SUSY breaking, the SUSY breaking vacuum is selected in the course of cosmological evolution.

## 1.2 Outline of the thesis

This thesis is composed of three parts. In part I, the thermal production of gravitino is studied in detail. We calculate the scattering amplitude of gravitino production using both the global SUSY Lagrangian and the supergravity Lagrangian and show that the production is suppressed for $\sqrt{s} > M_{\rm mess}$. This implies that the relic abundance of gravitino is proportional to $M_{\rm mess}$ rather than $T_R$ for $T_R > M_{\rm mess}$. Inspired by this feature, we present a scenario of gravitino DM which is compatible with the thermal leptogenesis.

In part II, we study general features of a O'Raifeartaigh-type model which serves as a low-energy description of wide class of DSB. SUSY is linearly realized and there is always a tree-level flat direction called the pseudo-moduli, which plays an important role in the cosmological scenario presented in part I. Several cosmological constraints on SUSY breaking sectors are also mentioned here.

Finally, we demonstrate the cosmological scenario in a simple model of gauge mediation in part III. We see that the cosmological constraints presented in part II is totally satisfied in the demonstration, and confirm the scenario indeed works as a mechanism to produce the right amount of the gravitino DM.

# Part I

# Thermal production of gravitino as the Dark Matter of the Universe

Gravitino is a hypothetical particle which has spin-3/2 and is always contained in local SUSY (supergravity) theories. Once SUSY is spontaneously broken, the mass is supplied by the SUSY-breaking sector, which is suppressed by Planck scale. At the same time, the goldstone-fermion (the goldstino) is absorbed into the longitudinal component of the gravitino. In GMSB models, gravitino is the leading candidate of DM since the superpartners of SM are much heavier than gravitino due to SM gauge interactions.

In this part, we first offer a comprehensive view about the thermal production of gravitino in section 2. The production rate has been calculated by using the supergravity Lagrangian [5, 6, 7, 8, 9, 10, 11, 12, 13, 14], which leads the result that the abundance is proportional to $T_R$. In GMSB models, the production is dominated by that of the longitudinal mode which can be evaluated by identifying the longitudinal mode as the goldstino in the global SUSY Lagrangian. Moreover, in GMSB models, one can use a framework of a linearly realized SUSY-breaking model with a singlet superfield $S$, whose $F$-component VEV breaks SUSY.

An explicit calculation of the goldstino production shows that the goldstino relic abundance is not necessarily proportional to $T_R$ [22, 56], which contradicts with the estimation in supergravity. We examine this apparent contradiction by calculating the scattering amplitudes of goldstino/gravitino production process both with a global SUSY Lagrangian and a supergravity Lagrangian. We confirm that the supergravity result should be modified at high energy.

In section 3, we present a new scenario of gravitino DM which incorporate the thermal leptogenesis. The scenario is based on the fact that the relic abundance of gravitino does not depend on $T_R$ once the temperature of the Universe exceeds the messenger scale $M_{\rm mess}$.

## 2 Thermal production of gravitino

We first review the production mechanism of gravitino and reproduce the famous result that the relic abundance is proportional to the reheating temperature of the Universe. Next we calculate the scattering amplitude of the gravitino production processes both with the global SUSY Lagrangian and the supergravity one and show that the amplitude is suppressed at

high energy region, which makes the relic abundance insensitive to the reheating temperature if $T_R > M_{\rm mess}$. The analysis is based on Ref. [56], and detailed calculations of the scattering amplitude are found in appendix A.

## 2.1 Generalities of gravitino thermal production

Since the interactions of gravitino are suppressed by the Planck scale $M_{\rm pl}$, it is never thermalized if the temperature of the Universe is lower than $M_{\rm pl}$. Nevertheless, gravitinos are produced from the scattering processes of the bath particles in the MSSM. The evolution of number density of the gravitino, $n_{3/2}$, in the expanding Universe is governed by the Boltzmann equation [4],

$$\dot{n}_{3/2} + 3Hn_{3/2} = \langle\sigma v\rangle n_R^2, \tag{2.1}$$

where $\langle\sigma v\rangle$ is the thermally averaged cross section of gravitino production, and $n_R$ is the number density of radiation, $n_R = \frac{\zeta(3)}{\pi^2}T^3$. $H$ is the Hubble parameter and defined by

$$H^2 = \frac{1}{3M_{\rm pl}^2}\rho_{\rm total}, \tag{2.2}$$

where $\rho_{\rm total}$ is the total energy density of the Universe. If the energy density of the Universe is dominated by radiation, i.e., $\rho_{\rm total} \simeq \rho_R = \frac{\pi^2}{30}g_*T^4$, the Hubble parameter can be represented as a function of the temperature,

$$H = \sqrt{\frac{\pi^2 g_*}{90}}\frac{T^2}{M_{\rm pl}}, \tag{2.3}$$

where $g_*$ is the effective number of the massless degrees of freedom. It is useful to define a yield value of gravitino,

$$Y_{3/2} = \frac{n_{3/2}}{s}, \tag{2.4}$$

where $s$ is the entropy density of the Universe, $s = \frac{2\pi^2}{45}g_*T^3$. As the number density of gravitino and the entropy density decrease both as $\sim a^{-3}$ along the expansion of the Universe ($a$ is the scale factor which defines the radius of the Universe), the yield is constant as long as the total entropy of the Universe is conserved. The Boltzmann equation (2.1) can be rewritten in terms of the yield value as

$$\frac{dY_{3/2}}{dT} = -\frac{\langle\sigma v\rangle n_R^2}{sHT}. \tag{2.5}$$

We also define the reaction rate,

$$\Gamma \equiv \langle \sigma v \rangle n_R, \tag{2.6}$$

and rewrite Eq. (2.5) in more suggestive way,

$$\frac{dY_{3/2}}{dT} = -\frac{45\zeta(3)}{2\pi^4}\frac{\Gamma}{g_* HT}. \tag{2.7}$$

We can estimate the gravitino relic abundance by integrating Eq. (2.7) from $T = T_R$ to $T_0 \ll T_R$, where $T_0$ is the temperature of the current Universe. As we see from Eq. (2.7), if the temperature dependence of the reaction rate $\Gamma$ is stronger than that of the Hubble parameter, namely $\Gamma \propto T^n$ with $n > 2$, the gravitino abundance at $T = T_0 \ll T_R$ is determined by $T_R$. For example, if the thermal averaged cross section has only a weak dependence on $T$ and the reaction rate is almost proportional to $\sim T^3$, the gravitino relic abundance is almost proportional to $T_R$,

$$Y_{3/2} \sim \frac{45\zeta(3)}{2\pi^4}\left[\frac{\Gamma}{g_* HT}\right]_{T_R} T_R. \tag{2.8}$$

This situation realizes, as we see later, if the temperature of the Universe is always lower than the messenger scale On the other hand, if the reaction rate has a weak dependence on temperature, $\Gamma \propto T^n$ with $n < 2$, the abundance is determined by the lowest temperature in the period when the interaction is effective. This is the case when the temperature of the Universe once exceeds $M_{\rm mess}$ in GMSB models.

### 2.2 Estimate in supergravity Lagrangian

Here we briefly review the studies on the thermal production of gravitino using the supergravity Lagrangian. The relic abundance is proportional to $T_R$. We first quote the known results of the relic abundance. Then we focus on one particular process of gravitino production and understand the origin of the $T_R$ dependence which is related to the high energy behavior of the reaction rate,

Gravitinos are produced from the scattering process of the MSSM fields and the amplitudes are calculated using the supergravity Lagrangian,

$$\mathcal{L}^{\rm MSSM}_{\rm sugra} \ni -\frac{1}{\sqrt{2}M_{\rm pl}}(D_\nu \phi_i)^* \bar{\psi}_{3/2\mu}\gamma^\nu\gamma^\mu P_L \psi_i - \frac{i}{4M_{\rm pl}}\bar{\lambda}^a\gamma^\mu[\gamma^\nu,\gamma^\rho]\psi_{3/2\mu}F^a_{\nu\rho} + \text{h.c.}, \tag{2.9}$$

where the gravitino field is denoted by $\psi_{3/2\mu}$. The gravitino has the tree-level interactions with every chiral multiplet $(\phi_i, \psi_i)$ or gauge multiplet $(A^a_\mu, \lambda^a)$ in the MSSM and the form of interactions is uniquely fixed by local SUSY.

For the gravitino production, there are ten two-body processes involving left-handed quarks ($q_i$), squarks ($\tilde{q}_i$), gluons ($g^a$) and gluinos ($\tilde{g}^a$), which are called process A to process J in the literatures [5, 6, 7, 9, 10]. The thermal averaged cross section has been calculated generally for $SU(N)$ super Yang-Mills model with $n_f$ pairs of fundamental and anti-fundamental chiral superfields [10],

$$\langle \sigma v \rangle = \left[ 1 + \frac{m_{\tilde{g}}^2}{3m_{3/2}^2} \right] \frac{g^2(N^2-1)}{32\pi M_{\rm pl}^2} \frac{\pi^2}{\zeta(3)} \left\{ \left[ \ln(T^2/m_{g,\rm th}^2) + 0.3224 \right] (N+n_f) + 0.5781 n_f \right\}, \tag{2.10}$$

where $m_{g,\rm th}$ is the thermal mass of the gauge boson which is given as $m_{g,\rm th}^2 = \frac{1}{6} g^2 (N+n_f) T^2$. The cross section is dominated by that of the QCD processes in the MSSM. The contribution proportional to 1 and $m_{\tilde{g}}^2/m_{3/2}^2$ is from the transverse and the longitudinal component of the gravitino, respectively.

The gravitino relic abundance is obtained by solving the Boltzmann equation (2.7) with the cross section in Eq. (2.10). Since the cross section depends very weakly on the temperature, the relic abundance is, as mentioned below Eq. (2.7), almost proportional to $T_R$. A numerical analysis is found in Ref. [14],

$$\begin{aligned} Y_{3/2} \simeq & 1.9 \times 10^{-12} \\ & \times \left( \frac{T_R}{10^{10}\ \text{GeV}} \right) \quad \left( 1 + \frac{m_{\tilde{g}}^2}{3m_{3/2}^2} \right) \left[ 1 + 0.045 \ln \left( \frac{T_R}{10^{10}\ \text{GeV}} \right) \right] \left[ 1 - 0.028 \ln \left( \frac{T_R}{10^{10}\ \text{GeV}} \right) \right]. \end{aligned} \tag{2.11}$$

In terms of the density parameter,

$$\begin{aligned} \Omega_{3/2} h^2 &\equiv \frac{m_{3/2} Y_{3/2} h^2}{(\rho_c/s)_0} \\ &\simeq 0.45 \left( \frac{T_R}{10^6 \text{GeV}} \right) \left( \frac{\text{GeV}}{m_{3/2}} \right) \left( \frac{m_{\tilde{g}}}{5\ \text{TeV}} \right)^2, \end{aligned} \tag{2.12}$$

where we assumed $m_{3/2} \ll m_{\tilde{g}}$ as is always the case in GMSB.

**High energy behavior of the scattering amplitude**

We have quoted the cross section and the resultant gravitino abundance from the literatures, and seen that the abundance is proportional to $T_R$. These are derived by the calculations using the supergravity Lagrangian Eq. (2.9). However, as we see below the cross section is modified for a high energy region by the contributions from the messenger fields. In

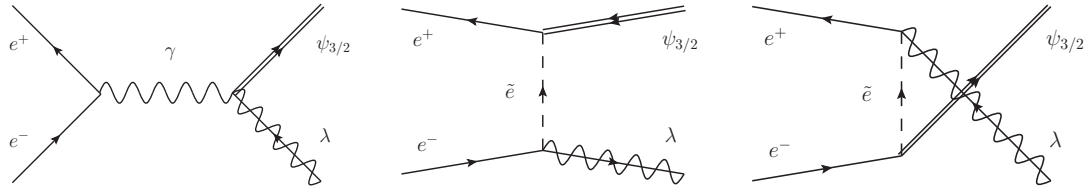


Figure 1: Gravitino production process $e^-e^+ \to \lambda\psi_{3/2}$.

order to understand the modification clearly, we focus on one particular process of gravitino production and write down the high energy behavior of the amplitude.

We focus on a particular process $e^-e^+ \to \lambda\psi_{3/2}$ (called process I in the literatures). The tree-level diagrams are shown in Fig. 1. The scattering amplitude is calculated by the supergravity Lagrangian in Eq. (2.9). Among the polarized amplitudes, the following turns out to have the highest power in the center-of-mass energy, $\sqrt{s}$, and thus dominates at high energies,

$$\mathcal{M}^{(\uparrow\downarrow\uparrow\uparrow)}_{e^-e^+\to\lambda\psi_{3/2}} = \frac{em_\lambda}{\sqrt{6}m_{3/2}M_{\rm pl}}\sqrt{s}\sin\theta, \tag{2.13}$$

where arrows in the parenthesis represent the spins of the electron, the positron, the gaugino and the gravitino, respectively. The angle $\theta$ is the production angle in the center-of-mass frame. The gauge coupling of QED is denoted by $e$. Although each of $s$-, $t$- and $u$-channel diagrams has an energy dependence of $O(s)$, they are canceled out when combined, remaining the energy dependence of $O(\sqrt{s})$. The above contribution is from the longitudinal component of the gravitino whose wave function is approximately proportional to $\sqrt{s}/m_{3/2}$ with $m_{3/2}$ the gravitino mass.

In order to estimate the relic abundance of the gravitino, we should calculate the reaction rate which is proportional to the square of the amplitude,

$$\Gamma_{e^-e^+\to\lambda\psi_{3/2}}(T) \propto \frac{m_\lambda^2}{m_{3/2}^2 M_{\rm pl}^2}T^3, \tag{2.14}$$

where the temperature dependence is determined by dimensional analysis. Note that the reaction rate is proportional to $\sim T^3$, which is higher in power than the Hubble parameter $H(T) \propto T^2$. Therefore, as mentioned in subsection 2.1, if the process $e^-e^+ \to \lambda\psi_{3/2}$ is effective and Eq. (2.14) is valid for an arbitrary temperature, the gravitino abundance is determined by $T_R$.

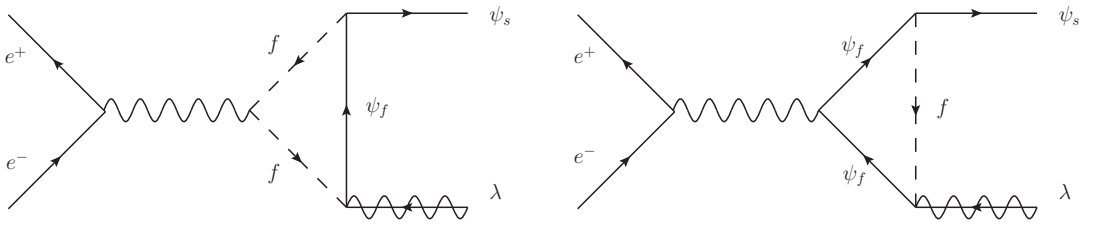


Figure 2: Goldstino production process $e^-e^+ \to \lambda\tilde{G}$.

### 2.3 Goldstino analysis

In GMSB models, effects of SUSY-breaking are transmitted to the MSSM sector through the messenger loop diagrams. A superpotential of the following form is usually assumed,

$$W = \lambda S f \bar{f}. \tag{2.15}$$

SUSY is broken by the $F$-component of the singlet superfield $S$. $f$ and $\bar{f}$ represent the messenger superfields which have SM gauge charges. If $F_S$ is the only source of the SUSY breaking, the fermion component of $S$ (we call it $\psi_S$) is the goldstino $\tilde{G}$, which is absorbed into the longitudinal component of the gravitino. In general, there are additional sources of SUSY breaking from the $F$-components of other chiral multiplets. In that case, the goldstino is composed of the liner combination of the fermions which belong to the multiplets whose $F$-components develop VEVs,

$$\tilde{G} = \frac{F_S}{F}\psi_S + \sum_i \frac{F_i}{F}\psi_i, \tag{2.16}$$

where $F = \sqrt{|F_S|^2 + \sum_i |F_i|^2}$. Therefore, the amplitude for the goldstino production is given by rescaling that for $\psi_S$ by a factor $F_S/F$. Unlike the gravitino in the supergravity Lagrangian, the goldstino does not couple directly to the MSSM fields. The goldstino is produced through the messenger loop diagrams shown in Fig. 2.3. We expect that the scattering amplitude of the process $e^-e^+ \to \lambda\tilde{G}$ coincides that of the gravitino production in Eq. (2.13).

By explicitly evaluating these diagrams, however, a different result from supergravity estimation comes out. For the same process and the same polarization to Eq. (2.13), the

scattering amplitude is calculated to be

$$\mathcal{M}^{(\uparrow\downarrow\uparrow\uparrow)}_{e^-e^+\to\lambda\tilde{G}} = -\frac{2\sqrt{2}e^3\lambda}{(4\pi)^2}\frac{F_S}{F}M_{\rm mess}C_0(\sqrt{s},M_{\rm mess})\sqrt{s}\sin\theta \tag{2.17}$$

$$= -\frac{2em_\lambda M^2_{\rm mess}}{\sqrt{6}m_{3/2}M_{\rm pl}}C_0(\sqrt{s},M_{\rm mess})\sqrt{s}\sin\theta, \tag{2.18}$$

where $M_{\rm mess} = \lambda\langle S\rangle$ is the messenger mass scale. We have translated the parameters of global SUSY, $\lambda$ and $\langle S\rangle$, to the parameters of the supergravity, $m_{3/2}$ and $M_{\rm pl}$ by using the formulae in GMSB,

$$m_\lambda = \frac{2e^2}{(4\pi)^2}\frac{F_S}{\langle S\rangle}, \tag{2.19}$$

and

$$m_{3/2} = \frac{F}{\sqrt{3}M_{\rm pl}}. \tag{2.20}$$

The function $C_0(\sqrt{s},M_{\rm mess})$ is the $C$-function defined in Ref. [21],

$$C_0(\sqrt{s},M_{\rm mess}) = \int_0^1 dx\frac{1}{s(1-x)}\log\left[1-\frac{s}{M^2_{\rm mess}}x(1-x)-i\epsilon\right]. \tag{2.21}$$

In a low energy limit, $\sqrt{s}\ll M_{\rm mess}$, $C_0$ is approximately given by $C_0\simeq -1/2M^2_{\rm mess}$ and reproduces the result of supergravity calculation in Eq. (2.13). However, for $\sqrt{s}\gg M_{\rm mess}$, $C_0$ scales as $1/s$ up to a logarithmic factor.

If the external energies are lower than the messenger mass scale, i.e., for $T < M_{\rm mess}$, the reaction rate depends on the temperature as $\propto T^3$,

$$\Gamma_{e^-e^+\to\lambda\tilde{G}}(T) \propto \frac{m^2_\lambda}{m^2_{3/2}M^2_{\rm pl}}T^3, \qquad \text{for}\ \ T\ll M_{\rm mess}, \tag{2.22}$$

which reproduces the result of the supergravity calculation in Eq. (2.14). Here we again squared the amplitude and fixed the temperature dependence by dimensional analysis. However, for $T > M_{\rm mess}$, the reaction rate is suppressed by $\sim M^2_{\rm mess}\ /\ T^2$ compared to Eq. (2.22), namely

$$\Gamma_{e^-e^+\to\lambda\tilde{G}}(T) \propto \frac{m^2_\lambda M^2_{\rm mess}}{m^2_{3/2}M^2_{\rm pl}}T, \qquad \text{for}\ \ T\gg M_{\rm mess}. \tag{2.23}$$

The point is that the temperature dependence of $\Gamma_{e^-e^+\to\lambda\tilde{G}}(T)/H(T)$ gets suppressed as $1/T$ at high temperatures, which makes the goldstino relic abundance irrelevant to the reheating temperature. Rather, the abundance is determined by the messenger mass scale.

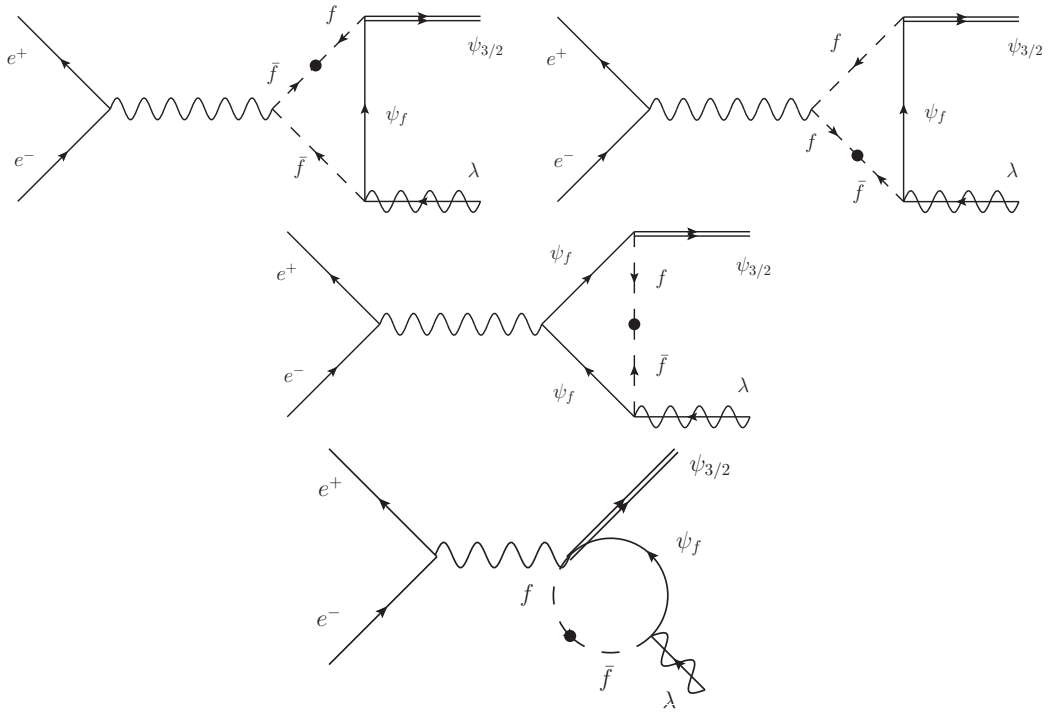


Figure 3: One-loop diagrams for the gravitino production $e^-e^+ \to \lambda\psi_{3/2}$.

### 2.4 Supergravity calculation in GMSB

We observe a difference between the two amplitudes, Eq. (2.13) and Eq. (2.18). One of them should be modified at high energy, $\sqrt{s} \gg M_{\rm mess}$, if we believe in the goldstino equivalence.

We find that the modification appears in the supergravity calculation. In GMSB models, there are messenger fields, which potentially affect the gravitino production process. In fact, they contribute to the gravitino production process $e^-e^+ \to \lambda\psi_{3/2}$ through the one-loop diagrams shown in Fig. 3. Even though they are diagrams at the one-loop level, they cannot be neglected compared to the tree-level ones in Fig. 1 since the gaugino mass in Eq. (2.13) is at the one-loop order in GMSB models. Note here that the diagrams in Fig. 3 are not the microscopic description of the first diagram in Fig. 1. Both diagrams exist as independent ones in supergravity. The explicit calculation shows

$$\mathcal{M}^{(\uparrow\downarrow\uparrow\uparrow)}_{e^-e^+\to\lambda\psi_{3/2}}(\text{one loop}) = -\frac{em_\lambda}{\sqrt{6}m_{3/2}M_{\rm pl}}\sqrt{s}\sin\theta\left[2M^2_{\rm mess}C_0(\sqrt{s},M_{\rm mess})+1\right], \qquad (2.24)$$

where $C_0$ is again the $C$-function in Eq. (2.21). The dots in Fig. 3 represent insertions of $F_S$. A few comments are in order. At a lower energy than the messenger mass scale, the messenger

fields can be integrated out and absent in the low energy theory. The gravitino interactions are then completely read off from the supergravity Lagrangian of the MSSM fields (2.9). The supergravity prediction in Eq. (2.13), therefore, should not be altered for $\sqrt{s} \ll M_{\rm mess}$. The additional contribution (2.24) indeed respects this consideration. The factor, $2M_{\rm mess}^2 C_0 + 1$, in Eq. (2.24) goes to zero as $\sqrt{s} \to 0$, and thus the amplitude is accurately represented by Eq. (2.13) at low energy. However, the one-loop contribution becomes comparable to that of tree-level for $\sqrt{s} \gg M_{\rm mess}$ since the factor, $2M_{\rm mess}^2 C_0 + 1$, approaches to 1.

Combined with the tree-level contribution (2.13), we confirmed that the growing amplitude at $\sqrt{s} \gg M_{\rm mess}$ in supergravity is completely cancelled by the one-loop diagrams, and the total supergravity calculation coincides with the result from global SUSY,

$$\begin{aligned}
\mathcal{M}^{(\uparrow\downarrow\uparrow\uparrow)}_{e^-e^+\to\lambda\psi_{3/2}} &= \mathcal{M}^{(\uparrow\downarrow\uparrow\uparrow)}_{e^-e^+\to\lambda\psi_{3/2}}(\text{tree}) + \mathcal{M}^{(\uparrow\downarrow\uparrow\uparrow)}_{e^-e^+\to\lambda\psi_{3/2}}(\text{one loop}) \\
&= \frac{em_\lambda}{\sqrt{6}m_{3/2}M_{\rm pl}}\sqrt{s}\sin\theta - \frac{em_\lambda}{\sqrt{6}m_{3/2}M_{\rm pl}}\sqrt{s}\sin\theta\left[2M_{\rm mess}^2 C_0(\sqrt{s}, M_{\rm mess}) + 1\right] \\
&= -\frac{2em_\lambda M_{\rm mess}^2}{\sqrt{6}m_{3/2}M_{\rm pl}} C_0(\sqrt{s}, M_{\rm mess})\sqrt{s}\sin\theta. \qquad (2.25)
\end{aligned}$$

## 2.5 Additional contribution from the tree-level messenger scatterings

For $T > M_{\rm mess}$, in addition to the scattering processes of the MSSM particles, the goldstino is also produced by scattering processes where the messenger fields are in the external lines. The reaction rate is calculated to be [22]

$$\begin{aligned}
\Gamma_{\rm messengers\to\lambda\tilde{G}}(T) &\propto \lambda^2\left(\frac{F_S}{F}\right)^2 T \\
&\propto \left(\frac{4\pi}{\alpha}\right)^2 \frac{m_\lambda^2 M_{\rm mess}^2}{m_{3/2}^2 M_{\rm pl}^2} T. \qquad (2.26)
\end{aligned}$$

As we see from Eq. (2.23) and Eq. (2.26), the reaction rate of the messenger particles is larger than that of the MSSM particles by a loop-factor since the messenger fields directly couple to the goldstino through the superpotential interaction.

## 2.6 The gravitino relic abundance

Summarizing the previous subsection, in GMSB models, the gravitino is produced from the scattering processes of the MSSM fields and the messenger fields. Depending on the value of $T_R$, the resultant gravitino relic abundance is determined by different values; if $T_R < M_{\rm mess}$,

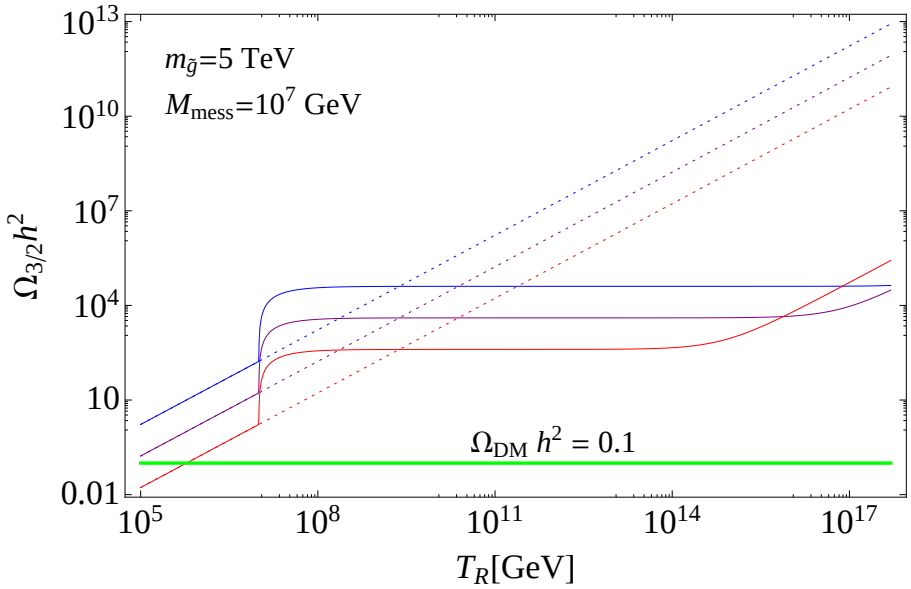


Figure 4: Gravitino relic abundance. Blue, purple, and red lines represent $m_{3/2} = 100$ MeV, $m_{3/2} = 1$ GeV and $m_{3/2} = 10$ GeV, respectively. The gravitino abundance become insensitive to the reheating temperature for $M_{\rm mess} < T_R$ (solid lines). Dotted lines are naive extrapolations of Eq. (2.27). For a very high reheating temperature ($T_R \gtrsim 10^{14}$ GeV), the transverse mode of the gravitino becomes important.

the abundance is fixed by $T_R$, and if $T_R > M_{\rm mess}$, it is the messenger mass scale to fix the abundance,

$$\Omega_{3/2}h^2 \simeq 0.45 \left(\frac{T_R}{10^6 {\rm GeV}}\right)\left(\frac{\rm GeV}{m_{3/2}}\right)\left(\frac{m_{\tilde{g}}}{5\ {\rm TeV}}\right)^2 \quad (T_R < M_{\rm mess}), \tag{2.27}$$

$$\Omega_{3/2}h^2 \simeq 3.7\times 10^2 \left(\frac{M_{\rm mess}}{10^6 {\rm GeV}}\right)\left(\frac{\rm GeV}{m_{3/2}}\right)\left(\frac{m_{\tilde{g}}}{5\ {\rm TeV}}\right)^2 \quad (T_R > M_{\rm mess}). \tag{2.28}$$

The abundance in Eq. (2.28) is not a straightforward replacement of $T_R$ to $M_{\rm mess}$ in Eq. (2.27) since the production through the messenger fields are not suppressed by a loop factor.

The estimates so far do not include a contribution of the transverse mode of the gravitino. For a very high reheating temperature, the transverse mode becomes relevant,

$$\Omega_{3/2}h^2({\rm transverse}) \simeq 0.53 \left(\frac{T_R}{10^{13}{\rm GeV}}\right)\left(\frac{m_{3/2}}{\rm GeV}\right). \tag{2.29}$$

Including both the longitudinal and the transverse modes, we show the gravitino relic abundance in GMSB with the messenger scale fixed to be $M_{\rm mess} = 10^7$ GeV in Fig. 4. As

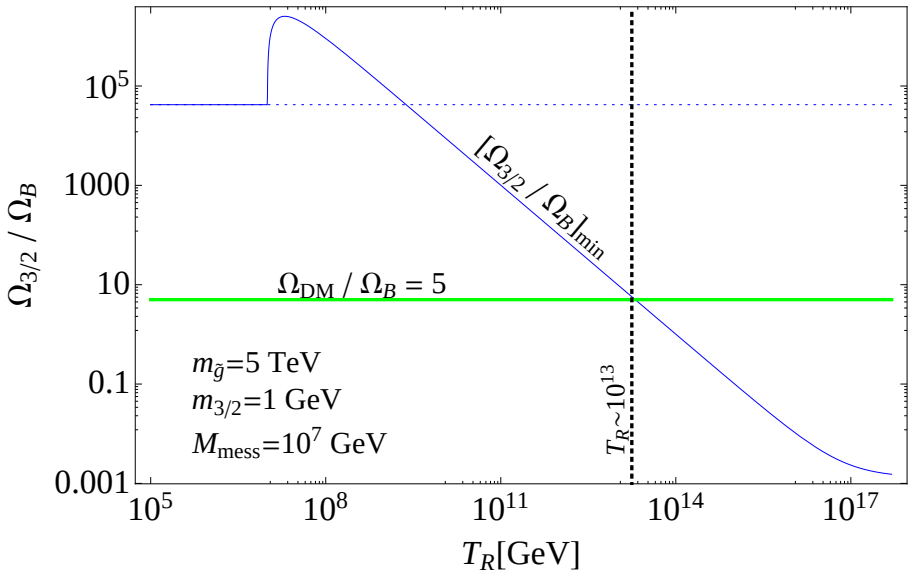


Figure 5: Since the gravitino abundance becomes constant for $M_{\rm mess} < T_R$ whereas the maximum value of $\Omega_B$ is always proportional to $T_R$, the ratio $\Omega_{3/2}/\Omega_B$ eventually reaches the observed value as $T_R$ becomes higher. We plotted a minimum value of the prediction for $\Omega_{3/2}/\Omega_B$ as a function of $T_R$. We see that the observed value of $\Omega_{\rm DM}/\Omega_B$ can be reproduced for $T_R \gtrsim 10^{13}$GeV.

we see from the figure, the gravitino relic abundance is predicted to be constant in a wide range of the reheating temperature, but the amount is too large compared to the observed dark matter energy density $\Omega_{\rm DM}h^2 \simeq 0.1$. The overproduced gravitinos must be diluted by some mechanism. Although the prediction to $\Omega_{3/2}$ is too large, the insensitivity to $T_R$ brings us a new scenario of gravitino DM.

## 3 A new scenario of gravitino Dark Matter

As we have confirmed in the previous section, the gravitino relic abundance becomes insensitive to $T_R$ once the temperature of the Universe exceeds the messenger mass scale. The results have a crucial impact on the possible mechanism of baryogenesis. In this section, we present a new cosmological scenario of gauge mediation, where gravitino dark matter and thermal leptogenesis are compatible. The scenario requires a late-time entropy release by some mechanism. A promising candidate of entropy production is that from the decay of the pseudo-moduli field which, as we see later in section 4, always exists in low energy models of SUSY-breaking.

### 3.1 Compatibility with thermal leptogenesis

In a light gravitino scenario, thermal leptogenesis and gravitino DM are thought to be incompatible with each other. The possible maximum amount of baryon asymmetry produced by the thermal leptogenesis is proportional to the reheating temperature [17, 18, 19, 20],

$$\Omega_B \lesssim 0.04 \left( \frac{T_R}{10^9 \mathrm{GeV}} \right), \tag{3.1}$$

which puts a lower bound on $T_R$ ($T_R \gtrsim 10^9$GeV) to realize the observed value $\Omega_B \simeq 0.045$. If the gravitino relic abundance is represented as Eq. (2.27) for any $T_R$, the thermal production of gravitino DM and the thermal leptogenesis are incompatible; even if we assume a late-time entropy production to dilute overproduced gravitino to match the abundance to the observation, baryons are also diluted at the same time and the abundance never reproduces the observation. In other words, the ratio $\Omega_{3/2}/\Omega_B$ is constant as long as the abundances are both proportional to $T_R$, and always larger than the observed ratio, $\Omega_{\rm DM}/\Omega_B \sim 5$.

However, in GMSB, if the reheating temperature is higher than the messenger mass scale, the gravitino relic abundance becomes insensitive to $T_R$. Then, the observed ratio of the energy densities, $\Omega_{\rm DM}/\Omega_B \sim 5$, can be realized with thermally produced gravitino and the thermal leptogenesis. We plot the prediction for $\Omega_{3/2}/\Omega_B$ to visualize the situation in Fig. 5. If the gravitino abundance is proportional to $T_R$ for any $T_R$, the theoretical prediction never reaches the observed value $\Omega_{\rm DM}/\Omega_B \sim 5$ (dotted line). However, if the reheating temperature is higher than the messenger scale, $\Omega_{3/2}$ becomes independent of $T_R$ in GMSB, which allows $\Omega_{3/2}/\Omega_B$ to achieve the observed value.

### 3.2 Late-time entropy release

The ratio of the energy densities $\Omega_{\rm DM}/\Omega_B \sim 5$ can be realized by thermally produced gravitino and thermal leptogenesis with an appropriate reheating temperature as we saw above. However, as is obvious from Fig. 4, the predicted gravitino abundance is too large compared to the observation, $\Omega_{\rm DM}h^2 \simeq 0.1$. The overproduced gravitino should be diluted by a late-time entropy release by some mechanism. The required amount of dilution is

$$\Delta_{3/2} \equiv \frac{\Omega_{3/2}h^2}{\Omega_{\rm DM}h^2} \tag{3.2}$$

$$\simeq 7.5 \times 10^4 \left( \frac{M_{\rm mess}}{10^7 \text{ GeV}} \right) \left( \frac{500 \text{ MeV}}{m_{3/2}} \right) \left( \frac{m_{\tilde{g}}}{5 \text{ TeV}} \right)^2, \tag{3.3}$$

where $T_R > M_{\rm mess}$ is assumed.

Actually, a source of entropy production is already incorporated in the scenario: the scalar component of the singlet superfield $S$, which is called the pseudo-moduli field. In the early Universe, it is possible that the pseudo-moduli is displaced from the vacuum and starts oscillation around the minimum. Since the pseudo-moduli is massless at tree-level and gets mass only through the quantum effects, it is often much lighter than the SUSY breaking scale, $\sqrt{F}$, and is long-lived if there is a weakly coupled description for the SUSY breaking sector. In such a case, the pseudo-moduli can eventually dominate the energy density of the Universe, and a sizable amount of entropy is produced from its decay.

In part II, we see that the pseudo-moduli always exists in a class of SUSY-breaking models which serve as low-energy descriptions of a wide class of dynamical SUSY-breaking models. Therefore, the cosmological scenario presented in this section has a chance to be realized in many models of SUSY-breaking.

# Part II
# SUSY-breaking and pseudo-moduli

If supersymmetry truly explains the hierarchy problem, it should be broken not only spontaneously, but also dynamically [26]. Before the appearance of the ISS model [33], the effort toward making a dynamical SUSY-breaking (DSB) is based on the argument of Witten index [27]. According to the argument, any $\mathcal{N} = 1$ supersymmetric gauge theory with massive, vector-like matters has supersymmetric vacua. So theories which break SUSY at their ground state must either be chiral [28, 29, 30], or if they are vector-like, they must have massless matters [31, 32]. These models look somewhat complicated, so DSB had been thought to be non-generic phenomenon in SUSY gauge theories.

Once we abandon SUSY breaking at the ground state and accept meta-stable vacua, however, the constraints from the Witten index do not have to be taken into account. As found in Ref [33], a SUSY gauge theory with massive vector-like matters has in general a meta-stable SUSY-breaking local minimum, and the life-time of the vacuum can be much longer than the age of the Universe, which suggests that the DSB is a generic phenomenon. Furthermore, the DSB models turn out to reduce to weakly-coupled descriptions at low-energy where SUSY is linearly realized. In the low-energy descriptions, SUSY is broken at tree-level, and there is always a tree-level flat direction called the pseudo-moduli, which potentially has a sizable impacts on thermal history of the Universe.

In section 4, we study a class of low-energy descriptions of SUSY breaking called O'Raifeartaigh-type models which break SUSY at tree-level. Several important features of the models are presented, which include the existence of pseudo-moduli, and the prevalence of meta-stable SUSY breaking. As we see below, meta-stable SUSY breaking is suggested not only from the viewpoint of model buildings of DSB, but also from the phenomenological requirements. Few examples of O'Raifeartaigh-type models are examined in section 5. Later in part III, we demonstrate the gravitino DM scenario presented in part I using one of the O'Raifeartaigh models in section 5.

## 4 General properties of O'Raifeartaigh-type models

In this section we define O'Raifeartaigh-type models and study general features of them. The discussion consists mostly of a review of Refs. [38, 39, 25].

## 4.1 The existence of pseudo-moduli

Here we define O'Raifeartaigh-type models (we often call them just O'Raifeartaigh models) and see that there is always a tree-level flat direction called pseudo-moduli. O'Raifeartaigh models are defined as theories of chiral superfields $\phi_i$ with a general super potential,

$$W = f_i\phi_i + \frac{1}{2}m_{ij}\phi_i\phi_j + \frac{1}{6}\lambda_{ijk}\phi_i\phi_j\phi_k. \tag{4.1}$$

Kähler potential is assumed to be canonical. The tree-level scalar potential is

$$V = \sum_i |W_i|^2, \tag{4.2}$$

where $W_i = \partial W/\partial\phi_i$. SUSY breaking requires $V > 0$, so at least one $W_i$ must be nonzero for some $\phi_i$. It is well known that there is a massless fermion called the goldstino at a SUSY-breaking vacuum. We can easily see the existence from Eq. (4.2). If $V$ has an extremum,

$$\partial_i V = W_{ij}W_j^* = 0, \tag{4.3}$$

is satisfied for some $\phi_i$, say $\phi_i = \phi_i^{(0)}$, which means matrix $W_{ij}$ has an zero eigenvalue if SUSY is broken. Since the matrix $W_{ij}$ is equivalent to the fermion mass matrix $(\mathcal{M}_F)_{ij}$, the zero-eigenvalue corresponds to the massless fermion, which is the goldstino. The corresponding zero-eigenvector is, as we see from Eq. (4.3), $W_j^*$.

### KS-lemma

From this simple set-up, an interesting lemma follows; in any SUSY-breaking vacuum of O'Raifeartaigh model, if there is a massless fermion at tree-level, then its scalar partner must also be massless at tree-level.

Let us follow the proof in Ref. [39]. The tree level boson mass-squared matrix is

$$\mathcal{M}_B^2 = \begin{pmatrix} \mathcal{M}_F^*\mathcal{M}_F & \mathcal{F}^* \\ \mathcal{F} & \mathcal{M}_F\mathcal{M}_F^* \end{pmatrix}, \tag{4.4}$$

where

$$\mathcal{F}_{ij} \equiv W_k^* W_{ijk} \tag{4.5}$$

is the effect of SUSY breaking. The sketch of the proof is to show that the $\mathcal{M}_B$ has always a zero-eigenvalue if there is a massless fermion. Suppose $\mathcal{M}_F$ has a zero eigenvector $v$ at some field configuration $\phi_i = \phi_i^{(0)}$,

$$(\mathcal{M}_F)_{ij}v_j = W_{ij}v_j = 0, \tag{4.6}$$

where $W_{ij}$ is evaluated at $\phi_i = \phi_i^{(0)}$. At SUSY-breaking vacuum, $v$ can be identified as goldstino and, according to Eq. (4.3), we can write $v_i = W_i^*$. Along its scalar partner direction $(v, v^*)$, the boson mass term is evaluated as

$$\begin{pmatrix} v \\ v^* \end{pmatrix}^\dagger \mathcal{M}_B^2 \begin{pmatrix} v \\ v^* \end{pmatrix} = \begin{pmatrix} v \\ v^* \end{pmatrix}^\dagger \begin{pmatrix} \mathcal{M}_F^* \mathcal{M}_F & \mathcal{F}^* \\ \mathcal{F} & \mathcal{M}_F \mathcal{M}_F^* \end{pmatrix} \begin{pmatrix} v \\ v^* \end{pmatrix} = v_i \mathcal{F}_{ij} v_j + \text{h.c.}, \tag{4.7}$$

where again all derivatives of $W$ is evaluated at $\phi_i = \phi_i^{(0)}$. For positive semi-definite $\mathcal{M}_B^2$, this must vanish, since otherwise we could make it negative by rotating the phase of $v$. Then, $(v, v^*)$ is a null eigenvector of $\mathcal{M}_B^2$. Therefore there is a massless boson at the vacuum $\phi_i = \phi_i^{(0)}$, and this completes the proof.

**Existence of pseudo-moduli space**

The lemma immediately leads the existence of pseudo-moduli space: the tree-level flat direction. Consider a SUSY-breaking vacuum at $\phi_i = \phi_i^{(0)}$ and shift the field value toward the massless direction $v$. At a SUSY-breaking vacuum, $v$ can be identified as goldstino, and $v_i = W_i^* = F_i$,

$$\phi_i = \phi_i^{(0)} + z F_i, \tag{4.8}$$

where $z \in \mathbb{C}$ is any complex number and $F_i$ is the $F$-term expectation value of the field $\phi_i$. As we can see below, along the pseudo-moduli direction, the $F$-term and so the tree-level potential does not change.

To see the above statement, let us utilize the argument below Eq. (4.7). If there is no tachyon at $\phi_i = \phi_i^{(0)}$, the right side of Eq. (4.7) should be vanish, which means

$$\mathcal{F}_{ij} v_j = 0. \tag{4.9}$$

For $v_i = W_i^*$, this identity can be rewritten as

$$W_{ijk} W_j^* W_k^* = 0. \tag{4.10}$$

Let us now evaluate the $F$-term at $\phi_i = \phi_i^{(0)} + z F_i$,

$$\begin{aligned} W_i(\phi_i = \phi_i^{(0)} + z F_i) &= W_i + W_{ij}(z F_j) + \frac{1}{2} W_{ijk}(z F_j)(z F_k) \\ &= W_i + z W_{ij} W_j^* + \frac{1}{2} z^2 W_{ijk} W_j * W_k^* \\ &= W_i(\phi = \phi_i^{(0)}), \end{aligned} \tag{4.11}$$

where we used Eqs. (4.3) and (4.10). All derivatives of $W$ other than the most left side one are again assumed to be evaluated at the SUSY-breaking vacuum $\phi_i = \phi_i^{(0)}$. We see that the scalar potential is flat along the pseudo-moduli direction parameterized by $F_i$.

Here after, we denote the pseudo-moduli direction as $S$, and write the superpotential as

$$W = S(f + \frac{1}{2}\lambda_{ab}\varphi_a\varphi_b) + \frac{1}{2}m_{ab}\varphi_a\varphi_b + \frac{1}{6}\lambda_{abc}\varphi_a\varphi_b\varphi_c. \tag{4.12}$$

The fields $\varphi_a$ represent the directions orthogonal to $S$.

**One-loop lifting of pseudo-moduli**

We saw that there is always a degenerate, SUSY-breaking vacua in O'Raifeartaigh models. The tree-level flat direction is, however, in general lifted once the quantum corrections are taken into account. This is why the flat direction is called "pseudo"-moduli. The leading correction to the potential for the pseudo-moduli can be calculated using the one-loop correction to the vacuum energy,

$$\begin{aligned} V_{\rm eff}^{(1)} &= \frac{1}{64\pi^2}{\rm STr}\mathcal{M}^4 \log\frac{\mathcal{M}^2}{\Lambda^2} \\ &= \frac{1}{64\pi^2}\left({\rm Tr}\ \mathcal{M}_B^4 \log\frac{\mathcal{M}_B^2}{\Lambda^2} - {\rm Tr}\ \mathcal{M}_F^4 \log\frac{\mathcal{M}_F^2}{\Lambda^2}\right), \end{aligned} \tag{4.13}$$

where $\mathcal{M}_B^2$ and $\mathcal{M}_F^2$ are the tree-level boson and fermion mass matrices, as functions of the expectation value of the pseudo-moduli. The UV cutoff $\Lambda$ can be absorbed into the renormalization of the coupling constants appearing in the tree-level vacuum energy.

The pseudo-moduli is stabilized at somewhere along the tree-level flat direction by the Coleman-Weinberg potential in Eq. (4.13). Although the pseudo-moduli gets mass from the quantum corrections, it is often much lighter than the SUSY-breaking scale, $\sqrt{F}$, and is long-lived, which potentially affects the thermal history of the Universe.

## 4.2 SUSY breaking at a meta-stable vacuum

As mentioned in the beginning of part II, SUSY breaking at a meta-stable vacuum is suggested from the viewpoint of model building of DSB. There are also two hints from phenomenological considerations which imply meta-stable SUSY breaking. One is closely connected to the $R$-symmetry, and the other is relevant to the vacuum structure of the SUSY-breaking models.

### 4.2.1 $R$-symmetry and SUSY-breaking

There is a strong constraint from $R$-symmetry for SUSY to be broken. As found in Ref. [34], SUSY is broken if and only if there is an $R$-symmetry. Also, according to Ref. [35], there is broken SUSY in a meta-stable state if and only if there is an approximate $R$-symmetry. For building realistic models, an unbroken $R$-symmetry is problematic since it forbid Majorana gaugino masses. Then, to realize broken SUSY and non-zero gaugino mass simultaneously, meta-stable SUSY breaking is a realistic solution. Let us confirm the statement that the existence of an $R$-symmety is a necessary condition for SUSY breaking.

**Proof**

Consider a generic theory with chiral superfields $\phi_i$ with $i = 1, ..., n$. If SUSY is broken, we cannot solve all the equations

$$\partial_i W(\phi) = 0 \qquad \text{for all} \quad i = 1, ..., n. \tag{4.14}$$

If $W$ is a generic superpotential, however, Eq. (4.14) involves $n$ equations for $n$ quantities $\phi_i$, so generally they can all be solved.

Even if there is a global non-$R$ symmetry, the situation does not change. For example, consider there is a non-$R$ U(1) symmetry with charges $Q(\phi_i) = q_i$. Then, the superpotential can be rewritten by $n - 1$ independent quantities as

$$W = W(X_j), \tag{4.15}$$

where

$$X_j \quad = \quad \phi_j \ \phi_1^{-q_j/q_1} \qquad \text{for} \quad j = 2, ..., n, \tag{4.16}$$

which is neutral under the U(1) symmetry, $Q(X_j) = q_j + (-q_j/q_1)q_1 = 0$. The equation

$$\frac{\partial W(X_i)}{\partial \phi_1} = 0 \tag{4.17}$$

is always satisfied, and

$$\frac{\partial W(X_j)}{\partial X_j} = 0 \tag{4.18}$$

give $n - 1$ equations for $n - 1$ quantities, so again they can all be solved.

In contrast, if there is an $R$-symmetry, since the superpotential carries charge 2 under an $R$-symmetry, $W$ is rewritten as

$$W = \Phi_1 \ f(\Phi_j), \tag{4.19}$$

where

$$\Phi_1 = \phi_1^{2/r_1}, \tag{4.20}$$

$$\Phi_j = \phi_j \, \phi_1^{-r_j/r_1} \quad \text{for} \quad j = 2, ..., n, \tag{4.21}$$

with $r_1 \neq 0$. In this case, for SUSY to be unbroken, the $n$ equations

$$f(\Phi_j) = 0 \tag{4.22}$$

and

$$\frac{\partial f(\Phi_j)}{\partial \Phi_j} = 0 \tag{4.23}$$

must be satisfied. They are $n$ equations for $n-1$ independent quantities, so generally they cannot be solved.

There is, however, an exception when a solution with $\Phi_1 = 0$ and therefore $\phi_1 = 0$ is allowed. This is the case when $r_1 = 2$ and all other $r_j = 0$. In this case, the condition $\partial W/\partial \Phi_j = 0$ can be always satisfied with $\Phi_1 = 0$, and there is a $n-2$ dimensional space of supersymmetric vacua at $\Phi_1 = 0$, $f(\Phi_j) = 0$. Later we see this phenomenon in the model of section 5.2.

**An approximate $R$-symmetry and SUSY-breaking at meta-stable state**

We see that the an $R$-symmetry is an essential ingredient for broken SUSY. Although the argument above is restricted to an exact $R$-symmetry, as discussed in detail in Ref. [35], the argument can be extended to models which have an approximate $R$-symmetry. They consider a theory with exact $R$-symmetry, and slightly deform it by a superpotential of the form

$$\delta W = \epsilon g(\phi_i), \tag{4.24}$$

where $\epsilon$ is a small parameter and this deformation breaks the $R$-symmetry. Although SUSY is restored by the deformation, they expect that the SUSY-breaking vacuum which exists for $\epsilon = 0$ is not affected by the small deformation, remaining the vacuum as a local, meta-stable state. In section 5.1, we see in a explicit example of meta-stable SUSY breaking with an approximate $R$-symmetry. Since an exact $R$-symmetry forbid the Majorana gaugino mass term, a realistic model is suggested to have an approximate $R$-symmetry and a meta-stable SUSY-breaking vacuum.

### 4.2.2 Vacuum structure and the gaugino mass

A broken $R$-symmetry is a necessary condition to obtain a sizable gaugino mass, but it is not a sufficient condition. As shown in Ref. [39], the size of the gaugino mass is closely related to the global structure of the pseudo-moduli space. The lemma in Ref. [39] says that if the pseudo-moduli space represented by $S$ is locally stable everywhere, in other words there is no tachyonic direction at any $S$, the determinant of the matrix $(\lambda S + m)$ is a constant,

$$\det(\lambda S + m) = \det m, \tag{4.25}$$

where $\lambda$ and $m$ are defined in Eq. (4.12), so $(\lambda S + m)$ is a mass matrix for the fields $\varphi_a$ which parameterize the directions orthogonal to $S$.

This has a crucial impact on models of gauge mediation where the SUSY-breaking sector is described by O'Raifeartaigh models, such as models of direct gauge mediation [42, 43, 44, 45, 46, 47, 48]. In such models, a subset of global symmetries is identified as the SM gauge group, and the fields $\varphi_a$ play a role of messenger fields. Since the formula for the gaugino mass at leading order in SUSY breaking is [49, 50]

$$\begin{aligned} m_\lambda &\sim f^\dagger \frac{\partial}{\partial S} \log \mathcal{M}_{messengers} \\ &\sim f^\dagger \frac{\partial}{\partial S} \log \det(\lambda S + m), \end{aligned} \tag{4.26}$$

if the determinant $\det(\lambda S + m)$ is constant, gauginos become massless at least at the leading orders in SUSY breaking, at the vacuum. Since there is no such cancellation for the sermon masses, this generally implies that gauginos are much lighter than the sfermions in such models. The connection between the gaugino mass and the structure of the pseudo-moduli space is further examined in Refs. [40, 41].

#### Proof

Let us prove the lemma by contradiction. Suppose that the determinant $\det(\lambda S + m)$ has $S$ dependence; then it can be written as a polynomial in $S$,

$$\det(\lambda S + m) = \sum c_i(\lambda, m) S^i, \tag{4.27}$$

there must be some place, say $S = S_0$, in the complex $S$ plane where it vanishes,

$$\det(\lambda S_0 + m) = 0. \tag{4.28}$$

This means that the matrix $(\lambda S_0 + m)$ has at least one null eigenvalue. The corresponding eigenvector $v$ annihilate the matrix,

$$(\lambda S_0 + m)v = 0. \tag{4.29}$$

This corresponds to a massless fermion direction. Then, from the KS-lemma proved in subsection 4.1, there exists a massless boson $(v, v^*)$ or there is a tachyon at $S = S_0$. If there is a massless boson,

$$\mathcal{M}_B^2 \begin{pmatrix} v \\ v^* \end{pmatrix} = \begin{pmatrix} \mathcal{M}_F^* \mathcal{M}_F & \mathcal{F}^* \\ \mathcal{F} & \mathcal{M}_F \mathcal{M}_F^* \end{pmatrix} \begin{pmatrix} v \\ v^* \end{pmatrix} = 0, \tag{4.30}$$

where SUSY / SUSY-breaking mass matrices are evaluated at $S = S_0$. This implies

$$\mathcal{F}_{ab} v_b = (W_i^* W_{abi}) v_b = (f^* \lambda_{ab}) v_b = 0, \tag{4.31}$$

where we have used a superpotential of the form in Eq. (4.12). From Eq. (4.29) and Eq. (4.31), we see that $\lambda v = mv = 0$, which contradicts the assumption that $\det(\lambda S + m)$ is not identically zero. Therefore, there must be a tachyonic direction at $S = S_0$, but this contradicts the assumption that the pseudo-moduli space is stable everywhere. So the determinant $\det(\lambda S + m)$ cannot have $S$ dependence if the pseudo-moduli space is stable everywhere. This proves the desired result. The pseudo-moduli space must have a tachyonic direction at some point $(S = S_0)$ if the determinant has a $S$ dependence.

**Meta-stable SUSY-breaking at tree-level**

The lemma implies that models of tree-level SUSY-breaking is not useful for gauge mediation. Note here that "tree-level SUSY-breaking" is defined as a phenomenon that SUSY is broken at minima of tree-level potential, and the pseudo-moduli space is locally stable everywhere. Such a situation is realized in, for example, the ISS model [33]. There, SUSY is broken at tree-level in a low-energy description. Since SUSY is only recovered by a non-perturbative effects of the strong gauge interactions, the SUSY-breaking pseudo-moduli space are meta-stable but do not have any tachyonic directions. In accord with this vacuum structure, the gaugino mass is observed to be vanish in the ISS model even if the pseudo-moduli is stabilized at a non-$R$-symmetric point.

On the other hand, it is still possible that SUSY is broken along the pseudo-moduli, but there is a tachyonic direction at some point along the pseudo-moduli space. In such a model, if the pseudo-moduli is stabilized at an $R$-symmetry breaking and non-tachyonic point by the quantum corrections, it can serve as a realistic model of SUSY breaking which generates

a sizable gaugino mass. The SUSY breaking vacuum is then inevitably an excited state. Therefore, also from the argument of the vacuum structure, SUSY is suggested to be broken at a meta-stable vacuum.

# 5 Examples of low-energy SUSY breaking models

We present several examples of O'Raifeartaigh type models of SUSY breaking. The aim is to confirm general features of O'Raifeartaigh models proved above in concrete models. We see the existence of tree-level flat direction (pseudo-moduli space) and also the connections between the $R$-symmetry and the SUSY-breaking, and also between the gaugino mass and the structure of the pseudo-moduli space.

## 5.1 The basic O'Raifeartaigh model

First example is the basic O'Raifeartaigh model [37] which contains three chiral superfields $S$, $\phi_1$ and $\phi_2$,

$$W = fS + \frac{1}{2}\lambda S\phi_1^2 + m\phi_1\phi_2. \tag{5.1}$$

The model has an $R$-symmetry with $R(S) = R(\phi_2) = 2$ and $R(\phi_1) = 0$. So we expect SUSY to be broken at tree-level. The tree-level scalar potential is

$$\begin{aligned} V &= \left|\frac{\partial W}{\partial S}\right|^2 + \left|\frac{\partial W}{\partial \phi_1}\right|^2 + \left|\frac{\partial W}{\partial \phi_2}\right|^2 \\ &= |f + \frac{1}{2}\lambda\phi_1^2|^2 + |\lambda S\phi_1 + m\phi_2|^2 + |m\phi_1|^2 . \end{aligned} \tag{5.2}$$

The structure of the vacuum depends on the parameter

$$y = \left|\frac{\lambda f}{m^2}\right|. \tag{5.3}$$

We focus on the case $y < 1$ for simplicity. At $\phi_1 = \phi_2 = 0$ and arbitrary $S$,

$$V = |f|^2 > 0 \tag{5.4}$$

and SUSY is indeed broken. There is a flat direction along $S$, which is the pseudo-moduli space. We show the structure of the vacuum in the $\phi_2 = 0$ direction in Fig. 6. We can check that the pseudo-moduli space is locally stable everywhere. The lemma showed in subsection 4.2 then says that the determinant of the mass matrix for the fields orthogonal to

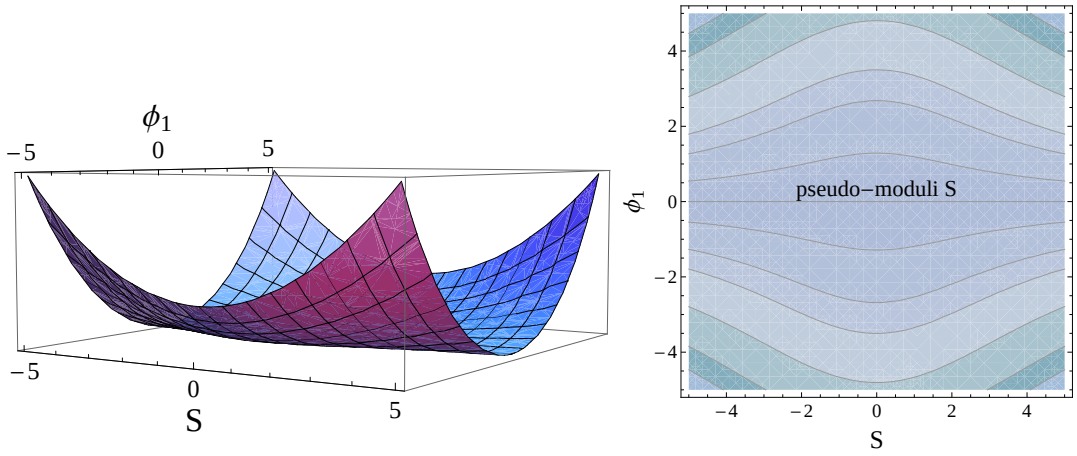


Figure 6: Vacuum structure of the basic O'Raifeartaigh model.

$S$, i.e., fields $\phi_1$ and $\phi_2$, is constant along the pseudo-moduli space. Calculating the fermion mass matrix from the superpotential,

$$(\mathcal{M}_F)_{ij} = W_{ij} = \begin{pmatrix} \lambda S & m \\ m & 0 \end{pmatrix}, \tag{5.5}$$

we see that $\det \mathcal{M}$ is actually constant for arbitrary $S$. So even if fields $\phi_1$ and $\phi_2$ are charged under the Standard Model gauge groups, we cannot get a sizable gaugino mass from this SUSY breaking model.

**Deformation by $R$-symmetry breaking operators**

The basic O'Raifeartaigh model of Eq. (5.1) has an exact $R$-symmetry and it exhibits tree-level SUSY breaking. Let us deform the model with a small parameter $\epsilon$ to break the $R$-symmetry and examine the vacuum structure. We expect the modified model has a meta-stable SUSY-breaking vacuum as in the discussion in section 4.2.1.

Consider a model

$$W = fS + \frac{1}{2}\lambda S\phi_1^2 + m\phi_1\phi_2 + \frac{1}{2}\epsilon m\phi_2^2. \tag{5.6}$$

Since the $R$-symmetry is broken by the last term, there should be a SUSY preserving vacuum according to the argument in section 4.2.1. The scalar potential is

$$V = |f + \frac{1}{2}\lambda\phi_1^2|^2 + |\lambda S\phi_1 + m\phi_2|^2 + |m\phi_1 + \epsilon m\phi_2|^2 . \tag{5.7}$$

Thanks to the $R$-symmetry breaking deformation, we can minimize the potential to zero at two supersymmetric vacua,

$$\langle\phi_1\rangle_{susy} = \pm\sqrt{-2f/\lambda}, \quad \langle\phi_2\rangle_{susy} = \mp\frac{1}{\epsilon}\sqrt{-2f/\lambda}, \quad \langle S\rangle_{susy} = \frac{m}{\lambda\epsilon}. \tag{5.8}$$

Although there are SUSY vacua, for small $\epsilon$ and $y = |\lambda f/m^2| < 1$, the potential near the previous SUSY-breaking minimum $\phi_1 = \phi_2 = 0$ is not modified a lot. It is found that for a parameter region

$$\left|S - \frac{m}{\lambda\epsilon}\right| > \left(\frac{1}{|\epsilon|^2} + 1\right)\left|\frac{f}{\lambda}\right|, \tag{5.9}$$

the $\phi_1$ and $\phi_2$ directions are non-tachyonic along the pseudo-moduli space $S$. Therefore, most of the pseudo-moduli space of the previous model remains locally stable, and the tachyon exists only in a neighborhood of the SUSY vacua [35]. In particular, for small $\epsilon$ and $y < 1$, the region near $S = 0$ is locally stable. This is an explicit example of the models which have an approximate $R$-symmetry and a meta-stable SUSY breaking state. In the deformed model of Eq. (5.6), the fermion mass matrix for $\phi_1$ and $\phi_2$ directions are

$$(\mathcal{M}_F)_{ij} = W_{ij} = \begin{pmatrix} \lambda S & m \\ m & \epsilon m \end{pmatrix}, \tag{5.10}$$

so the determinant $\det\mathcal{M}_F$ depends on the VEV of the pseudo-moduli $S$. This is also consistent with the argument in section 4.2.2 in that the model has tachyon at some point along $S$ and hence $\det\mathcal{M}_F$ has $S$-dependence. The deformed model may serve as a model of gauge mediation.

## 5.2 The minimal gauge mediation

Next we consider a model so called the minimal gauge mediation composed of two chiral fields, $S$ and $\phi$,

$$W = fS - \frac{1}{2}\lambda S\phi^2. \tag{5.11}$$

The model has an $R$-symmetry with $R(S) = 2$ and $R(\phi) = 0$. The tree-level scalar potential is

$$V = |f - \frac{1}{2}\lambda\phi^2|^2 + |\lambda S\phi|^2. \tag{5.12}$$

Since the model has an exact $R$-symmetry, we naively expect broken SUSY. In the present model, however, the scalar potential can be minimized at $S = 0$, and there are SUSY vacua at

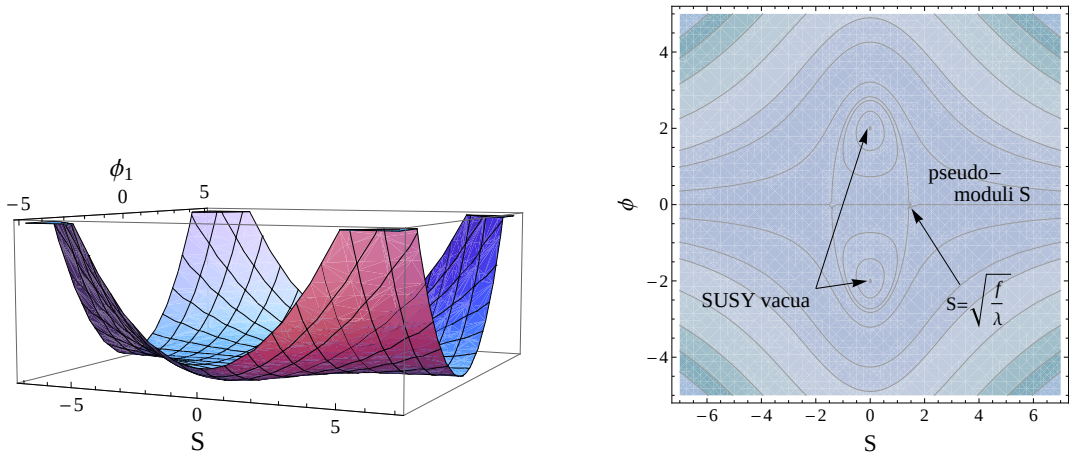


Figure 7: Vacuum structure of the minimal gauge mediation model.

this point. This is the exception of the argument in section 4.2.1 mentioned below Eq. (4.23). As we see from the potential, the model has two supersymmetric vacua at

$$\langle S\rangle_{\rm SUSY} = 0, \quad \langle\phi\rangle_{\rm SUSY} = \pm\sqrt{2f/\lambda}. \tag{5.13}$$

So the model does not break SUSY at tree-level. However, there is also a SUSY breaking pseudo-moduli space with arbitrary $\langle S\rangle$ and $\langle\phi\rangle = 0$, with $V = |f|^2$. So if $S$ is stabilized at $\langle S\rangle \neq 0$ by some radiative corrections, the model could serve as a model of SUSY breaking. The vacuum structure of the model is in Fig. 7.

Let us examine the mass matrix for the field $\phi$, which is the direction orthogonal to the pseudo-moduli space. The fermion mass is

$$\mathcal{M}_F = W_{\phi\phi} = -\lambda S, \tag{5.14}$$

and the boson squared mass matrix is

$$\mathcal{M}_B = \begin{pmatrix} \lambda^2 S^2 & -\lambda f \\ -\lambda f & \lambda^2 S^2 \end{pmatrix}. \tag{5.15}$$

We see that the pseudo-moduli space has a tachyon for

$$|S| < \sqrt{\frac{f}{\lambda}}. \tag{5.16}$$

Since the model has a tachyon along the pseudo-moduli space, the lemma in section 4.2 is not applicable to this model, namely the fermion mass matrix of $\phi$ direction could have a $S$

dependence, and actually it has as in Eq. (5.14). So if the field $\phi$ has Standard Model gauge charges, gauginos get SUSY-braking masses at leading order in SUSY breaking,

$$m_\lambda = \frac{g^2}{(4\pi)^2} f \frac{\partial}{\partial S} \log \det \mathcal{M} = -\frac{g^2}{(4\pi)^2} \frac{f}{\langle S \rangle}. \tag{5.17}$$

### 5.3 SUSY breaking by rank condition

The last example is a O'Raifeartaigh-type model with global symmetry groups

$$SU(N) \times SU(N_f)_L \times SU(N_f)_R \times U(1)_B \times U(1)' \times U(1)_R, \tag{5.18}$$

with $N_f > N$ and the following matter content

| | $SU(N)$ | $SU(N_f)_L$ | $SU(N_f)_R$ | $U(1)_B$ | $U(1)'$ | $U(1)_R$ |
|---|---|---|---|---|---|---|
| $\Phi$ | $\mathbf{1}$ | $\mathbf{N_f}$ | $\mathbf{N_f}$ | 0 | -2 | 2 |
| $\varphi$ | $\mathbf{N}$ | $\overline{\mathbf{N}}_\mathbf{f}$ | $\mathbf{1}$ | 1 | 1 | 0 |
| $\tilde{\varphi}$ | $\overline{\mathbf{N}}$ | $\mathbf{1}$ | $\overline{\mathbf{N}}_\mathbf{f}$ | $-1$ | 1 | 0 |

The Kähler potential is assumed to be canonical and the superpotential is

$$W = h\mathrm{Tr}\ \varphi\Phi\tilde{\varphi} - h\mu^2\mathrm{Tr}\ \Phi, \tag{5.19}$$

where $h$ is coupling constant and trace is over the global symmetry indices. The first term in Eq. (5.19) is the most general form of superpotential consistent with the global symmetries. The second term in Eq. (5.19) breaks the global symmetries to $SU(N) \times SU(N_f) \times U(1)_B \times U(1)_R$, where the unbroken $SU(N_f)$ is the diagonal subgroup of the original $SU(N_f)_L \times SU(N_f)_R$.

SUSY is broken when at least one of the $F$-component does not vanish, which occurs when $N_f > N$ is satisfied. We treat $\Phi$ as a $N_f \times N_f$ matrix and write it as $\Phi_{ij}$. The $F$-component of $\Phi_{ij}$ is

$$\begin{aligned} -(F_\Phi^\dagger)_{ij} &= \frac{\partial W}{\partial \Phi_{ij}} \\ &= h\varphi_i\tilde{\varphi}_j - h\mu^2\delta_{ij}, \end{aligned} \tag{5.20}$$

where the indices $i$ and $j$ are for the global symmetries $SU(N_f)_L$ and $SU(N_f)_R$. This is an $N_f \times N_f$ matrix relation. Since $N_f > N$, the first term is a matrix of rank $N$. So the $F$-term cannot be simultaneously set to zero, and SUSY is broken.

The minimum of the potential is

$$V = (N_f - N)|h\mu^2|^2 \tag{5.21}$$

and it occurs along the pseudo-moduli space

$$\Phi = \begin{pmatrix} 0 & 0 \\ 0 & \Phi_0 \end{pmatrix}, \quad \varphi = \begin{pmatrix} \varphi_0 \\ 0 \end{pmatrix}, \quad \tilde{\varphi} = \begin{pmatrix} \tilde{\varphi}_0 \\ 0 \end{pmatrix}, \quad \text{with} \ \ \varphi_0\tilde{\varphi}_0 = \mu^2 \mathbb{1}_N. \tag{5.22}$$

Here $\Phi_0$ is an arbitrary $(N_f - N) \times (N_f - N)$ matrix, and $\varphi_0$ and $\tilde{\varphi}$ are $N \times N$ matrices. Since SUSY is broken by the VEV of the $F$-component of $\Phi_0$, $F^\dagger_{\Phi_0} = h\mu^2 \mathbb{1}_{N_f - N}$, the massless goldstino comes from the fermionic component of $\Phi_0$.

The symmetry enhanced point is

$$\Phi_0 = 0, \quad \varphi_0 = \tilde{\varphi}_0 = \mu \mathbb{1}_N, \tag{5.23}$$

where an unbroken $SU(N) \times SU(N_f - N) \times U(1)_{B'} \times U(1)_R$ is preserved. It turns out that the symmetry enhanced point is stabilized by one-loop effective potential [33], so we expand the theories around the point, and again see the connection between the stability of the pseudo-moduli space and the gaugino mass. As one can see that the pseudo-moduli space is locally stable everywhere in the model, we expect that the gaugino mass vanishes at the leading order in SUSY breaking according to the lemma showed in subsection 4.2. We parameterize the fluctuations around this vacuum to be

$$\Phi = \begin{pmatrix} Y & Z \\ \tilde{Z} & \hat{\Phi} \end{pmatrix}, \quad \varphi = \begin{pmatrix} \chi \\ \rho \end{pmatrix}, \quad \tilde{\varphi} = \begin{pmatrix} \tilde{\chi} \\ \tilde{\rho} \end{pmatrix}, \tag{5.24}$$

where $\hat{\Phi}$ is a $(N_f - N) \times (N_f - N)$ matrix, and $\rho$, $\tilde{\rho}$ are $N \times (N_f - N)$ matrices.

If the size of the global symmetries are $N \geq 5$ or $N_f - N \geq 5$, we can embed the SM gauge group $SU(3) \times SU(2) \times U(1)$ into the $SU(N)$ or $SU(N_f - N)$, respectively. Then, the model can serve as a model of direct gauge mediation once we gauge the global symmetry $SU(N)$ or $SU(N_f - N)$. Since the fields $\rho$ and $\tilde{\rho}$ carry quantum numbers of both $SU(N)$ and $SU(N_f - N)$ and couple to $\hat{\Phi}$ which has a non-vanishing $F$-component, they play a role of the messenger fields. The relevant superpotential is

$$W = h\rho\hat{\Phi}\tilde{\rho} + h\mu(\rho\tilde{Z} + \tilde{\rho}Z). \tag{5.25}$$

In a matrix notation,

$$W = h \ (\rho, Z) \ \mathcal{M} \ \begin{pmatrix} \tilde{\rho} \\ \tilde{Z} \end{pmatrix}, \tag{5.26}$$

where the mass matrix for the messenger fields is written as

$$\mathcal{M} = \begin{pmatrix} \hat{\Phi} & \mu \\ \mu & 0 \end{pmatrix}. \tag{5.27}$$

The determinant of the mass matrix is constant. Then, as we can see from Eq. (4.26), the gaugino mass is zero at leading order in SUSY breaking. The results is consistent with the lemma of subsection 4.2.

In Ref. [33], it was shown that a supersymmetric QCD model with massive vector-like matters exhibits DSB at a meta-stable vacuum. The model turns out to reduce at low-energy to the model of Eq. (5.19) with the $SU(N)$ symmetry promoted to a gauge symmetry. Once the $SU(N)$ becomes a gauge symmetry, the $R$-symmetry becomes only an approximate one and a supersymmetric ground state appears far from the origin of the field space. The previous SUSY-breaking vacuum in Eq. (5.23) (ISS vacuum) then becomes a meta-stable state. Although it is meta-stable, the pseudo-moduli space parameterized by $\Phi$ is locally stable everywhere, so the gaugino mass is still identical to zero at the ISS vacuum.

### 5.4 Gravitational gauge mediation

Finally, we study a low-energy effective theory of O'Raifeartaigh type SUSY breaking model. It is a modified model of minimal gauge mediation presented in section 5.2, where the SUSY breaking pseudo-moduli space exists along the $S$ direction. The minimal gauge mediation model is phenomenologically favorable in that it can create a sizable gaugino mass. However, we should modify it and stabilize the pseudo-moduli at $S \neq 0$ in some way to use it as a complete model; we cannot integrate out the messenger fields at $S = 0$, and it is also a tachyonic region in the minimal gauge mediation model.

The model of interest is the following [51],

$$K = f^\dagger f + \bar{f}^\dagger \bar{f} + S^\dagger S - \frac{(S^\dagger S)^2}{\Lambda^2} + \cdots , \tag{5.28}$$

$$W = m^2 S - \lambda S f \bar{f} + c, \tag{5.29}$$

where $S$ is a pseudo-moduli as usual, and we have two chiral superfields $f$ and $\bar{f}$ which act as messengers in GMSB. We take the messengers to transform as $\mathbf{5}$ and $\bar{\mathbf{5}}$ under SU(5), and the messenger number $N = 1$ for simplicity. The model includes radiative corrections in the Kähler potential. $\Lambda$ represents a cutoff scale of the model, which is typically a mass of heavy fields we have implicitly integrated out already.

The $R$-symmetry with $R(S) = 2$ and $R(f\bar{f}) = 0$ is explicitly broken by the supergravity corrections represented by the constant term $c$. Since the $R$-symmetry breaking is only through the supergravity corrections, we expect SUSY-breaking at a meta-stable state. There

is a quantum correction to the Kähler potential from the interaction term $\lambda S f \bar{f}$,

$$K_{1-\text{loop}} = -\frac{5\lambda^2}{(4\pi)^2} S^\dagger S \log \frac{S^\dagger S}{\Lambda^2}, \tag{5.30}$$

at the one-loop level. If this radiative correction is too large, the SUSY breaking vacuum turns out to be destabilize. So the messenger coupling $\lambda$ is bounded above.

**Vacuum structure**

Including the supergravity corrections, the scalar potential is calculated by [36]

$$V = e^G (G_S G_{S^\dagger} G^{SS^\dagger} + G_f G_{f^\dagger} + G_{\bar{f}} G_{\bar{f}^\dagger} - 3) + \frac{1}{2} D^2, \tag{5.31}$$

where $G \equiv K + \log |W|^2$ in a Planck unit. $G_X$ is the derivative of $G$ with respect to the field $X$, and $G^{SS^\dagger}$ is the inverse of the Kähler metric. The last term represents the $D$-term contribution. The dominant terms are

$$\begin{aligned} V = &- \frac{2}{\sqrt{3}} \frac{m^4}{M_{\text{pl}}} (S + S^\dagger) + 4 \frac{m^4}{\Lambda^2} |S|^2 \\ &- \lambda m^2 (f \bar{f} + f^\dagger \bar{f}^\dagger) + \lambda^2 |S|^2 (|f|^2 + |\bar{f}|^2) + \lambda^2 |f|^2 |\bar{f}|^2 + \frac{5\lambda^2}{(4\pi)^2} m^4 \log \frac{|S|^2}{\Lambda^2}. \end{aligned} \tag{5.32}$$

We see that there is a pseudo-moduli space at $f = \bar{f} = 0$ with an arbitrary $S$ as it was in the minimal gauge mediation model, but in this model $S$ is stabilized at $S \neq 0$ by the radiative corrections and the supergravity corrections,

$$\langle S \rangle = \frac{\sqrt{3}}{6} \frac{\Lambda^2}{M_{\text{pl}}}, \quad \langle f \rangle = \langle \bar{f} \rangle = 0, \tag{5.33}$$

where $M_{\text{pl}} \simeq 2.4 \times 10^{18}\text{GeV}$ is the reduced Planck scale. We take the VEV to be real and positive by redefining the fields by using the $\text{U}(1)_R$ symmetry. There is also a SUSY preserving vacuum at

$$\langle S \rangle_{\text{SUSY}} = 0, \quad \langle f \rangle_{\text{SUSY}} = \langle \bar{f} \rangle_{\text{SUSY}} = \sqrt{\frac{m^2}{\lambda}}, \tag{5.34}$$

so the SUSY-breaking vacuum (5.33) is a meta-stable state. The messenger directions are tachyonic for

$$|S| < S_{\text{rc}} \equiv \sqrt{\frac{m^2}{\lambda}}. \tag{5.35}$$

Therefore, in order to realize meta-stable SUSY breaking in this model, we have to take care for $S$ not to enter this dangerous region along the cosmological evolution. We mention this point again in the next section.

So far we have neglected the radiative correction (5.30), which could destabilize the SUSY breaking vacuum. In order to see its effect, let us study the mass terms of the $S$ field and the messenger fields ( we take $f = \bar{f}$), including the correction:

$$V_{\rm mass} = (S^\dagger \ S)\mathcal{M}_S^2 \begin{pmatrix} S \\ S^\dagger \end{pmatrix} + (f^\dagger \ f)\mathcal{M}_f^2 \begin{pmatrix} f \\ f^\dagger \end{pmatrix}, \tag{5.36}$$

$$\mathcal{M}_S^2 \simeq \frac{m^4}{\Lambda^2} \begin{pmatrix} 4 & -\frac{15\lambda^2}{8\pi^2}\frac{M_{pl}^2}{\Lambda^2} \\ -\frac{15\lambda^2}{8\pi^2}\frac{M_{pl}^2}{\Lambda^2} & 4 \end{pmatrix} \ , \tag{5.37}$$

$$\mathcal{M}_f^2 = \begin{pmatrix} \lambda^2\langle S\rangle^2 & -\lambda m^2 \\ -\lambda m^2 & \lambda^2\langle S\rangle^2 \end{pmatrix}, \tag{5.38}$$

where we have fixed the SUSY breaking vacuum as (5.33) for simplicity, and dropped terms proportional to $\lambda^2$ in the diagonal components of $\mathcal{M}_S^2$. In order for the SUSY breaking vacuum to be (meta)stable, The conditions $\det m_S^2 > 0$ and $\det m_f^2 > 0$ must be satisfied, namely,

$$\frac{12m^2 M_{\rm pl}}{\Lambda^4} < \lambda < \frac{4\sqrt{2}\pi}{\sqrt{15}}\frac{\Lambda}{M_{\rm pl}}. \tag{5.39}$$

Note that $\lambda$ is bounded both above and below.

**Independent parameters**

We have three independent parameters in this model: $\lambda, \Lambda, m$. These parameters can be converted to physical quantities, the gravitino mass ($m_{3/2}$), the gaugino mass ($m_{\tilde{g}}$) and the messenger mass scale ($M_{\rm mess}$), using formulae

$$m_{3/2} = \frac{m^2}{\sqrt{3}M_{\rm pl}}, \tag{5.40}$$

$$m_{\tilde{g}} = \frac{\alpha_3}{4\pi}\frac{m^2}{\langle S\rangle}, \tag{5.41}$$

$$M_{\rm mess} = \lambda\langle S\rangle, \tag{5.42}$$

with the VEV relation Eq. (5.33). In the following analysis, we fix the gaugino mass to be 5 TeV to realize the Higgs boson mass $m_h = 125$ GeV, and treat the two parameters $m_{3/2}$ and $M_{\rm mess}$ as independent parameters. For example, the mass of the pseudo-moduli is fixed by the gravitino mass,

$$m_S = \frac{2m^2}{\Lambda} = 756{\rm GeV}\left(\frac{m_{3/2}}{500{\rm MeV}}\right)^{1/2}. \tag{5.43}$$

The constraint (5.39) between $\Lambda$ and $\lambda$ is converted to that between $m_{3/2}$ and $M_{\rm mess}$. We show in Fig. 8 the allowed parameter region where the SUSY breaking vacuum (5.33) is meta-stable.

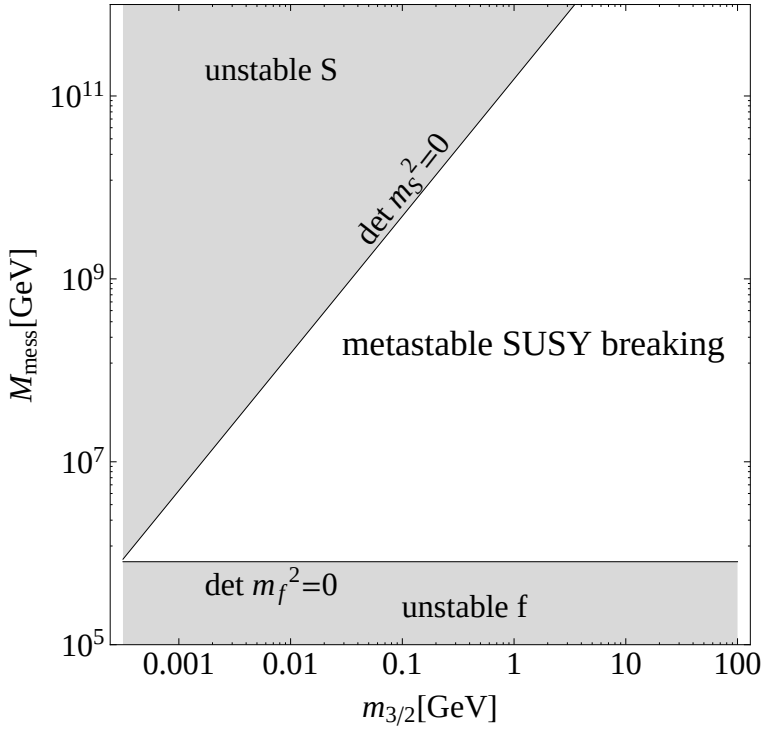


Figure 8: SUSY-breaking state is meta-stable for the white region.

# 6 Cosmological constraints on SUSY breaking sector

In the above two sections, we saw that a realistic model of SUSY breaking is suggested to have a meta-stable non-SUSY vacuum and an approximate $R$-symmetry. These implications come from the viewpoint of model building of DMS, or phenomenological requirements of obtaining sizable gaugino masses. In addition to these, there are also constraints from cosmological considerations which should be satisfied in realistic models of SUSY-breaking. We list those constraints in this section.

## 6.1 Moduli problem

The value of the SUSY-breaking pseudo-moduli $S$ after inflation can be displaced from the minimum due to the deformation of the scalar potential during inflation. If this is the case, $S$ starts coherent oscillation about the minimum and the oscillation energy eventually dominates the energy density of the Universe unless the oscillation amplitude is very small or the lifetime of $S$ is very short. Then, subsequent decays of $S$ may cause a cosmological

disaster.

One sever constraint comes from the study of Big-Ban nucleosynthesis (BBN). If a sizable energy is stored in the SUSY-breaking sector, the energy is released by the decay of $S$ and the entropy density of the Universe is modified significantly [59, 60]. If the lifetime of $S$ is as long as $\mathcal{O}(1)$ sec, the decay occurs in the middle of the nucleosynthesis, which destroys the light elements and spoils the success of the standard BBN scenario.

The decay of $S$ may also cause a problem by the pair production of gravitino. If gravitino is unstable, its subsequent decay is constrained by BBN in a same way to that of the decay of $S$. For a stable gravitino, the abundance is also constrained by the observed amount of dark matter abundance, $\Omega_{\rm DM}h^2 \simeq 0.1$. Non-thermal productions of gravitino from the SUSY-breaking moduli are studied in Refs. [61, 53, 54, 62]. Other than the SUSY-breaking moduli, non-thermal production of gravitino has been examined in the context of the decay of string moduli [63]-[67], and / or inflaton [68]-[72].

For a realistic cosmology, we must check in the SUSY-breaking sector (i) whether oscillation energy of $S$ dominates the energy density of the Universe, and if the domination happens, (ii) that BBN is not spoiled by the decay of $S$ and (iii) that gravitinos are not overproduced.

**Displacement from the minimum during inflation**

Let us see how the $S$ field is displaced from the minimum during inflation. To be concrete, we focus on the model of section 5.4. During inflation, since the inflaton potential largely breaks SUSY, the scalar potential of $S$ is modified through Planck-suppressed couplings. In particular, the $S$ field generically acquires a so-called Hubble-induced mass, and as long as the $\mathrm{U}(1)_R$ remains a good symmetry during inflation, the origin of $S$ is close to the extremum of the potential. If the Hubble-induced mass is positive, therefore, $S$ is stabilized near the origin during inflation, and it likely remains there even after the inflation.

On the other hand, it is also possible that the $S$ field couples to the inflaton sector in a more general manner. For example, $S$ may couple to the inflaton sector through the superpotential [53],

$$W = W_{\rm Inflaton}\left(1 - \xi\frac{\Lambda}{M_{\rm pl}}S + \cdots\right), \tag{6.1}$$

where $\xi$ is a coefficient of $\mathcal{O}(1)$, and $W_{\rm Inflaton}$ denotes the superpotential of the inflaton sector.

The scalar potential of $S$ during inflation is then given by

$$V(S) \simeq 3H^2 \left( |S|^2 - \frac{|S|^4}{\Lambda^4} + \cdots \right) + 3H^2 \left| M_{\rm pl} - \xi \frac{\Lambda}{M_{\rm pl}} S \right|^2 . \tag{6.2}$$

In the above expression, we have used the Hubble equation,

$$H^2 = \frac{|F_{\rm Inflaton}|^2}{3M_{\rm pl}^2}, \tag{6.3}$$

assuming that the $F$-component of the inflaton dominates the energy density during inflation. This potential has a minimum at $S_0 = \mathcal{O}(\Lambda)$.

In both cases, $S$ is displaced from the SUSY-breaking minimum $S = \langle S \rangle$, during inflation. Together with the small mass (remember that $S$ is massless at tree-level and gets mass only through the radiative corrections), it is likely that $S$ starts oscillations about the minimum $\langle S \rangle$ and the oscillation energy eventually dominates the Universe.

## 6.2 Vacuum selection in a model with multiple vacua

In the early Universe after inflation, the MSSM sector is reheated by the decay of inflaton to a very high temperature. In GMSB models, even if the SUSY breaking pseudo-moduli field does not couple to the MSSM field directly, its scalar potential can be modified by thermal corrections through the messenger fields which couple to the MSSM fields through SM gauge interactions. The minimum of the effective potential lies in general at different point than that at zero temperature. Then, if the SUSY breaking sector has multiple vacua at zero temperature, there is no guarantee that the SUSY breaking minimum is selected as the Universe cools down. The vacuum selection in meta-stable SUSY-breaking models has been discussed in the literatures for the ISS-type models [73, 74, 75, 76, 77, 78, 79] and the O'Raifeartaigh-type models [80, 81, 82, 57, 58]. They considered the finite temperature corrections to the scalar potential and followed the location of the minimum along the cooling of the Universe.

The finite temperature effective potential up to one-loop is given by[83, 84]

$$V = V_{\rm tree} + V_1 + V_{\rm thermal}, \tag{6.4}$$

where $V_{\rm tree}$ is the classical potential and $V_1$ is the zero-temperature one-loop potential. Finite

temperature one-loop correction is

$$V_{\rm thermal} = \frac{T^4}{2\pi^2}\left[\int_0^\infty dx x^2 \sum_i \log[1 - e^{-\sqrt{x^2+(M_S^2)_i/T^2}}]\right.$$
$$\left. -2\int_0^\infty dx x^2 \sum_r \log[1 + e^{-\sqrt{x^2+(M_F^2)_r/T^2}}] + 3\int_0^\infty dx x^2 \sum_a \log[1 - e^{-\sqrt{x^2+(M_V^2)_a/T^2}}]\right], \tag{6.5}$$

where the three terms represent the contributions from real scalar fields $\phi_i$, Weyl fermions $\psi_r$ and vector bosons $A_a^\mu$ with the eigenvalues of the squared mass matrices $(M_S^2)_i$, $(M_F^2)_r$ and $(M_V^2)_a$. For a high temperature limit of $T \gg M_S, M_F, M_V$, the potential can be expanded as

$$V_{\rm thermal} = -\frac{\pi^2 T^4}{90}\left(N_B + \frac{7}{8}N_F\right) + \frac{T^2}{24}\left[{\rm Tr}(M_S^2) + 3{\rm Tr}(M_V^2) + {\rm Tr}(M_F^2)\right] + \cdots, \tag{6.6}$$

where, for a supersymmetric model with no gauge groups, the sum of the real scalar / Weyl fermion squared masses is calculated by

$${\rm Tr}(M_S^2) = 2W_{ik}^* W^{ik}, \quad {\rm Tr}(M_F^2) = W_{ik}^* W^{ik}. \tag{6.7}$$

The point is that the minimum of the thermal potential (6.5) lies at the origin of the field space. For example, consider the minimal gauge mediation model in Eq. (5.11). Once the messenger superfield $\phi$ is thermalized, the vacuum energy is corrected by

$$V_{\rm thermal} \simeq \frac{T^2}{24}[2\lambda^2 S^2 + \lambda^2 S^2] = \frac{1}{8}\lambda^2 T^2 S^2, \tag{6.8}$$

which stabilize the pseudo-moduli $S$ at $S = 0$. Therefore, as pointed out in Ref. [74], if the SUSY-breaking vacuum lies near the origin and the SUSY-preserving ground state lies at far from the origin as in the ISS model, the minimum of the potential moves smoothly from the origin to the SUSY-breaking vacuum as the Universe cools down.

In addition to the conventional moduli problem, one should also take care the vacuum selection if SUSY is assumed to be broken at a meta-stable state.

# Part III

# Realization of the gravitino Dark Matter scenario

In part I, we saw a gravitino DM scenario which is compatible with thermal leptogenesis. The scenario is based on the fact that the relic abundance of thermally produced gravitino does not depend on $T_R$ in GMSB, once the temperature of the Universe exceeds the messenger scale. Although the scenario is simple, as described in part II, there are several requirements on SUSY-breaking sector from cosmological consideration which should be met along the thermal history of the Universe. In this part, to make sure that the scenario is actually viable, we demonstrate it with a concrete model of gauge mediation.

The model we use for the cosmological study is the gravitational gravitational gauge mediation presented in section 5.4. As the model exhibit meta-stable SUSY-breaking, we first check that the SUSY-breaking vacuum is preferred to the SUSY-preserving true vacuum. Next we estimate the oscillation energy of $S$ about the minimum, and see that the amount of entropy release is sufficiently large to realize the cosmological scenario.

Throughout our analysis, the SUSY scale is assumed to be $M_{\rm SUSY} \simeq 5$ TeV to realize $m_h = 125$ GeV [3] within the MSSM. Although it sounds difficult to confirm the scenario by the LHC experiments, the framework we use predicts a relatively small $\mu$-term and thus there is a light higgsino with $m_{\tilde{h}} \sim \mathcal{O}(100)$ GeV . We explain this point in appendix C. Such a light higgsino may be within the reach of future experiments such as at an International Linear Collider (ILC). Since the life-time of higgsino can be as long as $O(1)$ sec, we check the constraints from the Big-Bang nucleosynthesis (BBN) and find that the light higgsino is cosmologically safe if the gravitino mass is less than $\sim 500$ MeV.

## 7 Cosmological evolution of pseudo-moduli

In this section we follow cosmological evolution of the pseudo-moduli field and the messenger fields with the SUSY-breaking model presented in section 5.4. The goal is to confirm (i) the SUSY breaking vacuum is selected along the thermal history of the Universe and (ii) a sizable amount of entropy is produced from the decay of $S$.

## 7.1 Vacuum selection

Since the model breaks SUSY at a meta-stable state, we have to check whether the SUSY breaking minimum (5.33) is actually selected in the cosmological evolution. We examine the deformations of the scalar potential by the finite temperature corrections, and see that the minimum of the potential smoothly moves from the origin to the SUSY-breaking vacuum as the Universe cools down.

We assume that the MSSM superfields and the messenger superfields are in thermal equilibrium in the early Universe. Although $S$ superfield is not in thermal plasma, its scalar potential receives thermal corrections due to interactions with the messenger fields. The scalar potential at finite temperature along $f = \bar{f} = 0$ direction is, up to $\mathcal{O}(S^2)$,

$$V_S(T) = -\frac{2}{\sqrt{3}}\frac{m^4}{M_{\rm pl}}(S + S^\dagger) + \frac{4m^4}{\Lambda^2}S^\dagger S + \frac{5\lambda^2 T^2}{4}S^\dagger S, \tag{7.1}$$

where we have used the high temperature approximation in Eq. (6.6). At that time, the potential minimum does not lie at (5.33) but at

$$S_{\rm min}(T) \simeq \frac{\sqrt{3}}{6}\frac{\Lambda^2}{M_{\rm pl}}\frac{m_S^2}{m_S^2 + m_S^{\rm th}(T)^2}, \tag{7.2}$$

where

$$m_S \;=\; \frac{2m^2}{\Lambda} \tag{7.3}$$

is the tree-level mass of $S$ at zero-temperature and

$$m_S^{\rm th}(T) = \frac{\sqrt{5}\lambda T}{2} \tag{7.4}$$

is the thermal mass. We can see from this formula that the potential minimum is near the origin for a high temperature and moves toward the SUSY-breaking one as the temperature decreases.

In the absence of the thermal potential, $S$ would fall into the SUSY-preserving vacuum if $|S| < S_{\rm cr} = \sqrt{m^2/\lambda}$, since the messenger fields become tachyonic. For a sufficiently high temperature, however, $S$ does not fall into the SUSY-preserving vacuum because the thermal effects lift the messenger direction. The messenger fields get thermal potentials through interactions with the standard model gauge bosons, [57, 58],

$$V_{\ell,\bar{\ell}}(T) = \frac{T^2}{16}(3g^2 + g'^2)(|\ell|^2 + |\bar{\ell}|^2), \tag{7.5}$$

$$V_{q,\bar{q}}(T) = \frac{T^2}{16}(8g_s^2 + g'^2)(|q|^2 + |\bar{q}|^2), \tag{7.6}$$

where $\ell(\bar{\ell})$ and $q(\bar{q})$ denote the scalar components of the messenger superfields $f(\bar{f})$. For $T = 0$, the vicinity of $S = 0$ is a dangerous region because the messenger directions are tachyonic (see Eq. (5.35)). However, the messengers are stabilized at $f = \bar{f} = 0$ by the thermal potential for a high temperature and do not fall into the SUSY-preserving true vacuum. The vicinity of $S = 0$ becomes tachyonic only after the temperature of the Universe drops below the critical temperature $T_{\rm cr}$:

$$\begin{aligned} T_{\rm cr} &= 4m\sqrt{\frac{\lambda}{3g+g'^2}} \\ &\simeq 7.1\times 10^6 {\rm GeV}\left(\frac{M_{\rm mess}}{10^7\ {\rm GeV}}\right)^{1/2}\left(\frac{m_{\tilde{g}}}{5\ {\rm TeV}}\right)^{1/2}. \end{aligned} \tag{7.7}$$

We also define a temperature $T_S$ at which the potential minimum of $S$ direction, $S_{\rm min}(T)$, exits the region where the messenger direction is unstable at zero temperature, i.e.,

$$S_{\rm min}(T_S) \equiv S_{\rm cr}, \tag{7.8}$$

which gives

$$T_S^2 \simeq \frac{8\sqrt{3}}{15}\frac{m^3}{\lambda^{3/2}M_{\rm pl}}. \tag{7.9}$$

In terms of $m_{3/2}$ and $M_{\rm mess}$,

$$T_S \simeq 6.5\times 10^8\ {\rm GeV}\left(\frac{m_{3/2}}{500\ {\rm MeV}}\right)^{3/2}\left(\frac{M_{\rm mess}}{10^7\ {\rm GeV}}\right)^{-3/4}\left(\frac{m_{\tilde{g}}}{5\ {\rm TeV}}\right)^{-3/4}. \tag{7.10}$$

In order for the potential minimum to smoothly reach the SUSY-breaking vacuum without straying into the SUSY-preserving one, the condition

$$T_S > T_{\rm cr} \tag{7.11}$$

has to be satisfied*, i.e., $S_{\rm min}(T)$ should leave the dangerous region (the vicinity of $S = 0$) before the messenger direction becomes tachyonic. This condition is converted to a constraint on the model parameters,

$$\lambda < \left[\frac{8\sqrt{3}}{15}\frac{3g^2+g'^2}{16}\frac{m}{M_{\rm pl}}\right]^{2/5}. \tag{7.12}$$

Again in terms of $m_{3/2}$ and $M_{\rm mess}$, the condition put an upper bound on the messenger scale,

$$M_{\rm mess} < 3.7\times 10^8\ {\rm GeV}\left(\frac{m_{3/2}}{500\ {\rm MeV}}\right)^{6/5}\left(\frac{m_{\tilde{g}}}{5\ {\rm TeV}}\right)^{-1}. \tag{7.13}$$

We show the allowed region in Fig. 9. From now on, we focus the discussion on the white region where the the SUSY-breaking vacuum is selected along the thermal history.

*Precisely speaking, this is a sufficient condition, but we have confirmed that this is consistent with the numerical results.

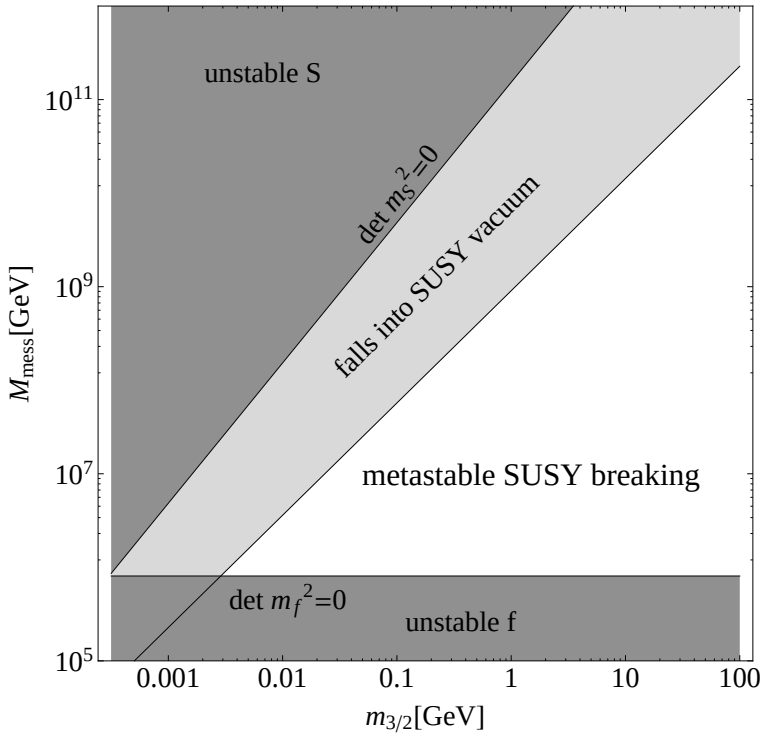


Figure 9: SUSY breaking vacuum is selected in the white region.

### 7.2 Coherent oscillations

Next we estimate the oscillation energy of $S$ by solving the equation of motion of $S$ taking into account the expansion of the Universe. Depending on the initial position of $S$ after inflation, $S$ exhibits different motions in its field space. As mentioned in section 6.1, $S$ is generally displaced from the zero temperature minimum of the potential, $\langle S \rangle$, during inflation. We examine two cases that the initial position of $S$, $S_0$, is at around the origin or the cutoff scale, $S_0 \sim 0$ or $S_0 \sim \Lambda$.

#### 7.2.1 The case with $S_0 \simeq 0$

The evolution of $S$ in this case has been studied in detail in Ref. [55]. We assume that $S$ was stabilized near the origin by the positive Hubble-induced mass term during the inflation. After inflation, the $S$ follows the time-dependent minimum (7.2). When the thermal mass becomes comparable to the tree-level mass, the minimum $S_{\rm min}(T)$ quickly moves to the SUSY

breaking minimum. This transition takes place at $T \simeq T_0$, given by

$$T_0 \equiv \frac{4}{\sqrt{5}} \frac{m^2}{\Lambda\lambda} \tag{7.14}$$

$$\simeq 3.4 \times 10^8 \text{ GeV } \left(\frac{m_{3/2}}{500 \text{ MeV}}\right)^{5/2} \left(\frac{M_{\rm mess}}{10^7 \text{ GeV}}\right)^{-1} \left(\frac{m_{\tilde{g}}}{5 \text{ TeV}}\right)^{-1/2}. \tag{7.15}$$

Whether or not the $S$ field catches up the motion of the minimum depends on the competition between the effective mass of $S$ and the friction caused by the expansion of the Universe. Here it is assumed that the messenger fields remain thermalized at $T = T_0$. Later we study the case where the messenger fields decouple from the thermal plasma before the temperature of the Universe goes down to $T_0$.

The dynamics of $S$ field is governed by the equation of motion

$$\ddot{S} + 3H\dot{S} + \frac{\partial}{\partial S^\dagger} V = 0. \tag{7.16}$$

The effective mass of $S$ field is approximately given by the sum of the tree-level mass and the thermal mass,

$$m_S^2(T) \equiv m_S^2 + \frac{5}{4}\lambda^2 T^2, \tag{7.17}$$

where we have neglected the contribution from the radiative correction to the Kähler potential (5.30), since it does not affect results. In the numerical calculations, the effect of the radiative correction is properly taken into account.

First let us consider the case that the Hubble parameter is larger than the effective mass at $T = T_0$, i.e., $H(T_0) > m_S(T_0)$. In this case, even if the potential minimum moves to the zero temperature value at $T = T_0$, $S$ is still trapped near the origin because of the large friction. At a later time when the Hubble parameter becomes comparable to the effective mass, $H \sim m_S$, $S$ leaves the vicinity of the origin and starts oscillations about the minimum. We define the temperature $T_{\rm osc}$ as

$$H(T_{\rm osc}) = m_S(T_{\rm osc}), \tag{7.18}$$

where the temperature dependence of the Hubble parameter is given by $H(T) \sim \frac{T^2}{M_{\rm pl}}$ as in Eq. (2.3) in the radiation dominated era, and $H(T) \sim \frac{T^4}{M_{\rm pl} T_R^2}$ in the inflaton-matter dominated era, respectively. The condition $H(T_0) > m_S(T_0)$ is equivalent to $T_0 > T_{\rm osc}$. In the scenario presented in section 3, we take the reheating temperature to be very high , say $T_R \gtrsim 10^{13}$ GeV, so that the gravitino dark matter and thermal leptogenesis become compatible. With such a

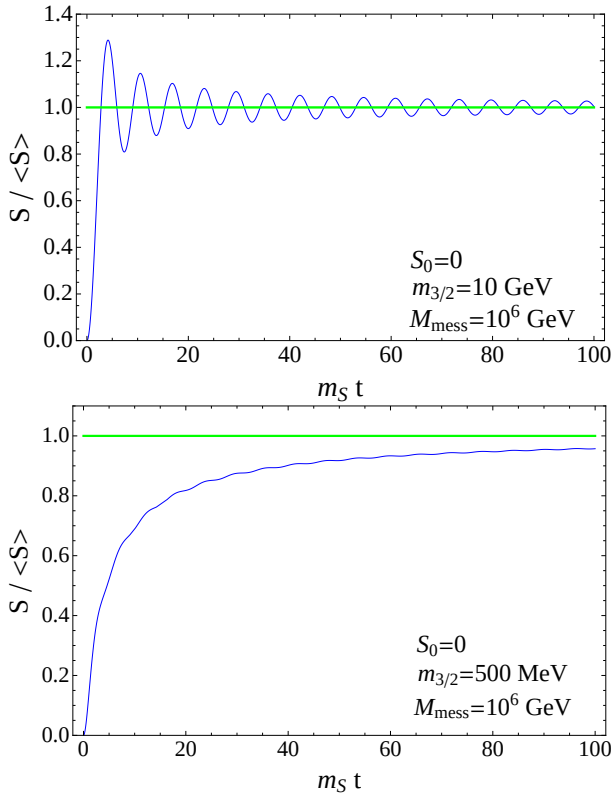


Figure 10: If the Hubble parameter is larger than the effective mass at $T = T_0$, $H(T_0) > m_S(T_0)$, $S$ is trapped to $S \simeq 0$ by a large friction from the expansion of the Universe. Later, $S$ starts oscillation about the minimum when the temperature reaches $T_{\rm osc}$ (upper figure). On the other hand, if $H(T_0) < m_S(T_0)$, $S$ follows the temperature dependent minimum $S_{\rm min}(T)$ and gradually reaches the SUSY-breaking minimum. The oscillation amplitude is suppressed in this case (lower figure).

high reheating temperature, $T_{\rm osc}$ is lower than $T_R$ in most of the parameter region of interest. Then, $T_{\rm osc}$ is

$$T_{\rm osc} \simeq 4.4 \times 10^{10}\ {\rm GeV}\ \left(\frac{m_{3/2}}{15\ {\rm GeV}}\right)^{-1} \left(\frac{M_{\rm mess}}{10^7\ {\rm Gev}}\right) \left(\frac{m_{\tilde{g}}}{5\ {\rm TeV}}\right). \quad (T_0 > T_{\rm osc}) \tag{7.19}$$

On the other hand, if the Hubble parameter is already smaller than the effective mass at $T = T_0$, $H(T_0) < m_S(T_0)$, or equivalently $T_0 < T_{\rm osc}$, the friction from the expansion of the Universe is small. This is the case if $\lambda$ is larger than the previous case. In this case $T_{\rm osc}$ is represented as

$$T_{\rm osc} \simeq 1.0 \times 10^{12}\ {\rm GeV}\ \left(\frac{m_{3/2}}{500\ {\rm MeV}}\right)^{-1} \left(\frac{M_{\rm mess}}{10^7\ {\rm GeV}}\right) \left(\frac{m_{\tilde{g}}}{5\ {\rm TeV}}\right). \quad (T_0 < T_{\rm osc}) \tag{7.20}$$

Then the $S$ field follows the time-dependent potential minimum and gradually reaches the SUSY-breaking vacuum. The amplitude of oscillations is highly suppressed in this case. The

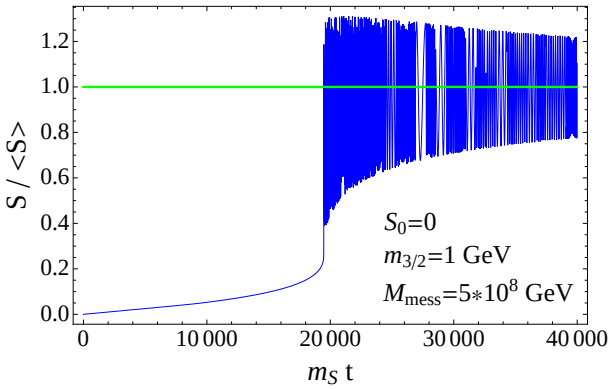


Figure 11: If the messenger fields become non-relativistic before $S$ reaches the SUSY-breaking minimum, $\langle S\rangle$, the potential minimum suddenly moves from $S_{\rm min}(T)$ to $\langle S\rangle$, and oscillations are triggered. This happens when $T_{\rm dec} > T_0$.

suppression was first found in Ref. [85], in which the oscillation amplitude was shown to be exponentially suppressed in a limiting case[†] in the context of the cosmological moduli problem. This adiabatic suppression mechanism was recently examined more carefully in Ref. [86]. We show in Fig. 10 the typical evolution of $S$ in the above two cases.

There is yet another possibility. As the temperature of the Universe decreases and the value of the pseudo-modului becomes sizable, the high temperature approximation in Eq.(7.1) breaks down at a certain point. The messenger fields become non-relativistic when the temperature of the Universe becomes comparable to the messenger mass. Then the finite temperature potential generated by messenger interactions gets suppressed by the Boltzmann factor $\sim e^{-\lambda S/T}$. We define the decoupling temperature $T_{\rm dec}$ as

$$T_{\rm dec} \equiv \lambda S(T = T_{\rm dec}). \tag{7.21}$$

If the messenger fields decouple after $S$ field reaches the SUSY-breaking vacuum, $T_{\rm dec}$ is simply the messenger mass scale,

$$T_{\rm dec} \simeq M_{\rm mess} \quad (T_{\rm dec} < T_0). \tag{7.22}$$

If the decoupling occurs when $S$ is still on the way to the SUSY-breaking vacuum, $T_{\rm dec}$ is

[†] The initial condition adopted in Ref. [85] was given at an infinitely large Hubble parameter. There are various additional contributions in general, which are only power-suppressed [86]. We have numerically confirmed that the pseudo-moduli abundance is power-suppressed in the present scenario.

calculated to be

$$T_{\rm dec} \simeq \left[\frac{8\sqrt{3}}{15}\frac{m^4}{\lambda M_{\rm pl}}\right]^{1/3} \tag{7.23}$$

$$\simeq 4.1\times 10^7\ {\rm GeV}\left(\frac{m_{3/2}}{1\ {\rm GeV}}\right)\left(\frac{M_{\rm mess}}{10^9\ {\rm GeV}}\right)^{-1/3}\left(\frac{m_{\tilde g}}{5\ {\rm TeV}}\right)^{-1/3}, \tag{7.24}$$

for $T_{\rm dec} > T_0$. In this case, at $T = T_{\rm dec}$, the position of the potential minimum instantly moves from $S_{\rm min}(T)$ to the SUSY-breaking vacuum, which triggers coherent oscillations about the minimum (see Fig. 11).

In summary, we have defined three temperatures: $T_0$, $T_{\rm osc}$ and $T_{\rm dec}$.

- The potential minimum quickly moves from the origin to the SUSY-breaking vacuum at $T = T_0$.
- The Hubble parameter $H$ becomes comparable to the pseudo-moduli mass $m_S(T)$ at $T = T_{\rm osc}$.
- The messenger fields become non-relativistic and disappear from the thermal plasma at $T = T_{\rm dec}$.

The evolution of $S$, and therefore, its abundance, sensitively depends on the relations among these temperatures. The following three cases are shown in Fig. 12. The reheating temperature is fixed to be $T_R = 10^{13}$ GeV, and the figure does not change as long as $T_R$ is higher than all of the $T_0$, $T_{\rm osc}$ and $T_{\rm dec}$. Note that the abundance of $S$ is suppressed in the second case (white region), while it is significant in the other cases.

- $T_0 > T_{\rm osc}$ (Green region) ; $S$ starts coherent oscillation about $\langle S\rangle$ at $T = T_{\rm osc}$.
- $T_{\rm osc} > T_0 > T_{\rm dec}$ (White region) ; $S$ follows $S_{\rm min}(T)$ and gradually reaches $\langle S\rangle$ without sizable oscillations.
- $T_{\rm osc} > T_{\rm dec} > T_0$ (Blue region) ; The messenger fields decouple from thermal plasma when $S$ is on the way to $\langle S\rangle$. Coherent oscillations are triggered at $T = T_{\rm dec}$.

### 7.2.2 The case with $S_0 \sim \Lambda$

Next we consider the case where $S$ was displaced at $S_0 \sim \Lambda$ after inflation. This situation may be lead by general interaction between $S$ and the inflaton sector as in Eq. (6.1). The evolution

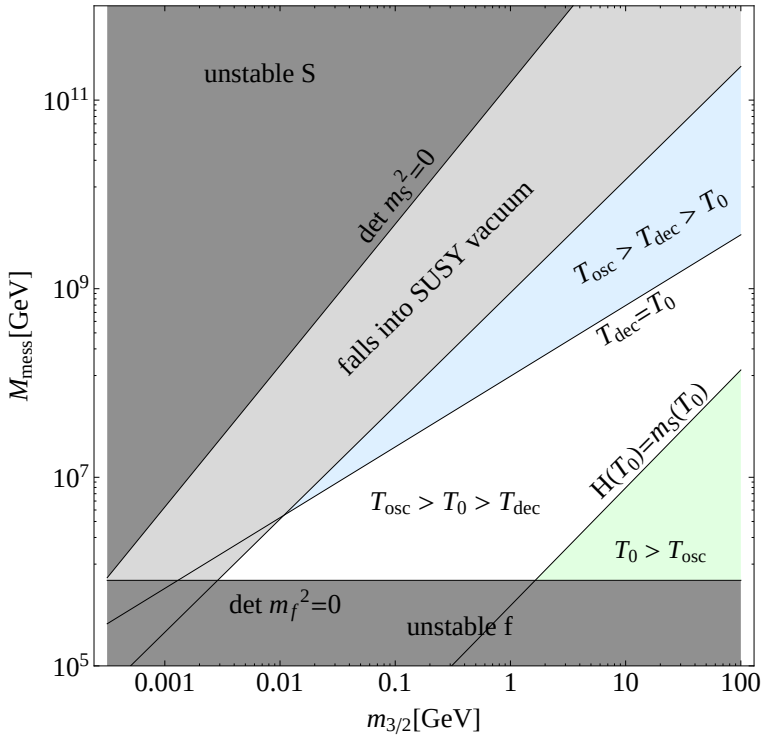


Figure 12: The evolution of $S$ exhibits distinctive behavior depending on the model parameters. In the green region ($T_0 > T_{\rm osc}$), $S$ starts oscillations when $H \approx m_S(T)$. The $S$ abundance is suppressed by the adiabatic suppression mechanism in the white region ($T_{\rm osc} > T_0 > T_{\rm dec}$). In the blue region ($T_{\rm osc} > T_{\rm dec} > T_0$) the coherent oscillations are triggered when the messenger fields disappear from thermal plasma.

in this case was studied in Refs. [53, 54, 56]. In Refs. [53, 54], the reheating temperature is took lower than the messenger scale, so that messenger fields are not thermalized. In this case, initial position of $S$ should have a sizable imaginary part so as not for $S$ to fall into SUSY-preserving minimum. In Ref. [56], on the contrary, the reheating temperature is assumed to be much higher than the messenger scale. Since the present scenario requires a very high $T_R$ to realize the observation, $\Omega_{\rm DM}/\Omega_B \sim 5$, we adopt the initial condition of Ref [56]. In this case, the arguments on vacuum selection in section 7.1 is applicable, so the SUSY-breaking vacuum is selected in the white region in Fig. 9.

In this case, $S$ stays at $S_0$ until the Hubble parameter decreases and becomes comparable to the effective mass of $S$. Then, at $T = T_{\rm osc}$, $S$ starts oscillation around the time-dependent minimum $S_{\rm min}(T)$. If $T_0 > T_{\rm osc}$, namely $S_{\rm min}(T = T_{\rm osc}) \simeq \langle S \rangle$, the center of the oscillation is the SUSY-breaking minimum from the beginning. On the other hand, if $T_{\rm osc} > T_0$, namely

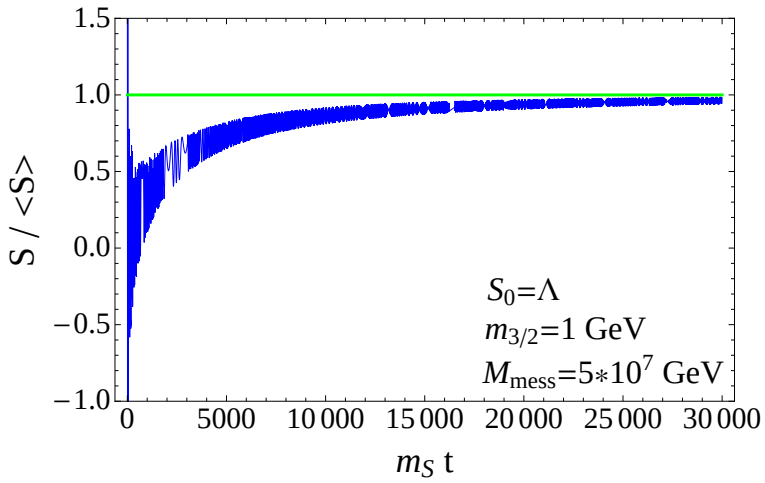


Figure 13: The evolution of $S$ with $S_0 = \Lambda$. If the temperature dependent minimum $S_{\rm min}(T)$ lies near the origin ant $T = T_{\rm osc}$, $S$ at first oscillates about $S_{\rm min}(T)$, and later the center of the oscillations moves from the origin to $\langle S \rangle$.

the potential minimum lies still near the origin when $S$ starts oscillation, $S$ starts oscillation around the origin at first. Then, as the temperature drops and reaches $T_0$, the center of the oscillation moves from the origin to the SUSY breaking-vacuum. A typical evolution of $S$ is in Fig. 13. $S$ eventually oscillate around the SUSY-breaking minimum, irrespective of the details of the initial condition.

## 8 Realization of the scenario

As mentioned in section 2 and 3, the gravitino relic abundance becomes insensitive to $T_R$ if $T_R > M_{\rm mess}$. However, they should be diluted by a late-time entropy release since the abundance is too large compared to the observation $\Omega_{\rm DM} \simeq 0.2$. We defined the required dilution to achieve the observation as $\Delta_{3/2}$ in Eq. (3.3). Now what we have to do is to estimate the dilution factor in the present model and check that $\Delta_{3/2}$ is supplied by the decay of $S$.

### 8.1 Gravitino Dark Matter

In order to estimate the amount of entropy production from the decay of $S$, we define the dilution factor $\Delta$ as

$$\frac{1}{\Delta} \equiv \frac{s_{\rm inf}}{s_S + s_{\rm inf}} \simeq {\rm Min}\left[1, \frac{s_{\rm inf}}{s_S}\right], \tag{8.1}$$

where $s_{\rm inf}$ and $s_S$ represent the entropy density produced by the decays of the inflaton and $S$, respectively. If $\Delta > 1$, $\Delta$ is well approximated by

$$\Delta \simeq \frac{s_S}{s_{\rm inf}} = \frac{4}{3T_d} \cdot \frac{\rho_S}{s_{\rm inf}}, \tag{8.2}$$

where $\rho_S$ is the energy density of $S$. Pre-existing gravitinos and baryons are diluted by $1/\Delta$. $T_d$ is the decay temperature of $S$, which is defined by

$$T_d \equiv \left(\frac{\pi^2 g_*}{90}\right)^{-1/4} \sqrt{M_{\rm pl}\Gamma_S}, \tag{8.3}$$

where $\Gamma_S$ is the total decay width of $S$. The formulae of $T_d$ and $\Gamma_S$ are found in appendix B.

If the magnitude of dilution factor $\Delta$ coincides $\Delta_{3/2}$ in Eq. (3.3), the overproduced gravitinos are diluted to realize the observed dark matter abundance, $\Omega_{\rm DM}h^2 \simeq 0.1$. In order to realize the right amount of baryons, $\Omega_B \simeq 0.045$, at the same time, we need an appropriate reheating temperature. Since the baryon asymmetry is also diluted by the entropy production, the reheating temperature should be high enough to produce abundant baryons in advance, namely $10^9 \times \Delta_{3/2} \lesssim T_R$ is required in the scenario. We show the required set of the dilution factor ($\Delta_{3/2}$) and the reheating temperature ($T_R$) in $m_{3/2}$ vs $M_{\rm mess}$ plane in Fig. 14.

In the present set-up, there exists a parameter region where the dark matter and the baryon asymmetry are explained by thermally produced gravitino and thermal leptogenesis simultaneously (blue and green regions), with an appropriate combination of $\Delta$ and $T_R$.

In order to estimate the magnitude of the dilution factor from the decay, we numerically solved the equation of motion of the pseudo-moduli with the initial condition set at the inflaton dominated era. The results depend on the initial location of the $S$ field. Unfortunately, if the initial position is close to the origin, $S_0 \simeq 0$, as studied in section 7.2.1, it turns out that the required dilution of $\Delta_{3/2}$ cannot be supplied by the decay. On the other hand, if $S_0 \sim \Lambda$ as studied in section 7.2.2, $\Delta_{3/2}$ can be achieved in most of the parameter regions. We choose the initial position of $S$ to be $\Lambda$ or $M_{\rm pl}$ for illustration. The results are shown in Fig. 15. As we see from the figure, by choosing an appropriate value of the initial condition of $S$ from between $\Lambda$ and $M_{\rm pl}$, the required amount of entropy can be supplied from the

oscillation energy everywhere in the blue and green regions in Fig. 14; we have confirmed that required entropy production can be obtained in this model if $S$ is displaced far from the origin during inflation.

**Non-thermal gravitino production**

While the dark matter is explained by thermally produced gravitino in the blue and green regions in Fig. 14, gravitinos are also produced non-thermally by the rare decay $S \to \psi_{3/2}\psi_{3/2}$. We calculate the non-thermally produced gravitino abundance in appendix B and found that the abundance coincides the observed dark matter abundance with $m_{3/2} \sim 2$ GeV. Taking into account possible theoretical errors, we show the parameter region where $0.03 \lesssim \Omega^{\rm NT}_{3/2}h^2 \lesssim 0.3$ is predicted as a green band in Fig. 14.

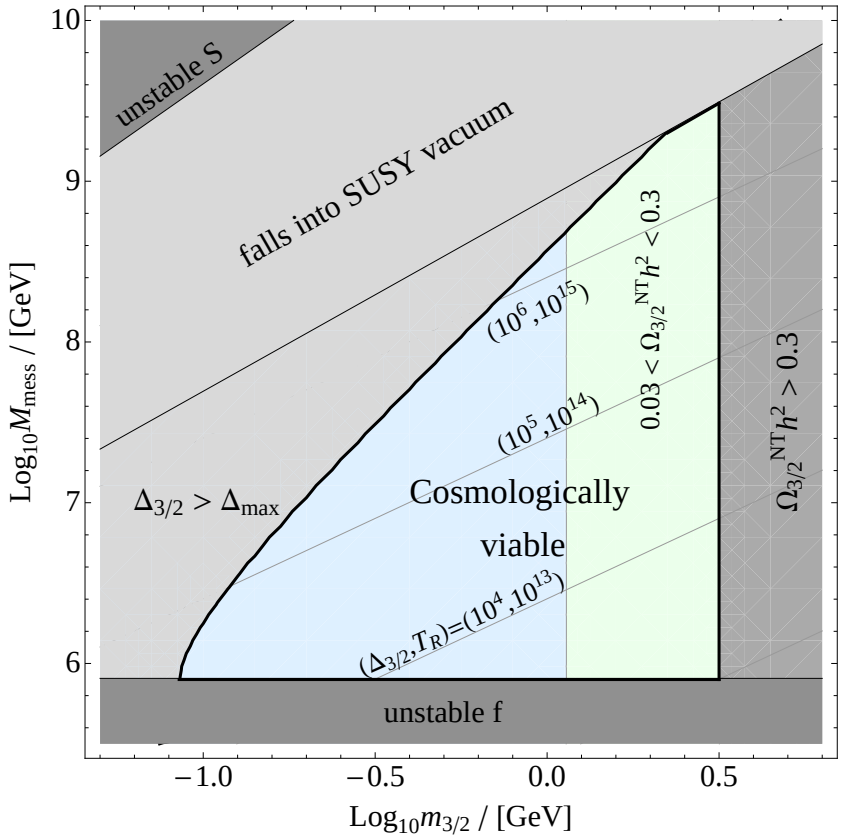


Figure 14: Required amount of the dilution factor ($\Delta_{3/2}$) and the reheating temperature ($T_R$) to realize the observation $\Omega_{\rm DM}h^2 \simeq 0.1$ and $\Omega_B \simeq 0.045$. In blue and green regions, the dark matter is explained by gravitino and baryon asymmetry is supplied by thermal leptogenesis with an appropriate choice of $\Delta$ and $T_R$. In the green region, the non-thermally produced gravitino abundance coincides the observed DM abundance. We should discard the parameter regions shaded by (light)gray color. For gray regions denoted as "unstable S" and "unstable f", the SUSY breaking minimum is unstable [51]. For a light gray region "fall into SUSY vacuum", the pseudo-moduli fall into SUSY preserving vacuum along the cosmological evolution and never reaches the SUSY breaking vacuum [55]. We define $\Delta_{\rm max}$ as the maximum dilution factor available under the condition that the oscillation amplitude is small so that $S$ does not fall into SUSY vacuum. So in the region $\Delta_{3/2} > \Delta_{\rm max}$ we cannot get a required amount of dilution factor $\Delta_{3/2}$ while $S$ successfully reaches the SUSY breaking minimum. Gravitinos are overproduced non-thermally in the gray region "$\Omega_{3/2}^{\rm NT} h^2 > 0.3$".

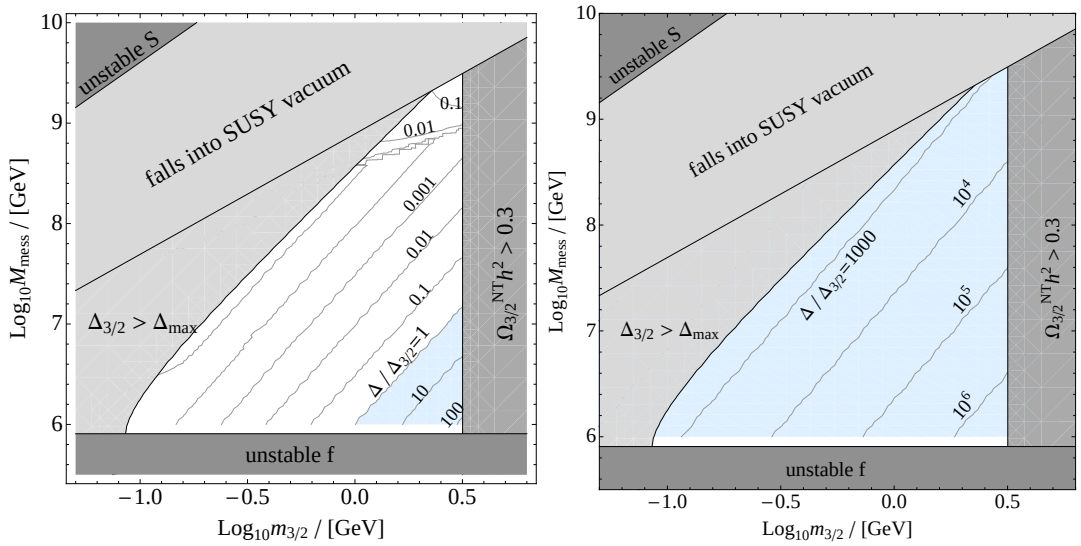


Figure 15: The results of numerical study. In the left(right) figure the initial condition of the position of $S$ right after the inflation is took to be $S_0 = \Lambda (S_0 = M_{\rm pl})$. The required amount of dilution factor and the theoretical prediction are denoted as $\Delta_{3/2}$ and $\Delta$. In the blue regions a sizable amount of entropy enough to dilute overabundant gravitino is produced by the decay of $S$. We see that a required amount of dilution factor read off from Eq. (3.3) can be always supplied by the decay by choosing an appropriate value of $S_0$ from between $\Lambda$ and $M_{\rm pl}$.

### 8.2 Comments on a light higgsino

So far we have studied a new cosmological scenario with a high SUSY scale $M_{\rm SUSY} \gtrsim 5$ TeV in order to realize a 125 GeV Higgs boson mass. If all the SUSY particles are as heavy as 5 TeV, it is difficult to confirm the scenario by the LHC experiments. However, it is possible that the $\mu$-parameter in the MSSM is much smaller than other superparticle masses. In the GMSB model we used for the cosmological study there is a natural solution to the $\mu$-problem (we mention the prescription in appendix C). The model predicts a light higgsino with its mass of $\mathcal{O}(100)$ GeV. The $\mu$-term is generated by a direct coupling between SUSY breaking chiral multiplet and Higgs multiplets assumed at the cutoff scale $\Lambda$, which results in a relatively small $\mu$-term compared to Higgs soft mass parameters. For a cosmologically favorable region of the gravitino mass, the lightest higgsino does not decay inside the detector. In that case, searches for mono-jet processes at LHC or mono-photon ones at the ILC will be able to find the light higgsino.

One should check if a light higgsino scenario is compatible with the constraint from the BBN. If the higgsino mass is so small that the life-time becomes as long as $\mathcal{O}(1)$ sec, the

decay may alter the abundance of the light elements. We have checked the BBN constraints in the case of $m_{\tilde{h}} = 300$ GeV and found that such a light higgsino is cosmologically safe if the gravitino is lighter than $\sim 500$ MeV. A detailed discussion is given in appendix C.

# 9 Summary

This thesis is composed of three parts. In part I, we investigated the thermal production of the gravitino in general framework of gauge mediation. Calculating the gravitino production cross section using both the goldstino Lagrangian and the supergravity one, we confirmed that the relic abundance become insensitive to the reheating temperature if the temperature of the Universe once exceeds the messenger mass scale. Inspired by this property, we presented a new cosmological scenario; the gravitino dark matter and the thermal leptogenesis are compatible, namely the ratio $\Omega_{3/2}/\Omega_B$ coincides the observation, $\Omega_{\rm DM}/\Omega_B \sim 5$, with an appropriate value of reheating temperature. To realize the correct absolute value of each quantity, $\Omega_{\rm DM}h^2 \simeq 0.1$ and $\Omega_B \simeq 0.045$, a late-time entropy release is required, which is automatically supplied by the oscillation energy of the pseudo-moduli.

In part II, we studied general properties of O'Raifeartaigh-type models which serve as low-energy descriptions of a wide class of dynamical SUSY-breaking models. We saw that a realistic model of SUSY-breaking has a meta-stable non-SUSY vacuum and an approximate $R$-symmetry. In order to understand deeply the connections between SUSY-breaking and $R$-symmetry, and also between the gaugino mass and the structure of the pseudo-moduli space, several example of O'Raifeartaigh-type models were introduced. We also showed several cosmological requirements which should be equipped with in a realistic model.

In part III, we examined cosmological evolution of the pseudo-moduli field in a concrete model of gauge mediation to demonstrate the scenario presented in part I. With an appropriate initial condition, we showed that the oscillation energy of the pseudo-moduli dominates the energy density of the Universe and a sizable amount of entropy needed to fix the energy densities of gravitino and baryon is released by the subsequent decay. The scenario is realized when the gravitino mass is 100 MeV $\lesssim m_{3/2} \lesssim 1$ GeV and the messenger scale is $10^6$ GeV $\lesssim M_{\rm mess} \lesssim 10^9$ GeV. Although we have studied the scenario with $M_{\rm SUSY} \gtrsim 5$ TeV to account for the 125 GeV Higgs boson, the higgsino can be asI light as $\mathcal{O}(100)$ GeV. Such a light higgsino can be discovered in a future experiments. We have checked that a light higgsino is safe from the BBN constraints if the gravitino mass is smaller than $\sim 500$ MeV.

## Acknowledgments

I would like to thank R. Kitano for all the guidance he has given me. I have learned so many things from him, and it is difficult for me to mention all of the valuable experiences in this limited margin. In a word, I have realized what it is to be a professional through the collaboration with him. I am also grateful to F. Takahashi for giving me lots of helpful comments and correcting my poor English when working together in Tohoku University. I am also grateful to M. Yamaguchi for recommending several textbooks or papers in the early stage of my graduate school life, which encouraged me to go into SUSY phenomenology, and also, for recognizing me as a good student which was needed for me to apply for the reduction or waving of tuition fees and to carry on studying physics with good physical conditions. I am also grateful to K. Hikasa for looking upon my research as well as teaching-assistant activities warmly.

I have truly led my study life supported by many colleagues. I would like to give special thanks to Y. Nakai for inviting me to the world of Nakai and constantly discussing physics and our future, which encouraged me in many ways. Also it was really lucky for me to have a chance to meet Y. Kikuta again at KEK and spend time with him and stimulate each other in many ways in my last year in graduate school. I would also like to express my appreciation to my seniors, S. Nakamura and K. Ishiwata. They sometimes kindly set up opportunities to exchange our recent news, which makes me take a vow to study hard each time. Finally, I would like to express my gratitude to all the members of the Particle Theory and Cosmology Group of Tohoku University and KEK Theory Center for their hospitality.

# A High energy behavior of gravitino production

In the appendix we calculate the scattering amplitude of gravitino production process both with global SUSY Lagrangian and supergravity Lagrangian, and study its high energy behavior. We focus on QED gauge interactions and calculate one particular process $e^- e^+ \to \lambda \psi_{3/2}$.

## A.1 Calculation with global SUSY Lagrangian

### Lagrangian

Let us consider a $U(1)$ model with chiral super fields

$$S, \quad f, \quad \bar{f} \tag{A.1}$$

and a vector superfield for $U(1)$ gauge field. $f$ and $\bar{f}$ are charged under $U(1)$ as $+1$ and $-1$ and $S$ is neutral. There is a superpotential

$$W = F_S S + \lambda S f \bar{f}. \tag{A.2}$$

SUSY is broken by the $F$-component of the singlet field $S$. $f$ and $\bar{f}$ act as messenger fields in gauge mediation. Lagrangian of the model is composed of the following three parts,

$$\mathcal{L} = \mathcal{L}_{\text{kinetic}} + \mathcal{L}_{\text{gaugino}} + \mathcal{L}_{S f \bar{f}}, \tag{A.3}$$

where

$$\begin{aligned} \mathcal{L}_{\text{kinetic}} =& -\frac{1}{4} F_{\mu\nu} F^{\mu\nu} + \frac{i}{2} \bar{\lambda} \gamma^\mu \partial_\mu \lambda + i \bar{\psi}_s \gamma^\mu \partial_\mu P_L \psi_s + i \bar{\psi}_f \gamma^\mu (\partial_\mu - i g A_\mu) \psi_f \\ &+ |\partial_\mu f - i g A_\mu f|^2 + |\partial_\mu f^* + i g A_\mu f^*|^2 \\ &+ i \bar{\psi}_e \gamma^\mu (\partial_\mu - i g A_\mu) P_L \psi_e + |\partial_\mu \tilde{e} - i g A_\mu \tilde{e}|^2, \end{aligned} \tag{A.4}$$

$$\mathcal{L}_{\text{gaugino}} = -i\sqrt{2} g (f^* \bar{\lambda} P_L \psi_f - f \bar{\psi}_f P_R \lambda) + i\sqrt{2} g (\bar{f}^* \bar{\lambda} P_L \psi_f^c - \bar{f} \bar{\psi}_f^c P_R \lambda), \tag{A.5}$$

$$\begin{aligned} \mathcal{L}_{S f \bar{f}} =& -\lambda \bar{\psi}_f P_L \psi_s f - \lambda \bar{\psi}_s P_R \psi_f f^* - \lambda \bar{\psi}_f^c P_L \psi_s \bar{f} - \lambda \bar{\psi}_s P_R \psi_f^c \bar{f}^* \\ &- M \bar{\psi}_f \psi_f - M^2 (|f|^2 + |\bar{f}|^2) - \lambda F_S (f \bar{f} + f^* \bar{f}^*). \end{aligned} \tag{A.6}$$

The last term comes from the superpotential. We have defined the supersymmetric mass of $f$ and $\bar{f}$ multiplet as

$$M \equiv \lambda \langle S \rangle \tag{A.7}$$

and taken the VEV to be real. $\psi_f$ and $\psi_f^c$ are Dirac fermions defined as

$$\psi_f \equiv \begin{pmatrix} \psi_{f\alpha} \\ \psi_{\bar{f}}^{\dagger\dot{\alpha}} \end{pmatrix}, \quad \psi_f^c \equiv \begin{pmatrix} \psi_{\bar{f}\alpha} \\ \psi_f^{\dagger\dot{\alpha}} \end{pmatrix}, \tag{A.8}$$

where $\psi_{f\alpha}$ and $\psi_{\bar{f}\alpha}$ represent the two component chiral fermions belong to $f$ and $\bar{f}$ superfields. Gaugino is treated as a Majorana fermion,

$$\lambda = \begin{pmatrix} \lambda_\alpha \\ \lambda^{\dagger\dot{\alpha}} \end{pmatrix}. \tag{A.9}$$

The Weyl fermion $\psi_S$ is the goldstino which is absorbed into the longitudinal component of gravitino once SUSY is promoted to a local symmetry. We study the production processes of goldstino and compare the result with that of supergravity calculation.

**Gaugino mass**

Throughout the study we assume that the gaugino mass is generated only via gauge mediation. Before entering the calculation of the gravitino (goldstino) production amplitudes, let us calculate the gaugino mass from the Lagrangian Eq. (A.6). At one-loop level, gaugino two point function has the following form:

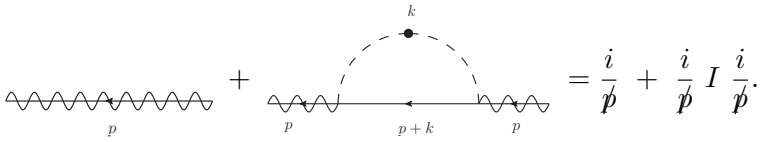


$$= \frac{i}{\not p} + \frac{i}{\not p} I \frac{i}{\not p}. \tag{A.10}$$

The particles in the loop are the messengers and the dot in the boson line represents the insertion of $F_S$. The integral $I$ is calculated to be

$$\begin{aligned} I &= \int \frac{d^4k}{(2\pi)^4} (\sqrt{2} g P_L) \frac{i(\not p + \not k + M)}{(p+k)^2 + M^2} (-\sqrt{2} g P_L) \frac{i}{k^2 - M^2} (-i\lambda F_S) \frac{i}{k^2 - M^2} \times 2 \\ &+ \int \frac{d^4k}{(2\pi)^4} (-\sqrt{2} g P_R) \frac{i(\not p + \not k + M)}{(p+k)^2 + M^2} (\sqrt{2} g P_R) \frac{i}{k^2 - M^2} (-i\lambda F_S) \frac{i}{k^2 - M^2} \times 2 \\ &= 4g^2 \lambda F_S M \int \frac{d^4k}{(2\pi)^4} \frac{1}{[k^2 - M^2]^2 [(p+k)^2 - M^2]} \\ &= 4g^2 \lambda F_S M \times \frac{-i}{2(4\pi)^2 M^2} \\ &= \frac{-2ig^2}{(4\pi)^2} \frac{\lambda F_S}{M}. \end{aligned} \tag{A.11}$$

Compare this with full propagator,

$$\text{ 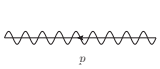 } = \frac{i}{\not{p} - m_\lambda} \tag{A.12}$$

$$= \frac{i}{\not{p}} \frac{1}{1 - \frac{m_\lambda}{\not{p}}} \tag{A.13}$$

$$\simeq \frac{i}{\not{p}} \left(1 + \frac{m_\lambda}{\not{p}}\right) = \frac{i}{\not{p}} + \frac{i}{\not{p}}(-im_\lambda)\frac{i}{\not{p}}, \tag{A.14}$$

we get a gaugino mass formula at one-loop level,

$$m_\lambda = \frac{2g^2}{(4\pi)^2} \frac{\lambda F_S}{M}. \tag{A.15}$$

Later we use the formula to compare the results of global SUSY calculation and supergravity calculation.

### Amplitude at one-loop level

Let us calculate the scattering amplitude of the goldstino production process $e^- e^+ \to \lambda \psi_S$. Since the goldstino couples to MSSM fields only through the messenger particles, tree-level diagrams are absent in the process. There are in total four 1-loop diagrams. We label the diagrams as A and B as in Fig. 16 and Fig. 17 and evaluate them in tern.

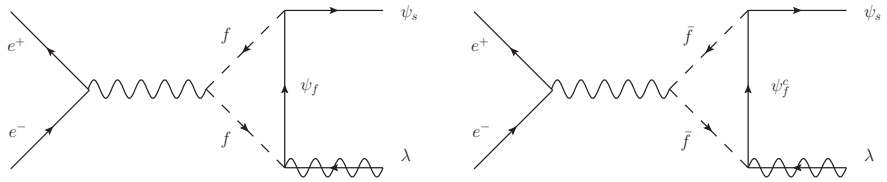


Figure 16: Goldstino production diagrams A

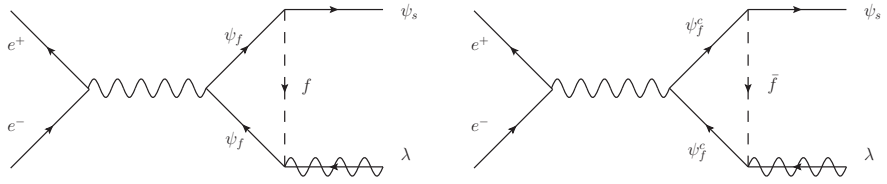


Figure 17: Goldstino production diagrams B

The amplitudes for diagrams A and B have a universal form,

$$\begin{aligned}\mathcal{M} &= [\bar{v}(p_2)(ig\gamma^\mu P_L)u(p_1)] \times \frac{-ig_{\mu\nu}}{(p_1+p_2)^2} \times \left[\tilde{\mathcal{M}}\right]^\nu \\ &= \frac{g}{s}[\bar{v}(p_2)\gamma^\mu P_L u(p_1)]g_{\mu\nu}\left[\tilde{\mathcal{M}}\right]^\nu, \end{aligned} \tag{A.16}$$

where $u(p_1)$ and $v(p_2)$ represent the wave functions of electron and positron. For diagrams A,

$$\begin{aligned}\left[\tilde{\mathcal{M}}^A\right]^\nu &= \int \frac{d^4k}{(2\pi)^4}\bar{u}_s(p_3)(-i\lambda P_R)\frac{i(\not{k}+\not{p}_3+M)}{(k+p_3)^2-M^2}(-\sqrt{2}gP_R)v_\lambda(p_4) \\ &\quad \times \frac{i}{k^2-M^2} \times ig(2k+p_3+p_4)^\nu \times \frac{i}{(k+p_3+p_4)^2-M^2} \\ &\quad \times 2 \\ &= i2\sqrt{2}\lambda g^2 M \int \frac{d^4k}{(2\pi)^4}\frac{1}{k^2-M^2}\frac{1}{(k+p_3)^2-M^2}\frac{1}{(k+p_3+p_4)^2-M^2} \\ &\quad \times \bar{u}_s(p_3)P_R v_\lambda(p_4) \times (2k+p_3+p_4)^\nu, \end{aligned} \tag{A.17}$$

where $u_s(p_3)$ and $v_\lambda(p_4)$ are the wave function of goldstino and gaugino. Diagrams B can be evaluated in a same manner,

$$\begin{aligned}\left[\tilde{\mathcal{M}}^B\right]^\nu &= i2\sqrt{2}\lambda g^2 M \int \frac{d^4k}{(2\pi)^4}\frac{1}{k^2-M^2}\frac{1}{(k+p_3)^2-M^2}\frac{1}{(k+p_3+p_4)^2-M^2} \\ &\quad \times \bar{u}_s(p_3)P_R v_\lambda(p_4) \times (-2k-2p_3)^\nu. \end{aligned} \tag{A.18}$$

Combining these contributions,

$$\begin{aligned}\left[\tilde{\mathcal{M}}\right]^\nu &= \left[\tilde{\mathcal{M}}^A\right]^\nu + \left[\tilde{\mathcal{M}}^B\right]^\nu \\ &= i2\sqrt{2}\lambda g^2 M \int \frac{d^4k}{(2\pi)^4}\frac{1}{k^2-M^2}\frac{1}{(k+p_3)^2-M^2}\frac{1}{(k+p_3+p_4)^2-M^2} \\ &\quad \times \bar{u}_s(p_3)P_R v_\lambda(p_4) \times (p_4-p_3)^\nu. \end{aligned} \tag{A.19}$$

The integral can be written as a so called $C$-function defined in Ref.[21],

$$\frac{i}{(4\pi)^2}C_0(\sqrt{s},M) \equiv \int \frac{d^4k}{(2\pi)^4}\frac{1}{k^2-M^2}\frac{1}{(k+p_3)^2-M^2}\frac{1}{(k+p_3+p_4)^2-M^2}. \tag{A.20}$$

Then,

$$\mathcal{M} = \frac{-2\sqrt{2}\lambda g^3}{(4\pi)^2}\frac{M}{s}C_0(\sqrt{s},M^2)[\bar{v}(p_2)\gamma^\mu P_L u(p_1)][\bar{u}_s(p_3)P_R v_\lambda(p_4)](p_4-p_3)_\mu. \tag{A.21}$$

Inserting the explicit formulae for the wave functions, we get a helicity amplitudes:

$$\mathcal{M}^{(\uparrow\downarrow\uparrow\uparrow)} = -\frac{2\sqrt{2}g^3\lambda}{(4\pi)^2}MC_0(\sqrt{s},M)\sqrt{s}\sin\theta, \tag{A.22}$$

$$\mathcal{M}^{(\uparrow\downarrow\downarrow\downarrow)} = \frac{2\sqrt{2}g^3\lambda}{(4\pi)^2}MC_0(\sqrt{s},M)\sqrt{s}\sin\theta. \tag{A.23}$$

The formula in Eq. (A.22) has been quoted in Eq. (2.18) in section 2. As mentioned below Eq. (2.18), the amplitude for the goldstino production is suppressed for the energy region of $\sqrt{s} \gg M_{\rm mess}$ by $\sim M_{\rm mess}^2/s$ compared to that of $\sqrt{s} \ll M_{\rm mess}$.

## A.2 Calculation with supergravity Lagrangian

Next we evaluate the amplitude for the gravitino production process $e^- e^+ \to \lambda \psi_{3/2}$ using supergravity Lagrangian. In addition to the tree-level diagrams, there are messenger one-loop diagrams which turn out to contribute the amplitude with the same magnitude to that of tree-level diagrams.

### Lagrangian

We consider a supergravity model with vector like matters $f$ and $\bar{f}$ which are charged under $U(1)$ gauge symmetry. Lagrangian of the model is the following:

$$\mathcal{L} = \mathcal{L}_{\rm kinetic} + \mathcal{L}_{\rm gaugino} + \mathcal{L}_{\rm sugra} + \mathcal{L}_{\rm mass}, \tag{A.24}$$

where

$$\begin{aligned}
\mathcal{L}_{\rm kinetic} =& -\frac{1}{4} F_{\mu\nu} F^{\mu\nu} + \frac{i}{2} \bar{\lambda} \gamma^\mu \partial_\mu \lambda - \frac{1}{2} \epsilon^{\mu\nu\rho\sigma} \bar{\psi}_\mu \gamma_5 \gamma_\nu \partial_\rho \psi_\sigma \\
&+ i \bar{\psi}_f \gamma^\mu (\partial_\mu - i g A_\mu) \psi_f + |\partial_\mu f - i g A_\mu f|^2 + |\partial_\mu f^* + i g A_\mu f^*|^2 \\
&+ i \bar{\psi}_e \gamma^\mu (\partial_\mu - i g A_\mu) P_L \psi_e + |\partial_\mu \tilde{e} - i g A_\mu \tilde{e}|^2,
\end{aligned} \tag{A.25}$$

$$\begin{aligned}
\mathcal{L}_{\rm sugra} =& -\frac{1}{\sqrt{2} M_{\rm pl}} (\partial_\nu f^* + i g A_\nu f^*) \bar{\psi}_\mu \gamma^\nu \gamma^\mu P_L \psi_f - \frac{1}{\sqrt{2} M_{\rm pl}} (\partial_\nu f - i g A_\nu f) \bar{\psi}_f P_R \gamma^\mu \gamma^\nu \psi_\mu \\
&- \frac{1}{\sqrt{2} M_{\rm pl}} (\partial_\nu \bar{f}^* - i g A_\nu \bar{f}^*) \bar{\psi}_\mu \gamma^\nu \gamma^\mu P_L \psi_{\bar{f}}^c - \frac{1}{\sqrt{2} M_{\rm pl}} (\partial_\nu \bar{f} + i g A_\nu \bar{f}) \bar{\psi}_{\bar{f}}^c P_R \gamma^\mu \gamma^\nu \psi_\mu \\
&- \frac{i}{8 M_{\rm pl}} \bar{\psi}_\mu [\gamma^\nu, \gamma^\rho] \gamma^\mu \lambda F_{\nu\rho},
\end{aligned} \tag{A.26}$$

$$\mathcal{L}_{\rm gaugino} = -i\sqrt{2} g (f^* \bar{\lambda} P_L \psi_f - f \bar{\psi}_f P_R \lambda) + i\sqrt{2} g (\bar{f}^* \bar{\lambda} P_L \psi_{\bar{f}}^c - \bar{f} \bar{\psi}_{\bar{f}}^c P_R \lambda, \tag{A.27}$$

$$\mathcal{L}_{\rm mass} = -M \bar{\psi}_f \psi_f - M^2 (|f|^2 + |\bar{f}|^2) - \lambda F_S (f \bar{f} + f^* \bar{f}^*). \tag{A.28}$$

Gravitino is denoted by $\psi_\mu$. We have assumed that the chiral multiplets $f$ and $\bar{f}$ get their SUSY / SUSY-breaking masses from the superpotential Eq. (A.2).

**Wave function of gravitino**

The wave function of gravitino is given by the products of the spinor $u(\mathbf{p}, s)$ and the polarization vector $\epsilon_\mu(\mathbf{p}, m)$ as [7]

$$\tilde{\psi}_\mu(\mathbf{p}, \lambda) = \sum_{s,m} \left\langle \left(\frac{1}{2}, \frac{s}{2}\right)(1, m) \;\middle|\; \left(\frac{3}{2}, \lambda\right) \right\rangle u(\mathbf{p}, s)\epsilon_\mu(\mathbf{p}, m), \tag{A.29}$$

where $\langle\left(\frac{1}{2}, \frac{s}{2}\right)(1, m)|\left(\frac{3}{2}, \lambda\right)\rangle$ is the Clebsch-Gordan coefficient. Since we are interested in the parameter region where $m_{3/2} \ll m_\lambda$ is always satisfied (this is the case in GMSB), dominant contribution to the amplitude comes from the longitudinal mode of gravitino. So we only extract the spin-half component of the gravitino which is proportional to $1/m_{3/2}$,

$$\tilde{\psi}_\mu(\mathbf{p}, \frac{s}{2}) \;\ni\; \sqrt{\frac{2}{3}}\; u(\mathbf{p}, s)\; \epsilon_\mu(\mathbf{p}, 0), \tag{A.30}$$

where $s$ is a spin quantum number and take $\pm 1$ and the polarization vector for a massive particle ($p_\mu p^\mu = m_{3/2}^2 \neq 0$)with the momentum vector $p^\mu = (E, |\mathbf{p}|\sin\theta\cos\phi, |\mathbf{p}|\sin\theta\sin\phi, |\mathbf{p}|\cos\theta)$ is ,

$$\epsilon_\mu(\mathbf{p}, 0) = \frac{1}{m_{3/2}}(|\mathbf{p}|, -E\sin\theta\cos\phi, -E\sin\theta\sin\phi, -E\cos\theta). \tag{A.31}$$

The wave function $\tilde{\psi}_\mu$ satisfies the following equations;

$$\gamma^\mu \tilde{\psi}_\mu(\mathbf{p}, \lambda) = 0, \tag{A.32}$$

$$p^\mu \tilde{\psi}_\mu(\mathbf{p}, \lambda) = 0, \tag{A.33}$$

$$(\not{p} - m_{3/2})\tilde{\psi}_\mu(\mathbf{p}, \lambda) = 0. \tag{A.34}$$

We repeatedly use these equations in evaluating the amplitude.

**Amplitudes at tree-level**

First we calculate the amplitude at tree-level. There are three diagrams of $s$-, $t$- and $u$-channels.

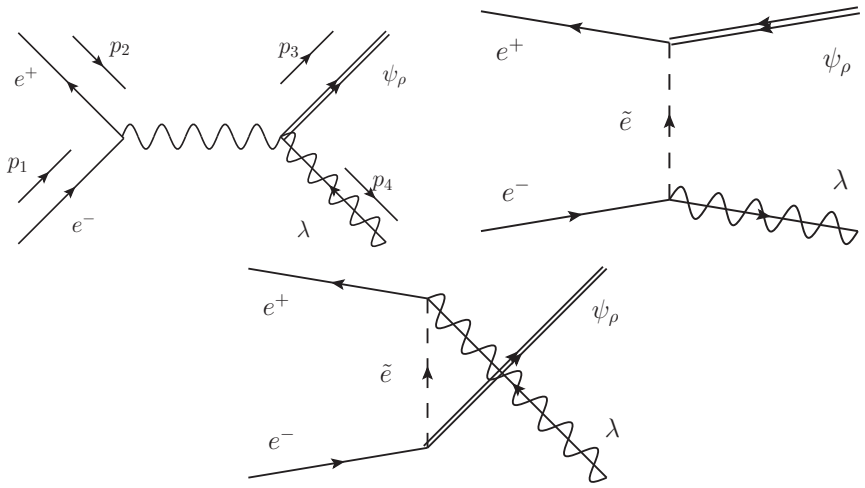


Figure 18: Gravitino production process at tree-level.

**s-channel**

Let us evaluate the diagrams in turn. For the $s$-channel,

$$\begin{aligned}\mathcal{M}_s &= [\bar{v}(p_2)(ig\gamma^\mu P_L)u(p_1)] \times \frac{-ig_{\mu\nu}}{(p_1+p_2)^2} \times \left[\bar{\tilde{\psi}}_\rho(p_3)\left[-\frac{i}{4M_{\rm pl}}(p_1+p_2)_\sigma[\gamma^\sigma,\gamma^\nu]\gamma^\rho\right]v(p_4)\right] \\ &= \frac{-ig}{4M_{\rm pl}}\frac{1}{s}\left[\bar{v}(p_2)\gamma^\mu P_L u(p_1)\right]\left[\bar{\tilde{\psi}}_\rho(p_3)\left((\not{p}_1+\not{p}_2)\gamma_\mu\gamma^\rho-\gamma_\mu(\not{p}_1+\not{p}_2)\gamma^\rho\right)v(p_4)\right]. \qquad \text{(A.35)}\end{aligned}$$

Inserting the explicit formula for wave functions, we get helicity amplitudes,

$$\mathcal{M}_s^{(\uparrow\downarrow\uparrow\downarrow)} = \frac{ig}{\sqrt{6}M_{\rm pl}m_{3/2}}s\left(1-\frac{m_\lambda^2}{s}\right)^{3/2}(1+\cos\theta), \qquad \text{(A.36)}$$

$$\mathcal{M}_s^{(\uparrow\downarrow\downarrow\uparrow)} = \frac{-ig}{\sqrt{6}M_{\rm pl}m_{3/2}}s\left(1-\frac{m_\lambda^2}{s}\right)^{3/2}(1-\cos\theta), \qquad \text{(A.37)}$$

$$\mathcal{M}_s(\text{others}) = 0. \qquad \text{(A.38)}$$

**t-channel**

For $t$-channel,

$$\begin{aligned}\mathcal{M}_t &= \left[\bar{v}(p_2)\left[-\frac{1}{\sqrt{2}M}(p_1-p_4)_\nu P_R\gamma^\rho\gamma^\nu\right]\tilde{\psi}^c_\rho(p_3)\right]\times\frac{i}{(p_1-p_4)^2}\times\left[\bar{u}(p_4)(\sqrt{2}gP_L)u(p_1)\right] \\ &= \frac{-ig}{M}\frac{1}{t}\left[\bar{v}(p_2)P_R\gamma^\rho(\not{p}_1-\not{p}_4)\tilde{\psi}^c_\rho(p_3)\right]\left[\bar{u}(p_4)P_L u(p_1)\right], \qquad \text{(A.39)}\end{aligned}$$

and

$$\mathcal{M}_t^{(\uparrow\downarrow\uparrow\downarrow)} = \frac{-ig}{\sqrt{6}M_{\rm pl}m_{3/2}} s \left(1 - \frac{m_\lambda^2}{s}\right)^{1/2} (1+\cos\theta), \tag{A.40}$$

$$\mathcal{M}_t^{(\uparrow\downarrow\uparrow\uparrow)} = \frac{igm_\lambda}{\sqrt{6}M_{\rm pl}m_{3/2}} \sqrt{s} \left(1 - \frac{m_\lambda^2}{s}\right)^{1/2} \sin\theta, \tag{A.41}$$

$$\mathcal{M}_t(\text{others}) = 0. \tag{A.42}$$

**u-channel**

For $u$-channel,

$$\begin{aligned}\mathcal{M}_u &= \left[\bar{\tilde{\psi}}_\rho(p_3)\left[\frac{1}{\sqrt{2}M}(p_1-p_3)_\nu\gamma^\nu\gamma^\rho P_L\right]u(p_1)\right] \times \frac{i}{(p_1-p_3)^2} \times \left[\bar{v}(p_2)(-\sqrt{2}gP_R)v(p_4)\right] \\ &= \frac{-ig}{M}\frac{1}{u}\left[\bar{\tilde{\psi}}_\rho(p_3)(\not{p}_1 - \not{p}_3)\gamma^\rho P_L u(p_1)\right][\bar{v}(p_2)P_R u(p_4)], \end{aligned} \tag{A.43}$$

and

$$\mathcal{M}_u^{(\uparrow\downarrow\downarrow\uparrow)} = \frac{-ig}{\sqrt{6}M_{\rm pl}m_{3/2}} s \left(1 - \frac{m_\lambda^2}{s}\right)^{1/2} (1-\cos\theta), \tag{A.44}$$

$$\mathcal{M}_u^{(\uparrow\downarrow\downarrow\downarrow)} = \frac{igm_\lambda}{\sqrt{6}M_{\rm pl}m_{3/2}} \sqrt{s} \left(1 - \frac{m_\lambda^2}{s}\right)^{1/2} \sin\theta, \tag{A.45}$$

$$\mathcal{M}_u(\text{others}) = 0. \tag{A.46}$$

**Combine**

At first sight, the amplitude behaves as $\mathcal{M} \sim s$ for a high energy. However, as pointed out in Ref. [7], the leading high energy behavior should cancel out in the total amplitude. The reason can be understood in the following way. The helicity $\pm\frac{1}{2}$ components of gravitino is unphysical in the supersymmetric phase; they become physical only after absorbing the goldstino. So the total amplitude should vanish for a supersymmetric limit if the gravitino has helicity $\pm\frac{1}{2}$. That is ,the total amplitude for the helicity $\pm\frac{1}{2}$ gravitino production should be proportional to some SUSY-breaking parameters. We can explicitly confirm the statement by summing up the three diagrams,

$$\mathcal{M} = \mathcal{M}_s + \mathcal{M}_t - \mathcal{M}_u. \tag{A.47}$$

The relative minus sign comes from the exchange of fermionic quantities. For each helicity, we get

$$\mathcal{M}^{(\uparrow\downarrow\uparrow\downarrow)} = \frac{-igm_\lambda^2}{\sqrt{6}M_{\rm pl}m_{3/2}}\left(1-\frac{m_\lambda^2}{s}\right)^{1/2}(1+\cos\theta) \tag{A.48}$$

$$\mathcal{M}^{(\uparrow\downarrow\downarrow\uparrow)} = \frac{igm_\lambda^2}{\sqrt{6}M_{\rm pl}m_{3/2}}\left(1-\frac{m_\lambda^2}{s}\right)^{1/2}(1-\cos\theta) \tag{A.49}$$

$$\mathcal{M}^{(\uparrow\downarrow\uparrow\uparrow)} = \frac{igm_\lambda}{\sqrt{6}M_{\rm pl}m_{3/2}}\sqrt{s}\left(1-\frac{m_\lambda^2}{s}\right)^{1/2}\sin\theta \tag{A.50}$$

$$\mathcal{M}^{(\uparrow\downarrow\downarrow\downarrow)} = \frac{-igm_\lambda}{\sqrt{6}M_{\rm pl}m_{3/2}}\sqrt{s}\left(1-\frac{m_\lambda^2}{s}\right)^{1/2}\sin\theta \tag{A.51}$$

$$\mathcal{M}(\text{others}) = 0 \tag{A.52}$$

We see that the high energy behavior $\mathcal{M}\sim s$ is actually canceled out and the amplitude is proportional to the SUSY-breaking parameter, the gaugino mass $m_\lambda$, for every helicity.

**Amplitudes at one-loop level**

In GMSB models, there are messenger fields which contribute to the gravitino production through one-loop diagrams. There are 16 diagrams in total. We part them into four groups and label them as diagrams C, D, E and F.

**Diagram C**

There are four diagrams in group C which have a universal form

$$\begin{aligned}\mathcal{M}_s^{(1)C} &= [\bar v(p_2)(ig\gamma^\mu P_L)u(p_1)]\times\frac{-ig_{\mu\nu}}{(p_1+p_2)^2}\times\left[\tilde{\mathcal{M}}_s^{(1)C_1}+\tilde{\mathcal{M}}_s^{(1)C_2}+\tilde{\mathcal{M}}_s^{(1)C_3}+\tilde{\mathcal{M}}_s^{(1)C_4}\right]^\nu \\ &= \frac{g}{s}\left[\bar v(p_2)\gamma^\mu P_L u(p_1)\right]g_{\mu\nu}\left[\tilde{\mathcal{M}}_s^{(1)C_1}+\tilde{\mathcal{M}}_s^{(1)C_2}+\tilde{\mathcal{M}}_s^{(1)C_3}+\tilde{\mathcal{M}}_s^{(1)C_4}\right]^\nu .\end{aligned} \tag{A.53}$$

For the first and second diagrams,

$$\begin{aligned}\left[\tilde{\mathcal{M}}_s^{(1)C_1}\right]^\nu &= \int\frac{d^4k}{(2\pi)^4}\bar{\bar\psi}_\rho(p_3)\left[\frac{1}{\sqrt{2}M_{\rm pl}}\not{k}\gamma^\rho P_L\right]\frac{i(\not{k}+\not{p}_3+M)}{(k+p_3)^2-M^2}(-\sqrt{2}gP_L)v(p_4) \\ &\qquad\times\frac{i}{k^2-M^2}(-i\lambda F_S)\times ig(2k+p_3+p_4)^\nu\times\frac{i}{(k+p_3+p_4)^2-M^2} \\ &= \frac{-g^2\lambda F_S M}{M_{\rm pl}}\int\frac{d^4k}{(2\pi)^4}\frac{1}{[k^2-M^2]^2}\frac{1}{(k+p_3)^2-M^2}\frac{1}{(k+p_3+p_4)^2-M^2} \\ &\qquad\times\bar{\bar\psi}_\rho(p_3)P_L v(p_4)\times 2k^\rho(2k+p_3+p_4)^\nu,\end{aligned} \tag{A.54}$$

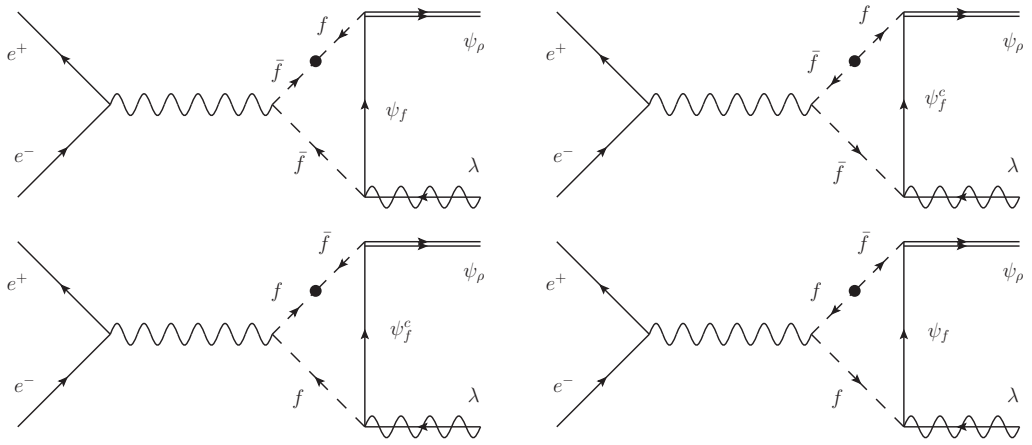


Figure 19: Gravitino production process at at one-loop level: diagrams C

and

$$\left[\tilde{\mathcal{M}}_s^{(1)C_2}\right]^\nu = \int \frac{d^4k}{(2\pi)^4} \bar{\tilde{\psi}}_\rho(p_3) \left[\frac{1}{\sqrt{2}M_{\rm pl}} P_R \not{k} \gamma^\rho\right] \frac{i(\not{k}+\not{p}_3+M)}{(k+p_3)^2-M^2} (\sqrt{2}gP_R) v(p_4)$$
$$\times \frac{i}{k^2-M^2}(-i\lambda F_S) \times -ig(2k+p_3+p_4)^\nu \times \frac{i}{(k+p_3+p_4)^2-M^2}$$
$$= \frac{-g^2\lambda F_S M}{M_{\rm pl}} \int \frac{d^4k}{(2\pi)^4} \frac{1}{[k^2-M^2]^2} \frac{1}{(k+p_3)^2-M^2} \frac{1}{(k+p_3+p_4)^2-M^2}$$
$$\times \bar{\tilde{\psi}}_\rho(p_3) P_R v(p_4) \times 2k^\rho (2k+p_3+p_4)^\nu. \tag{A.55}$$

Diagram $C_3/C_4$ gives exactly the same contribution as $C_1/C_4$. Then,

$$\left[\tilde{\mathcal{M}}_s^{(1)C}\right]^\nu = 2\left[\tilde{\mathcal{M}}_s^{(1)C_1}\right]^\nu + 2\left[\tilde{\mathcal{M}}_s^{(1)C_2}\right]^\nu$$
$$= \frac{-2g^2\lambda F_S M}{M_{\rm pl}} \int \frac{d^4k}{(2\pi)^4} \frac{1}{[k^2-M^2]^2} \frac{1}{(k+p_3)^2-M^2} \frac{1}{(k+p_3+p_4)^2-M^2}$$
$$\times \bar{\tilde{\psi}}_\rho(p_3) v(p_4) \times 2k^\rho (2k+p_3+p_4)^\nu. \tag{A.56}$$

The denominators in the integral can be combined using the Feynman parameters,

$$\frac{1}{[k^2-M^2]^2} \frac{1}{(k+p_3)^2-M^2} \frac{1}{(k+p_3+p_4)^2-M^2} = \int_0^1 dxdydx\delta(x+y+z-1)\frac{6x}{D^4}, \tag{A.57}$$

where

$$D = x(k^2-M^2) + y((k+p_3)^2-M^2) + z((k+p_3+p_4)^2-M^2)$$
$$= k^2 + 2((y+z)p_3 + zp_4)\cdot k + sz - M^2. \tag{A.58}$$

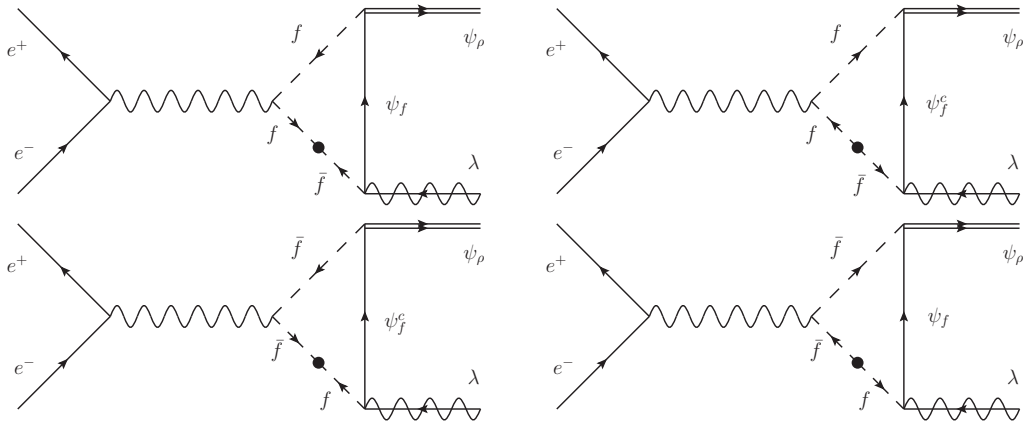


Figure 20: Gravitino production process at at one-loop level: diagrams D

We have used the relations

$$p_3^2 = m_{3/2}^2, \quad p_4^2 = m_\lambda^2, \quad 2p_3 \cdot p_4 = s - m_\lambda^2 \tag{A.59}$$

and took the limit of $m_{3/2} \to 0$. We shift the loop momentum $k$ to complete the square,

$$D = \ell^2 - \Delta, \tag{A.60}$$

where

$$\ell = k + (y+z)p_3 + zp_4, \tag{A.61}$$

and

$$\Delta = -z(1-y-z)s - yzm_\lambda^2 + M^2. \tag{A.62}$$

We get

$$\begin{aligned}\left[\tilde{\mathcal{M}}_s^{(1)C}\right]^\nu = \frac{-2g^2\lambda F_S M}{M_{\rm pl}}[\bar{\tilde{\psi}}_\rho(p_3)v(p_4)] \int_0^1 dxdydz\delta(x+y+z-1)6x \\ \times \int \frac{d^4\ell}{(2\pi)^4} \frac{\ell^2 g^{\nu\rho} - 2z(1-2y-2z)p_3^\nu p_4^\rho - 2z(1-2z)p_4^\nu p_4^\rho}{(\ell^2-\Delta)^4}.\end{aligned} \tag{A.63}$$

**Diagrams D**

With almost the same calculation to diagrams C, the amplitude for the diagrams D is

$$\mathcal{M}_s^{(1)D} = \frac{g}{s}\left[\bar{v}(p_2)\gamma^\mu P_L u(p_1)\right] g_{\mu\nu}\left[\tilde{\mathcal{M}}_s^{(1)D}\right]^\nu, \tag{A.64}$$

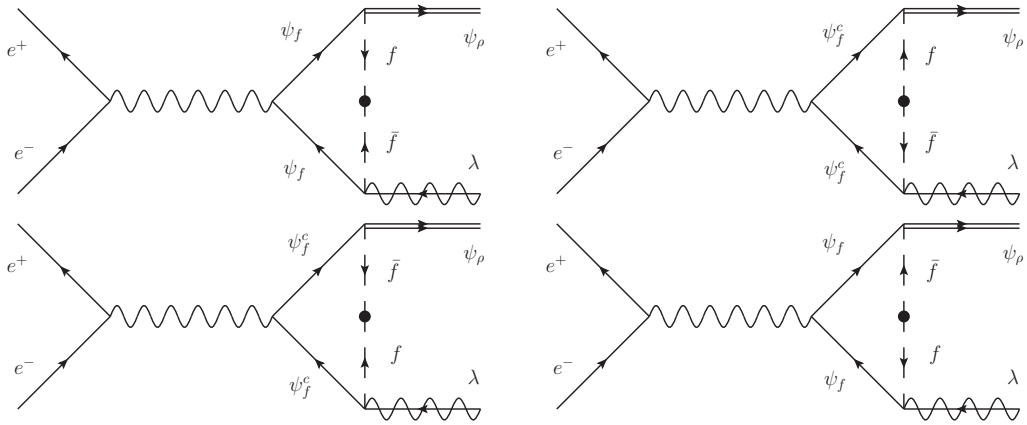


Figure 21: Gravitino production process at at one-loop level: diagrams E

with

$$\left[\tilde{\mathcal{M}}_s^{(1)D}\right]^\nu = \frac{-2g^2\lambda F_S M}{M_{\rm pl}}[\bar{\tilde{\psi}}_\rho(p_3)v(p_4)]\int_0^1 dxdydz\delta(x+y+z-1)6z \\ \times\int\frac{d^4\ell}{(2\pi)^4}\frac{\ell^2 g^{\nu\rho}-2z(1-2y-2z)p_3^\nu p_4^\rho-2z(1-2z)p_4^\nu p_4^\rho}{(\ell^2-\Delta)^4}. \tag{A.65}$$

**Diagrams E**

The loop structure of diagrams E is somewhat different from that of diagrams C and D in that there are two fermion lines in diagrams E, but the final formula reduces to a similar one to that of C and D,

$$\mathcal{M}_s^{(1)E} = \frac{g}{s}\left[\bar{v}(p_2)\gamma^\mu P_L u(p_1)\right] g_{\mu\nu}\left[\tilde{\mathcal{M}}_s^{(1)E}\right]^\nu, \tag{A.66}$$

with

$$\left[\tilde{\mathcal{M}}_s^{(1)E}\right]^\nu = \frac{-2g^2\lambda F_S M}{M_{\rm pl}}[\bar{\tilde{\psi}}_\rho(p_3)v(p_4)]\int_0^1 dxdydz\delta(x+y+z-1)6y \\ \times\int\frac{d^4\ell}{(2\pi)^4}\frac{\ell^2 g^{\nu\rho}-4z(1-y-z)p_3^\nu p_4^\rho+4z^2 p_4^\nu p_4^\rho}{(\ell^2-\Delta)^4}. \tag{A.67}$$

**Diagrams F**

Also for diagrams F,

$$\mathcal{M}_s^{(1)F} = \frac{g}{s}\left[\bar{v}(p_2)\gamma^\mu P_L u(p_1)\right] g_{\mu\nu}\left[\tilde{\mathcal{M}}_s^{(1)F}\right]^\nu, \tag{A.68}$$

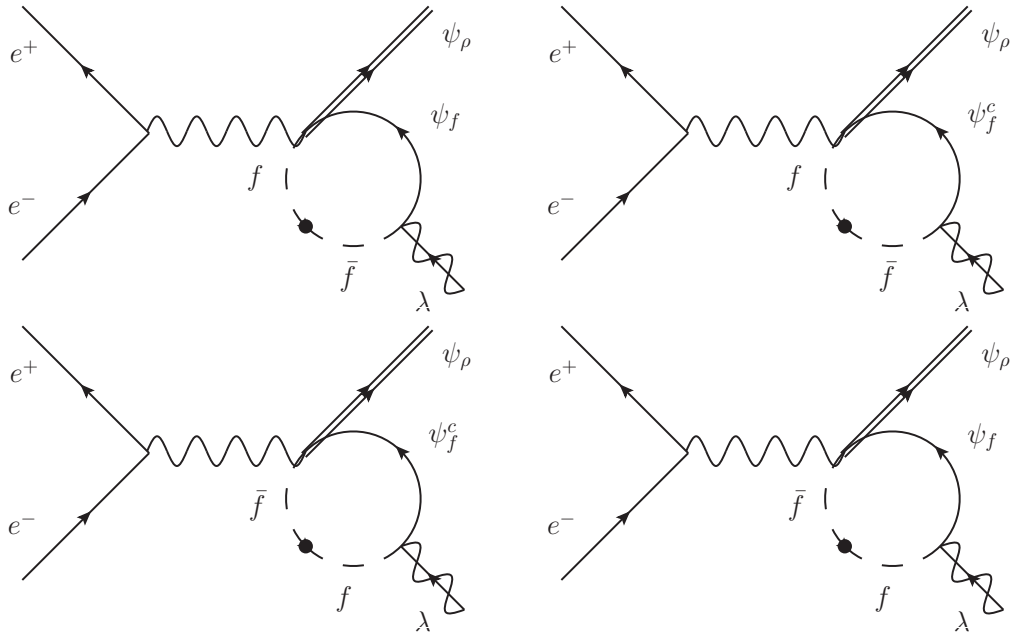


Figure 22: Gravitino production process at at one-loop level: diagrams F

with

$$\left[\tilde{\mathcal{M}}_s^{(1)F}\right]^\nu = \frac{2g^2\lambda F_S M}{M_{\rm pl}} \int \frac{d^4k}{(2\pi)^4} \frac{1}{[k^2-M^2]^2} \frac{1}{(k-p_4)^2-M^2} \times \bar{\tilde{\psi}}_\rho(p_3)\gamma^\nu\gamma^\rho v(p_4)$$
$$= \frac{4g^2\lambda F_S M}{M_{\rm pl}} [\bar{\tilde{\psi}}^\nu(p_3)v(p_4)] \int \frac{d^4k}{(2\pi)^4} \frac{1}{[k^2-M^2]^2} \frac{1}{(k-p_4)^2-M^2}. \tag{A.69}$$

The integral can be explicitly implemented,

$$\int \frac{d^4k}{(2\pi)^4} \frac{1}{[k^2-M^2]^2} \frac{1}{(k-p_4)^2-M^2} = -\frac{i}{2(4\pi)^2} \frac{1}{M^2}. \tag{A.70}$$

We get

$$\left[\tilde{\mathcal{M}}_s^{(1)F}\right]^\nu = -\frac{2ig^2\lambda F_S}{(4\pi)^2 M_{\rm pl} M} [\bar{\tilde{\psi}}^\nu(p_3)v(p_4)]. \tag{A.71}$$

**Combine**

First let us combine the amplitudes of diagrams C, D and E,

$$\left[\tilde{\mathcal{M}}_s^{(1)C}\right]^\nu + \left[\tilde{\mathcal{M}}_s^{(1)D}\right]^\nu + \left[\tilde{\mathcal{M}}_s^{(1)E}\right]^\nu = \frac{-12g^2\lambda F_S M}{M_{\rm p}} [\bar{\tilde{\psi}}_\rho(p_3)v(p_4)] \int_0^1 dxdydz\delta(x+y+z-1)$$
$$\times \int \frac{d^4\ell}{(2\pi)^4} \frac{\ell^2 g^{\nu\rho} - 2z(x-z)(p_3^\nu p_4^\rho + p_4^\nu p_4^\rho)}{(\ell^2-\Delta)^4}. \tag{A.72}$$

Integrals can be implemented explicitly,

$$\int \frac{d^4\ell}{(2\pi)^4}\frac{\ell^2}{(\ell^2-\Delta)^4} = -\frac{i}{3}\frac{1}{(4\pi)^2}\frac{1}{\Delta}, \tag{A.73}$$

$$\int \frac{d^4\ell}{(2\pi)^4}\frac{1}{(\ell^2-\Delta)^4} = \frac{i}{6}\frac{1}{(4\pi)^2}\frac{1}{\Delta^2}. \tag{A.74}$$

Inserting these formula,

$$\left[\tilde{\mathcal{M}}_s^{(1)C}\right]^\nu + \left[\tilde{\mathcal{M}}_s^{(1)D}\right]^\nu + \left[\tilde{\mathcal{M}}_s^{(1)E}\right]^\nu = \frac{4ig^2\lambda F_S M}{(4\pi)^2 M_{\rm p}}[\bar{\tilde{\psi}}_\rho(p_3)v(p_4)]\int_0^1 dxdydz\delta(x+y+z-1) \times\left[\frac{1}{\Delta}g^{\nu\rho}+\frac{1}{\Delta^2}z(x-z)(p_3^\nu p_4^\rho+p_4^\nu p_4^\rho)\right]. \tag{A.75}$$

We define dimensionless functions $f_1(s,M^2)$ and $f_2(s,M^2)$,

$$f_1(s,M^2) \equiv M^2\int_0^1 dxdydz\delta(x+y+z-1)\frac{2}{\Delta}, \tag{A.76}$$

$$f_2(s,M^2) \equiv M^4\int_0^1 dxdydz\delta(x+y+z-1)\frac{2}{\Delta^2}z(x-z), \tag{A.77}$$

to make the amplitude more simple,

$$\left[\tilde{\mathcal{M}}_s^{(1)C}\right]^\nu + \left[\tilde{\mathcal{M}}_s^{(1)D}\right]^\nu + \left[\tilde{\mathcal{M}}_s^{(1)E}\right]^\nu = \frac{2ig^2\lambda F_S}{(4\pi)^2 M_{\rm pl}M}[\bar{\tilde{\psi}}_\rho(p_3)v(p_4)]\left[f_1(s,M^2)\delta_\mu^\rho+\frac{1}{M^2}f_2(s,M^2)(p_{3\mu}p_4^\rho+p_{4\mu}p_4^\rho)\right]. \tag{A.78}$$

Together with the contribution from diagrams F,

$$\left[\tilde{\mathcal{M}}_s^{(1)C}\right]^\nu + \left[\tilde{\mathcal{M}}_s^{(1)D}\right]^\nu + \left[\tilde{\mathcal{M}}_s^{(1)E}\right]^\nu + \left[\tilde{\mathcal{M}}_s^{(1)F}\right]^\nu = \frac{2ig^2\lambda F_S}{(4\pi)^2 M_{\rm pl}M}[\bar{\tilde{\psi}}_\rho(p_3)v(p_4)]\left[[f_1(s,M^2)-1]\delta_\mu^\rho+\frac{1}{M^2}f_2(s,M^2)(p_{3\mu}p_4^\rho+p_{4\mu}p_4^\rho)\right]. \tag{A.79}$$

Altogether,

$$\mathcal{M}_s^{(1)} = \frac{g}{s}\left[\bar{v}(p_2)\gamma^\mu P_L u(p_1)\right] g_{\mu\nu}\left[\tilde{\mathcal{M}}_s^{(1)}\right]^\nu = \frac{2ig^3\lambda F_S}{(4\pi)^2 M_{\rm pl}M}\frac{1}{s}\left[\bar{v}(p_2)\gamma^\mu P_L u(p_1)\right][\bar{\tilde{\psi}}_\rho(p_3)v(p_4)]\left[[f_1(s,M^2)-1]\delta_\mu^\rho+\frac{1}{M^2}f_2(s,M^2)(p_{3\mu}p_4^\rho+p_{4\mu}p_4^\rho)\right]. \tag{A.80}$$

Inserting the explicit formula for each spinor, we get helicity amplitudes. We can see that the terms proportional to $f_2(s,M^2)$ vanish for a high energy limit. The function $f_1(s,M^2)$ can be rewritten by the $C$-function,

$$f_1(s,M^2) = -2M^2C_0(\sqrt{s},M). \tag{A.81}$$

The final results are

$$\mathcal{M}_s^{(1)(\uparrow\downarrow\uparrow\uparrow)} = -\frac{2ig^3\lambda F_S}{\sqrt{6}(4\pi)^2 M_{\rm pl} M}[2M^2 C_0(\sqrt{s}, M) + 1]\sqrt{s}\sin\theta, \tag{A.82}$$

$$\mathcal{M}_s^{(1)(\uparrow\downarrow\downarrow\downarrow)} = \frac{2ig^3\lambda F_S}{\sqrt{6}(4\pi)^2 M_{\rm pl} M}[2M^2 C_0(\sqrt{s}, M) + 1]\sqrt{s}\sin\theta, \tag{A.83}$$

$$\mathcal{M}_s^{(1)}(\text{others}) = 0. \tag{A.84}$$

Together with the tree-level contributions, we see that the calculations with supergravity Lagrangian indeed reproduce the formulae given by global SUSY calculations, as in Eq. (2.25).

# B Interactions and decays of $S$

## B.1 Pseudo-moduli interactions with the MSSM fields

The pseudo-moduli $S$ interacts with the MSSM fields through the messenger loop diagrams. The interactions can be read off from the $\langle S\rangle$ dependence of the low energy parameters [53, 54]. Since we follow the cosmological evolution of the real component of $S$ field, we only list the interactions between the real component of $S$ and the MSSM fields which are needed to study the decay of $S$. In the following in this section we have implicitly took the imaginary component of $S$ to be zero.

For scalar fields $\tilde{f}$, the effective interaction Lagrangian is written as

$$\mathcal{L}_{\tilde{f}} = \frac{(m_{\rm eff}^{\tilde{f}})^2}{\langle S\rangle} S\tilde{f}^\dagger\tilde{f} + \text{h.c.} \tag{B.1}$$

The effective mass parameter $(m_{\rm eff}^{\tilde{f}})^2$ is a part of the scalar mass that is proportional to $1/|\langle S\rangle|^2$. One element of the scalar mass is the contribution from the gauge mediation,

$$(m_{\rm GM}^{\tilde{f}})^2 = \left[\frac{g^2}{(4\pi)^2}\right]^2 \cdot 2C_2 \left|\frac{m^2}{\langle S\rangle}\right|^2, \tag{B.2}$$

which is induced at the messenger mass scale $M_{\rm mess}$. If the gauge mediation is the only source of the scalar mass, $m_{\rm eff}^{\tilde{f}}$ is identical to their mass. In that case, $m_{\rm eff}^{\tilde{f}}$ is the gauge mediation contribution plus the radiative corrections. In the model of interest, $m_{H_u}$ consists of two sources; one is from the gauge mediation and the other is from the direct coupling to the pseudo-moduli (C.1). The latter piece does not depend on $\langle S\rangle$ so is nothing to do with the effective coupling constant.

Since we evaluate the abundance of non-thermally produced higgsino to check the BBN constraint later, we list the interaction with higgsino,

$$\mathcal{L}_{\tilde{h}} = -\frac{\mu_{\rm eff}}{\langle S\rangle} S\ (\bar{h}_d^c \cdot P_L h_u) + \text{h.c.} \tag{B.3}$$

The coefficient $\mu_{\rm eff}$ is a part of $\mu$ that is proportional to $1/\langle S\rangle$. Actually, in the model $\mu$-term is generated at the cutoff scale $\Lambda$ through the Kähler potential Eq. (C.1) and it does not have $\langle S\rangle$ dependence. The VEV dependence of $\mu_{\rm eff}$ appears only through the renormalization group running, but the effect is very small for the $\mu$-term. The effective coupling $\mu_{\rm eff}$ is suppressed compared to the $\mu$-term, typically

$$|\mu_{\rm eff}| \sim 0.01 \times |\mu|. \tag{B.4}$$

Among the effective coupling, the Higgs mass parameter $m_{\rm eff}^{H_u}$ is enhanced by the large renormalization group running [54],

$$-(m_{\rm eff}^{H_u})^2 = (\kappa m_{\tilde{B}})^2, \tag{B.5}$$

with

$$\kappa \simeq 3 - 4. \tag{B.6}$$

## B.2 Decays of pseudo-moduli

### Main decay mode

The $S$ field mainly decays into the MSSM particles. Since the mass parameter $m_{\rm eff}^{H_u}$ is enhanced over other SUSY breaking parameters, the decay rate into the Higgs boson is enhanced. For $m_S > 2m_h$, the main decay channel turns out to be $S \to hh, ZZ$ and $WW$, where the gauge bosons are longitudinally polarized [54],

$$\Gamma_{S\to hh} + \Gamma_{S\to ZZ} + \Gamma_{S\to WW} \simeq \frac{1}{8\pi m_S}\left(\frac{(m_{\rm eff}^{H_u})^2 \sin^2\beta}{\langle S\rangle}\right)^2. \tag{B.7}$$

We define the decay temperature of $S$ by

$$T_d \equiv \left(\frac{\pi^2 g_*}{90}\right)^{-1/4} \sqrt{M_{\rm pl}\Gamma_S}, \tag{B.8}$$

where $\Gamma_S$ is the total decay width of $S$. By approximating the total decay width by that of the main channel, we get

$$T_d \simeq 68\text{GeV}\left(\frac{g_*}{15}\right)^{-1/4}\left(\frac{m_{\rm eff}^{H_u}}{5\ \text{TeV}}\right)^2\left(\frac{m_{\tilde{g}}}{5\ \text{TeV}}\right)^{3/4}\left(\frac{m_{3/2}}{500\ \text{MeV}}\right)^{-5/4}. \tag{B.9}$$

**Non-thermal gravitino production**

Gravitinos are also produced non-thermally by the rare decay $S \to \psi_{3/2}\psi_{3/2}$. The interaction between the pseudo-moduli field and the gravitino (goldstino) appears from the higher term of the Kähler potential in Eq. (5.28), and the decay width is calculated to be [53, 54]

$$\Gamma_{3/2} = \frac{1}{96\pi}\frac{m_S^3}{M_{\rm pl}^2}\left(\frac{m_S}{m_{3/2}}\right)^2. \tag{B.10}$$

If $S$ dominates the energy density of the Universe, non-thermal gravitino abundance is calculated to be

$$\Omega_{3/2}^{\rm NT} = \frac{3}{4}m_{3/2}\frac{T_d}{m_S} \times 2B_{3/2}/(\rho_c/s)_0, \tag{B.11}$$

where $(\rho_c/s)_0 \simeq 1.8 \times 10^{-9}$GeV is the critical density divided by the entropy density at present. The main decay mode of $S$ is $S \to hh, ZZ$ and $WW$, and the non-thermal gravitino is estimated as

$$\Omega_{3/2}^{\rm NT} \simeq 0.2\left(\frac{m_{3/2}}{2\ {\rm GeV}}\right)^{9/4}\left(\frac{m_{\tilde g}}{5\ {\rm TeV}}\right)^{5/4}\left(\frac{m_{\rm eff}^{H_u}}{5\ {\rm TeV}}\right)^{-2}. \tag{B.12}$$

The Dark Matter is also explained by non-thermally produced gravitino with $m_{3/2} \sim 2$GeV. This statement does not depend on the initial condition of $S$ as long as the pseudo-moduli once dominates the energy density of the Universe. Taking into account possible theoretical errors, we show the parameter region where $0.03 \lesssim \Omega_{3/2}^{\rm NT}h^2 \lesssim 0.3$ is predicted as a pink band in Fig. **??**. In the pink region thermal leptogenesis is also possible with a suitable value of the reheating temperature

# C $\mu$-problem and a light higgsino

## C.1 A solution to the $\mu$-problem

Here we present a possible solution to the $\mu$-problem. As we see below, the solution predicts a relatively light higgsino compared to $M_{\rm SUSY}$. We check whether a light higgsino scenario is allowed by the BBN constraint.

In order to avoid too large $\mu$-term, we assume an approximate Peccei-Quinn (PQ) U(1) symmetry with a charge assignment $PQ(H_u) = PQ(H_d) = 1$. Also, to realize the relation $\mu^2 \sim m_{H_u}^2$, we assume the following general interactions between $S$ and the Higgs superfields at the cutoff scale [52],

$$K^{\rm (Higgs)} = \left(c_\mu\frac{S^\dagger H_u H_d}{\Lambda} + {\rm h.c.}\right) - c_H\frac{S^\dagger S(H_u^\dagger H_u + H_d^\dagger H_d)}{\Lambda^2}, \tag{C.1}$$

where the PQ charge of $S$ is fixed as $PQ(S) = 2$. Once the $F$-component of $S$ develops a VEV, $\mu$-term and the Higgs scalar mass terms emerge at the scale $\Lambda$. The relation $\mu^2 \sim m_{H_u}^2$, which is needed for satisfying the condition of electroweak symmetry breaking without a serious fine-tuning, naturally realizes if the coefficients $c_\mu$ and $c_H$ are both $\mathcal{O}(1)$.

Possible origins of the Kähler potential (C.1) are discussed in Ref. [52] by studying dynamics of UV models above the cutoff scale $\Lambda$. There, it is found that the coefficients $c_\mu$ and $c_H$ tend to have a mild hierarchy, and we typically have $\mu/m_H \sim 1/10$. This hierarchy implies that the Higgs scalar mass parameter $m_{H_u}$ tends to be above the order of TeV scale for a moderate value of $\mu$-term, namely $m_{H_u} \gtrsim \mathcal{O}(1)$ TeV for $\mu \gtrsim \mathcal{O}(100)$ GeV.

We do not regard this small hierarchy as catastrophic; actually, this hierarchy is consistent with the relatively heavy Higgs boson mass. In order for the electroweak symmetry to be broken radiatively, the condition

$$\frac{M_Z^2}{2} \simeq -\mu^2 - m_{H_u}^2(\Lambda) - \delta m_{H_u}^2 \tag{C.2}$$

must be satisfied. $\delta m_{H_u}^2$ is a contribution from the radiative corrections. With positive $m_{H_u}^2(\Lambda)$ and $\mu^2 \ll m_{H_u}^2(\Lambda)$, $\delta m_{H_u}^2$ must be negative and large to satisfy the condition (C.2), which is realized by the contributions from the stop-loop diagrams if the stop mass $m_{\tilde{t}}$ is large. Large stop mass subsequently induce a large contribution proportional to $m_{\tilde{t}}^2$ to the Higgs boson mass again through the stop-loop diagram to realize a relatively heavy Higgs boson. In summary, in this set-up, the $\mu$-problem is ameliorated by the generalized version of the Giudice-Masiero mechanism with the Kähler potential in Eq. (C.1), which in turn leads the relatively small $\mu$-term and the relatively heavy Higgs boson mass in accord with $m_h = 125$ GeV.

Although it is difficult to discover a SUSY particles at the LHC experiments when $M_{\rm SUSY} \sim 5$ TeV, it predicts a light higgsino with $m_{\tilde{h}} \simeq \mathcal{O}(100)$GeV. Therefore, in this scenario, there is a chance to discover a light higgsino in the future experiment.

## C.2 Constraints from BBN

The light higgsino in GMSB is subject to the constraints from BBN. The constraints on the primordial abundance of the lightest neutralino $\chi$ is studied in Ref. [87]. They analyzed the decay process of the neutralino and presented constraints on $Y_\chi = n_\chi/s$, the yield of $\chi$, in a Bino-like NLSP case. We use the constraints to derive those for the higgsino.

Since the life-time of a neutralino $\chi$ is approximately proportional to $m_{3/2}^2/m_\chi^5$, constraints

on the primordial abundance are more severe for larger $m_{3/2}$ or smaller $m_\chi$. We focus on a case that the mass of NLSP (in our case higgsino) is 300 GeV. According to Ref. [87], if the gravitino is heavier than $\sim 500$ MeV, the stringent bound on the bino abundance comes from the overproduction of the Deuterium. For 10 MeV $\lesssim m_{3/2} \lesssim$ 500 MeV, the bound is from the overproduction of $^4$He,

$$m_{\tilde{B}} Y_{\tilde{B}} \lesssim 10^{-13}\text{GeV} \quad (500\text{ MeV} \lesssim m_{3/2} \lesssim 100\text{ GeV}), \tag{C.3}$$

$$m_{\tilde{B}} Y_{\tilde{B}} \lesssim 10^{-9}\text{GeV} \quad (10\text{ MeV} \lesssim m_{3/2} \lesssim 500\text{ MeV}). \tag{C.4}$$

The bound is much weaker for $m_{3/2} \lesssim 10$ MeV. We estimate the higgsino abundance in the scenario and check whether a light higgsino is allowed by BBN.

Higgsinos are produced non-thermally from the decay of the pseudo-moduli,

$$Y_{\tilde{h}} = \frac{3}{4}\frac{T_d}{m_S} \times 2B_{\tilde{h}}, \tag{C.5}$$

where $B_{\tilde{h}}$ is the branching ratio of the decay process $S \to \tilde{h}\tilde{h}$ and the decay temperature $T_d$ is well approximated by Eq. (B.9). $Y_{\tilde{h}}$ depends on two effective couplings : $m_{\text{eff}}^{H_u}$ and $\mu_{\text{eff}}$ defined in appendix **??**. Remaining these parameters, the higgsino abundance is estimated as

$$m_{\tilde{h}} Y_{\tilde{h}} \simeq 1.2 \times 10^{-7}\text{GeV} \left(\frac{m_{3/2}}{500\text{ MeV}}\right)^{-3/4} \left(\frac{m_{\text{eff}}^{H_u}}{5\text{ TeV}}\right)^{-2} \left(\frac{\mu_{\text{eff}}}{5\text{ GeV}}\right)^{2}. \tag{C.6}$$

The abundance of the non-thermally produced higgsinos is decreased by the subsequent annihilation process. This effect can be taken into account by solving the Boltzmann equation,

$$\dot{n}_{\tilde{h}} + 3Hn_{\tilde{h}} = -\langle\sigma v\rangle n_{\tilde{h}}^2, \tag{C.7}$$

where $\langle\sigma v\rangle$ is the thermal averaged annihilation cross section of higgsino [88] [†] ,

$$\langle\sigma v\rangle = \frac{g^4}{128\pi\mu^2}\left(\frac{3}{2} + \tan^2\theta_W + \frac{\tan^2\theta_W}{2}\right), \tag{C.8}$$

where $\theta_W$ is Weinberg angle. The solution of the Boltzmann equation (C.7) is approximated by a simple analytic formula [89, 54]. In terms of the yield value $Y_{\tilde{h}} = n_{\tilde{h}}/s$,

$$Y_{\tilde{h}}(T) \simeq \left[\frac{1}{Y_{\tilde{h}}(T_d)} + \sqrt{\frac{8\pi^2 g_*(T_d)}{45}}\langle\sigma v\rangle M_{\text{pl}}(T_d - T)\right]^{-1}. \tag{C.9}$$

[†]We have not included co-annihilation effects to make a conservative estimate.

If the initial abundance $Y_{\tilde{h}}(T_d)$ produced by the decay of $S$ is large enough, the resultant abundance for $T \ll T_d$ is independent of $Y_{\tilde{h}}(T_d)$. In this case, the abundance is estimated by

$$Y_{\tilde{h}} \simeq 8.2 \times 10^{-13} \left(\frac{15}{g_*}\right)^{1/2} \left(\frac{10 \text{ GeV}}{T_d}\right) \left(\frac{10^{-8} \text{ GeV}^{-2}}{\langle \sigma v \rangle}\right). \tag{C.10}$$

For higgsino with $m_{\tilde{h}} = 300$ GeV,

$$m_{\tilde{h}} Y_{\tilde{h}} \simeq 3.9 \times 10^{-11} \text{GeV} \Big(\frac{15}{g_*}\Big)^{3/4} \Big(\frac{m_{\text{eff}}^{H_u}}{5 \text{ TeV}}\Big)^{-2} \Big(\frac{m_{\tilde{g}}}{5 \text{ TeV}}\Big)^{-3/4} \Big(\frac{m_{3/2}}{500 \text{ MeV}}\Big)^{5/4} \Big(\frac{\mu}{300 \text{ GeV}}\Big)^{2}. \tag{C.11}$$

Compared with Eq. (C.3) and (C.4), we see that the higgsino abundance is below the BBN constraint for $m_{3/2} \lesssim 500$ MeV with the help of the annihilation process.

## References


[1] M. Dine, W. Fischler and M. Srednicki, Nucl. Phys. B **189**, 575 (1981); S. Dimopoulos and S. Raby, Nucl. Phys. B **192**, 353 (1981); M. Dine and W. Fischler, Phys. Lett. B **110**, 227 (1982); Nucl. Phys. B **204**, 346 (1982); C. R. Nappi and B. A. Ovrut, Phys. Lett. B **113**, 175 (1982); L. Alvarez-Gaume, M. Claudson and M. B. Wise, Nucl. Phys. B **207**, 96 (1982); S. Dimopoulos and S. Raby, Nucl. Phys. B **219**, 479 (1983).

[2] M. Dine and A. E. Nelson, Phys. Rev. D **48**, 1277 (1993) [hep-ph/9303230]; M. Dine, A. E. Nelson, Y. Nir and Y. Shirman, Phys. Rev. D **53**, 2658 (1996) [hep-ph/9507378]; M. Dine, A. E. Nelson and Y. Shirman, Phys. Rev. D **51**, 1362 (1995) [hep-ph/9408384].

[3] P. Draper, P. Meade, M. Reece and D. Shih, Phys. Rev. D **85**, 095007 (2012) [arXiv:1112.3068 [hep-ph]].

[4] E.W. Kolb and M.S. Turner, *The Early Universe*, (Westview Press, 1994).

[5] T. Moroi, H. Murayama and M. Yamaguchi, Phys. Lett. B **303**, 289 (1993).

[6] M. Kawasaki and T. Moroi, Prog. Theor. Phys. **93**, 879 (1995) [hep-ph/9403364, hep-ph/9403061].

[7] T. Moroi, hep-ph/9503210.

[8] A. de Gouvea, T. Moroi and H. Murayama, Phys. Rev. D **56**, 1281 (1997) [hep-ph/9701244].

[9] M. Bolz, W. Buchmuller and M. Plumacher, Phys. Lett. B **443**, 209 (1998) [hep-ph/9809381].

[10] M. Bolz, A. Brandenburg and W. Buchmuller, Nucl. Phys. B **606**, 518 (2001) [Erratum-ibid. B **790**, 336 (2008)] [hep-ph/0012052].

[11] J. Pradler and F. D. Steffen, Phys. Rev. D **75**, 023509 (2007) [hep-ph/0608344].

[12] J. Pradler and F. D. Steffen, Phys. Lett. B **648**, 224 (2007) [hep-ph/0612291].

[13] V. S. Rychkov and A. Strumia, Phys. Rev. D **75**, 075011 (2007) [hep-ph/0701104].

[14] M. Kawasaki, K. Kohri and T. Moroi, Phys. Rev. D **71**, 083502 (2005) [astro-ph/0408426].

[15] E. Komatsu *et al.* [WMAP Collaboration], Astrophys. J. Suppl. **180**, 330 (2009) [arXiv:0803.0547 [astro-ph]].

[16] M. Fukugita and T. Yanagida, Phys. Lett. B **174**, 45 (1986).

[17] S. Davidson and A. Ibarra, Phys. Lett. B **535**, 25 (2002) [hep-ph/0202239].

[18] G. F. Giudice, A. Notari, M. Raidal, A. Riotto and A. Strumia, Nucl. Phys. B **685**, 89 (2004) [hep-ph/0310123].

[19] W. Buchmuller, R. D. Peccei and T. Yanagida, Ann. Rev. Nucl. Part. Sci. **55**, 311 (2005) [hep-ph/0502169].

[20] W. Buchmuller, P. Di Bari and M. Plumacher, Annals Phys. **315**, 305 (2005) [hep-ph/0401240].

[21] G. 't Hooft and M. J. G. Veltman, Nucl. Phys. B **153**, 365 (1979).

[22] K. Choi, K. Hwang, H. B. Kim and T. Lee, Phys. Lett. B **467**, 211 (1999) [hep-ph/9902291].

[23] K. Jedamzik, M. Lemoine and G. Moultaka, Phys. Rev. D **73**, 043514 (2006) [hep-ph/0506129].

[24] I. Dalianis, arXiv:1304.7673 [hep-ph].

[25] K. A. Intriligator and N. Seiberg, Class. Quant. Grav. **24**, S741 (2007) [hep-ph/0702069].

[26] E. Witten, Nucl. Phys. B **188**, 513 (1981).

[27] E. Witten, Nucl. Phys. B **202**, 253 (1982).

[28] I. Affleck, M. Dine and N. Seiberg, Nucl. Phys. B **241**, 493 (1984).

[29] I. Affleck, M. Dine and N. Seiberg, Phys. Rev. Lett. **52**, 1677 (1984).

[30] I. Affleck, M. Dine and N. Seiberg, Nucl. Phys. B **256**, 557 (1985).

[31] K. A. Intriligator and S. D. Thomas, Nucl. Phys. B **473**, 121 (1996) [hep-th/9603158].

[32] K. -I. Izawa and T. Yanagida, Prog. Theor. Phys. **95**, 829 (1996) [hep-th/9602180].

[33] K. A. Intriligator, N. Seiberg and D. Shih, JHEP **0604**, 021 (2006) [hep-th/0602239].

[34] A. E. Nelson and N. Seiberg, Nucl. Phys. B **416**, 46 (1994) [hep-ph/9309299].

[35] K. A. Intriligator, N. Seiberg and D. Shih, JHEP **0707**, 017 (2007) [hep-th/0703281].

[36] J. Wess and J. Bagger, *Supersymmetry and Supergravity*, (Princeton University Press, 1992)

[37] L. O'Raifeartaigh, Nucl. Phys. B **96**, 331 (1975).

[38] S. Ray, Phys. Lett. B **642**, 137 (2006) [hep-th/0607172].

[39] Z. Komargodski and D. Shih, JHEP **0904**, 093 (2009) [arXiv:0902.0030 [hep-th]].

[40] Y. Nakai and Y. Ookouchi, JHEP **1101**, 093 (2011) [arXiv:1010.5540 [hep-th]].

[41] Y. Ookouchi, Int. J. Mod. Phys. A **26**, 4153 (2011) [arXiv:1107.2622 [hep-th]].

[42] R. Kitano, H. Ooguri and Y. Ookouchi, Phys. Rev. D **75**, 045022 (2007) [hep-ph/0612139].

[43] C. Csaki, Y. Shirman and J. Terning, JHEP **0705**, 099 (2007) [hep-ph/0612241].

[44] S. Abel, C. Durnford, J. Jaeckel and V. V. Khoze, Phys. Lett. B **661**, 201 (2008) [arXiv:0707.2958 [hep-ph]].

[45] N. Haba and N. Maru, Phys. Rev. D **76**, 115019 (2007) [arXiv:0709.2945 [hep-ph]].

[46] R. Essig, J. -F. Fortin, K. Sinha, G. Torroba and M. J. Strassler, JHEP **0903**, 043 (2009) [arXiv:0812.3213 [hep-th]].

[47] A. Giveon, A. Katz and Z. Komargodski, JHEP **0907**, 099 (2009) [arXiv:0905.3387 [hep-th]].

[48] N. Maru, Phys. Rev. D **82**, 075015 (2010) [arXiv:1008.1440 [hep-ph]].

[49] G. F. Giudice and R. Rattazzi, Nucl. Phys. B **511**, 25 (1998) [hep-ph/9706540].

[50] N. Arkani-Hamed, G. F. Giudice, M. A. Luty and R. Rattazzi, Phys. Rev. D **58**, 115005 (1998) [hep-ph/9803290].

[51] R. Kitano, Phys. Lett. B **641**, 203 (2006) [hep-ph/0607090].

[52] M. Ibe and R. Kitano, JHEP **0708**, 016 (2007) [arXiv:0705.3686 [hep-ph]].

[53] M. Ibe and R. Kitano, Phys. Rev. D **75**, 055003 (2007) [hep-ph/0611111].

[54] K. Hamaguchi, R. Kitano and F. Takahashi, JHEP **0909**, 127 (2009) [arXiv:0908.0115 [hep-ph]].

[55] H. Fukushima, R. Kitano and F. Takahashi, JHEP **1302**, 140 (2013) [arXiv:1209.1531 [hep-ph]].

[56] H. Fukushima and R. Kitano, JHEP **1401**, 081 (2014) [arXiv:1311.6228 [hep-ph]].

[57] I. Dalianis and Z. Lalak, JHEP **1012**, 045 (2010) [arXiv:1001.4106 [hep-ph]].

[58] I. Dalianis and Z. Lalak, Phys. Lett. B **697**, 385 (2011) [arXiv:1012.3157 [hep-ph]].

[59] G. D. Coughlan, R. Holman, P. Ramond and G. G. Ross, Phys. Lett. B **140**, 44 (1984).

[60] T. Banks, D. B. Kaplan and A. E. Nelson, Phys. Rev. D **49**, 779 (1994) [hep-ph/9308292].

[61] I. Joichi and M. Yamaguchi, Phys. Lett. B **342**, 111 (1995) [hep-ph/9409266].

[62] K. Kamada, Y. Nakai and M. Sakai, Prog. Theor. Phys. **126**, 35 (2011) [arXiv:1103.5097 [hep-ph]].

[63] M. Hashimoto, K. I. Izawa, M. Yamaguchi and T. Yanagida, Prog. Theor. Phys. **100**, 395 (1998) [hep-ph/9804411].

[64] M. Endo, K. Hamaguchi and F. Takahashi, Phys. Rev. Lett. **96**, 211301 (2006) [hep-ph/0602061].

[65] S. Nakamura and M. Yamaguchi, Phys. Lett. B **638**, 389 (2006) [hep-ph/0602081].

[66] M. Dine, R. Kitano, A. Morisse and Y. Shirman, Phys. Rev. D **73**, 123518 (2006) [hep-ph/0604140].

[67] M. Endo, K. Hamaguchi and F. Takahashi, Phys. Rev. D **74**, 023531 (2006) [hep-ph/0605091].

[68] R. Kallosh, L. Kofman, A. D. Linde and A. Van Proeyen, Phys. Rev. D **61**, 103503 (2000) [hep-th/9907124].

[69] M. Kawasaki, F. Takahashi and T. T. Yanagida, Phys. Lett. B **638**, 8 (2006) [hep-ph/0603265].

[70] T. Asaka, S. Nakamura and M. Yamaguchi, Phys. Rev. D **74**, 023520 (2006) [hep-ph/0604132].

[71] M. Endo, F. Takahashi and T. T. Yanagida, Phys. Lett. B **658**, 236 (2008) [hep-ph/0701042].

[72] M. Endo, F. Takahashi and T. T. Yanagida, Phys. Rev. D **76**, 083509 (2007) [arXiv:0706.0986 [hep-ph]].

[73] S. A. Abel, C. -S. Chu, J. Jaeckel and V. V. Khoze, JHEP **0701**, 089 (2007) [hep-th/0610334].

[74] N. J. Craig, P. J. Fox and J. G. Wacker, Phys. Rev. D **75**, 085006 (2007) [hep-th/0611006].

[75] W. Fischler, V. Kaplunovsky, C. Krishnan, L. Mannelli and M. A. C. Torres, JHEP **0703**, 107 (2007) [hep-th/0611018].

[76] S. A. Abel, J. Jaeckel and V. V. Khoze, JHEP **0701**, 015 (2007) [hep-th/0611130].

[77] L. Anguelova, R. Ricci and S. Thomas, Phys. Rev. D **77**, 025036 (2008) [hep-th/0702168 [HEP-TH]].

[78] C. Papineau, JHEP **0805**, 068 (2008) [arXiv:0802.1861 [hep-th]].

[79] R. Auzzi, S. Elitzur and A. Giveon, JHEP **1003**, 094 (2010) [arXiv:1001.1234 [hep-th]].

[80] A. Katz, JHEP **0910**, 054 (2009) [arXiv:0907.3930 [hep-th]].

[81] E. F. Moreno and F. A. Schaposnik, JHEP **0910**, 007 (2009) [arXiv:0908.2770 [hep-th]].

[82] A. Ferrantelli and J. McDonald, JCAP **1002**, 003 (2010) [arXiv:0909.5108 [hep-ph]].

[83] L. Dolan and R. Jackiw, Phys. Rev. D **9**, 3320 (1974).

[84] M. Quiros, hep-ph/9901312.

[85] A. D. Linde, Phys. Rev. D **53**, 4129 (1996) [hep-th/9601083].

[86] K. Nakayama, F. Takahashi and T. T. Yanagida, Phys. Rev. D **84** (2011) 123523 [arXiv:1109.2073 [hep-ph]]; Phys. Rev. D **86**, 043507 (2012) [arXiv:1112.0418 [hep-ph]]; Phys. Lett. B **714**, 256 (2012) [arXiv:1203.2085 [hep-ph]].

[87] M. Kawasaki, K. Kohri, T. Moroi and A. Yotsuyanagi, Phys. Rev. D **78**, 065011 (2008) [arXiv:0804.3745 [hep-ph]].

[88] N. Arkani-Hamed, A. Delgado and G. F. Giudice, Nucl. Phys. B **741**, 108 (2006) [hep-ph/0601041].

[89] M. Fujii and K. Hamaguchi, Phys. Rev. D **66**, 083501 (2002) [hep-ph/0205044].